

ANALYTIC THEORY OF COUPLED-CAVITY TRAVELING WAVE TUBES

ALEXANDER FIGOTIN

ABSTRACT. Coupled-cavity traveling wave tube (CCTWT) is a high power microwave (HPM) vacuum electronic device used to amplify radio-frequency (RF) signals. CCTWTS have numerous applications, including radar, radio navigation, space communication, television, radio repeaters, and charged particle accelerators. The microwave-generating interactions in CCTWTs take place mostly in coupled resonant cavities positioned periodically along the electron beam axis. Operational features of a CCTWT particularly the amplification mechanism are similar to those of a multicavity klystron (MCK). We advance here a Lagrangian field theory of CCTWTs with the space being represented by one-dimensional continuum. The theory integrates into it the space-charge effects including the so-called debunching (electron-to-electron repulsion). The corresponding Euler-Lagrange field equations are ODEs with coefficients varying periodically in the space. Utilizing the system periodicity we develop the instrumental features of the Floquet theory including the monodromy matrix and its Floquet multipliers. We use them to derive closed form expressions for a number of physically significant quantities. Those include in particular the dispersion relations and the frequency dependent gain foundational to the RF signal amplification. Serpentine (folded, corrugated) traveling wave tubes are very similar to CCTWTs and our theory applies to them also.

1. INTRODUCTION

We start with the general principles of the microwave radiation generation and the amplification of RF signals, [Shev, 4]:

“ANY generating or amplifying device converts d.c. energy into high-frequency electric field energy, and this conversion is effected by means of an electron beam. All energy exchanges between the electron beam and the alternating electric field are a result of acceleration or retardation of the electrons. The kinetic energy of the electrons is converted into electromagnetic energy, and vice versa. Therefore, although the mechanisms of various devices are different, in each of them power is transferred from the constant voltage source to the alternating electromagnetic field. This is brought about in the oscillatory system by means of a density-modulated electron beam in which electrons are accelerated in the constant electric field, and retarded in the alternating electric field. Density modulation of the electron beam makes it possible to retard a greater number of electrons than are accelerated by the same alternating field, thus producing the transfer of energy.”

The last sentence in the above quote underlines the critical role played by the density modulation of the electron beam (known also as “electron bunching”) in the energy transfer from the electron beam to the electromagnetic (EM) radiation.

A coupled-cavity traveling wave tube (CCTWT) shown schematically in Fig. 1 is the primary subject we pursue here. The CCTWT is special type of traveling wave tube (TWT) that utilizes coupled-cavity structure (CCS) as a slow-wave structure (SWS), [Gilm1, 15], [MAEAD, 4]. The CCS commonly is a periodic linear chain of several tens of cavities coupled by coupling holes or slots and a beam tunnel, [Tsim, 8.7.5]. The cavities can be similar to those in klystrons. As to the

Key words and phrases. Coupled-cavity traveling wave tubes, serpentine (folded, corrugated) traveling wave tubes, instability, amplification, gain.

physical implementation cavities are often constructed of sections of a slow-wave structure that are made resonant by suitable terminations. The quality factor of each cavity is required to be sufficiently high so that the RF field distribution in each separate cavity is substantially unaffected by the interaction with the beam, [ChoWes].

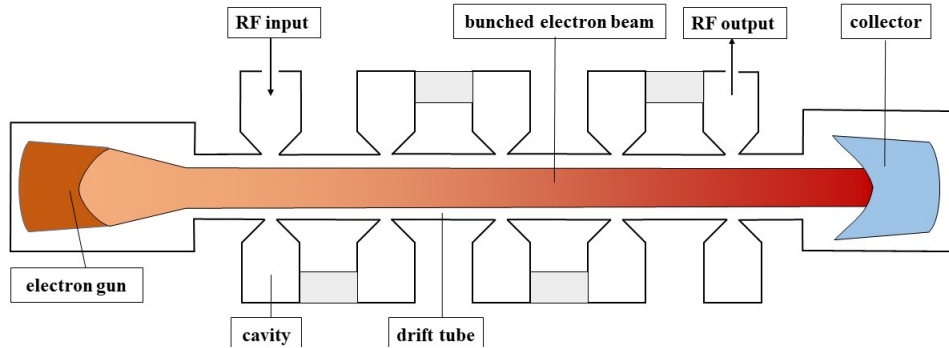


FIGURE 1. Schematic representation of a coupled-cavity traveling wave tube (CCTWT) composed of a periodic array of coupled cavities (often of toroidal shape) interacting with the pencil-like electron beam. The interaction causes the electron bunching and consequent amplification of the RF signal.

By its very design the CCS is mechanically and thermally more robust than a helix, which is often used as the SWS, allowing much greater average power, especially in the short-wave bands of microwave range, [ChoCra], [GraParArm], [Tsim, 8.3, 8.7.5]. Serpentine (folded, corrugated) TWTs are based on the corresponding waveguides that permit electron interaction below the velocity of light, [Gilm1, 15.1, 15.2]. They are very similar to CCTWTs and the results of our studies apply also to serpentine (folded, corrugated) TWTs.

A distinct and important feature of a CCTWT is that the interaction between the e-beam and the *coupled-cavity structure* (CCS), particularly the electron velocity modulation by high-frequency EM field, is limited mostly to the EM cavities positioned periodically along the e-beam axis. The cavity properties that are significant for an effective interaction with the e-beam are as follows, [Shev, 2]:

“In order to be used in an electron tube, a cavity resonator must have a region with a relatively strong high-frequency field which is polarized along the direction of electron flow. This region should, in the majority of cases, be so small that the electron transit time is less than the period of change of the field. Hollow toroidal resonators satisfy these conditions. Toroidal resonators consist of cylinders with a very prominent "bulge" in the middle.”

The region in the above quote is commonly referred to as the *cavity gap* or just *gap*, and it is there the electron velocity is modulated leading to the electron bunching and consequent RF signal amplification. If \dot{v} is the stationary (dc) velocity of the electron flow and l_g is the length of the cavity gap then the mentioned condition of smallness of l_g and the electron transit time $\tau_g = \frac{l_g}{\dot{v}}$ can be written as

$$l_g < \frac{2\pi\dot{v}}{\omega}, \quad (1.1)$$

It is a common assumption for one-dimensional models for charge-waves that the e-beam is not dense in the sense that the operational frequency ω satisfies, [Tsim, p. 277]:

$$\omega_p \ll \omega, \quad (1.2)$$

where ω_p is the relevant plasma frequency. Then combining inequalities (1.2) and (1.1) we obtain the following upper bound on the gap length:

$$l_g < \frac{2\pi\dot{v}}{\omega} \ll \lambda_p = \frac{2\pi\dot{v}}{\omega_p}. \quad (1.3)$$

Idealized theories including the one we advance here assume that the narrow cavity gaps are just of zero width corresponding to zero transit time of the electron, [Shev, II.5], [Werne, III.3]. That is we make the following simplifying assumption:

$$l_g = 0, \quad \tau_g = \frac{l_g}{\dot{v}} = 0. \quad (1.4)$$

The primary subject of our studies here is the construction of one-dimensional Lagrangian field theory of a coupled-cavity traveling wave tube (CCTWT) a schematic sketch of which is shown in Fig. 1 (compare it with Fig. 11 with a schematic sketch of a *multicavity klystron* (MCK)). This theory integrates into it (i) our one-dimensional Lagrangian field theory for TWTs introduced and studied in [FigTWTbk, 4, 24] and reviewed in Section 2; (ii) one-dimensional Lagrangian field theory for multicavity klystron we developed in [FigKly] in reviewed in Section 8. The theory takes into account the space-charge effects, and it applies also to serpentine (folded, corrugated) traveling wave tubes.

This paper is organized as follows. In Section 2, we review concisely the one-dimensional Lagrangian field theory for TWTs introduced and studied in [FigTWTbk, 4, 24]. In Section 3, we construct the Lagrangian of the CCTWT, derive the corresponding Euler-Lagrange equations and introduce the CCTWT constitutive subsystems: coupled cavity structure and the e-beam. In Section 4, we use the Floquet theory to study solutions to the Euler-Lagrange equations. In particular we construct the monodromy matrix. In Section 5, we analyze the Floquet multiplies which are solution to the characteristic equations. In Section 6 we construct the dispersion relations and study their properties. In Section 7, we derive expressions for the frequency dependent gain associated with the CCTWT eigenmodes. In Section 8, we review concisely the one-dimensional Lagrangian field theory for multicavity klystrons developed in [FigKly] that allows to see some of its features in the CCTWT. In Section 9, we study couple-cavity structure when it is not coupled to the e-beam. That is allows us to see some of its features in the properties of the CCTWT. In a numbers of appendices we review for the reader's convenience a number of mathematical and physical subjects relevant to the analysis of the CCTWT. The kinetic and field points of view on the gap interaction is considered in Section 10. The Lagrangian variational framework of our analytical theory is developed in Section 11. In Section 12, we consider special polynomials of the forth degree and their root degeneracies that are useful for our studies of the CCTWT exceptional points of degeneracy. In a number of Appendices we review some mathematical and physical subject relevant to our studies.

While quoting monographs, we identify the relevant sections as follows. Reference [X,Y] refers to Section/Chapter “Y” of monograph (article) “X”, whereas [X, p. Y] refers to page “Y” of monograph (article) “X”. For instance, reference [2, VI.3] refers to monograph [2], Section VI.3; reference [2, p. 131] refers to page 131 of monograph [2].

2. SKETCH OF THE ANALYTIC MODEL OF THE TRAVELING WAVE TUBE

When constructing the CCTWT Lagrangian, we use the elements of the analytic theory of TWTs developed in [FigTWTbk, 4, 24]. The purpose of this section is to introduce those elements

as well as the relevant variables of the analytic model of TWT. TWT converts the energy of the electron beam (e-beam) into the EM energy of the amplified RF signal. A schematic sketch of typical TWT is shown in Fig. 2. To facilitate the energy conversion and signal amplification, the e-beam is enclosed in the so-called *slow wave structure* (SWS), that supports waves that are slow enough to effectively interact with the electron flow. As a result of this interaction, the kinetic energy of electrons is converted into the EM energy stored in the field, [Gilm1], [Tsim], [Nusi, 2.2], [SchaB, 4]. Consequently, the *key operational principle of a TWT is a positive feedback interaction between the slow-wave structure and the flow of electrons*. The physical mechanism of the radiation generation and its amplification is the electron bunching caused by the acceleration and deceleration of electrons along the e-beam (see quotes in Section 1).

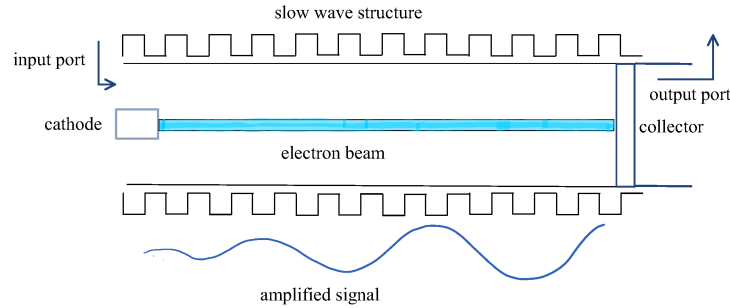


FIGURE 2. The upper picture is a schematic representation of a traveling wave tube. The lower picture shows an RF perturbation in the form of a space-charge wave which is amplified exponentially as it propagates through the traveling wave tube.

A typical TWT consists of a vacuum tube containing the e-beam that passes down the middle of an SWS such as an RF circuit. It operates as follows. The left end of the RF circuit is fed with a low-powered RF signal to be amplified. The SWS electromagnetic field acts upon the e-beam causing electron bunching and the formation of the so-called *space-space-charge wave*. In turn, the electromagnetic field generated by the space-charge wave induces more current back into the RF circuit with a consequent enhancement of electron bunching. As a result, the EM field is amplified as the RF signal passes down the structure until a saturation regime is reached and a large RF signal is collected at the output. The role of the SWS is to provide slow-wave modes to match up with the velocity of the electrons in the e-beam. This velocity is usually a small fraction of the speed of light. Importantly, synchronism is required for effective in-phase interaction between the SWS and the e-beam with optimal extraction of the kinetic energy of the electrons. A typical simple SWS is the helix, which reduces the speed of propagation according to its pitch. The TWT is designed so that the RF signal travels along the tube at nearly the same speed as electrons in the e-beam to facilitate effective coupling. Technical details on the designs and operation of TWTs can be found in [Gilm1], [Nusi, 4] [PierTWT], [Tsim]. As for a rich and interesting history of traveling wave tubes, we refer the reader to [MAEAD] and references therein.

An effective mathematical model for a TWT interacting with the e-beam was introduced by Pierce [Pier51, I], [PierTWT]. The Pierce model is one-dimensional; it accounts for the wave amplification, energy extraction from the e-beam and its conversion into microwave radiation in the TWT [Gilm1], [Gilm], [Nusi, 4], [SchaB, 4], [Tsim]. This model captures remarkably well significant features of the wave amplification and the beam-wave energy transfer, and is still used for basic design estimates. In our paper [FigRey1], we have constructed a Lagrangian field theory by generalizing and extending the Pierce theory to the case of a possibly inhomogeneous MTL

coupled to the e-beam. This work was extended to an analytic theory of multi-stream electron beams in traveling wave tubes in [FigTWTbk]. We concisely review here this theory. According to the simplest version of the theory an ideal TWT is represented by a single-stream electron beam (e-beam) interacting with a single transmission line (TL) just as in the Pierce model [Pier51, I]. The main parameter describing the single-stream e-beam is e-beam intensity

$$\beta = \frac{\sigma_B}{4\pi} R_{sc}^2 \omega_p^2 = \frac{e^2}{m} R_{sc}^2 \sigma_B \dot{n}, \quad \omega_p^2 = \frac{4\pi \dot{n} e^2}{m}, \quad (2.1)$$

where $-e$ is the electron charge with $e > 0$, m is the electron mass, ω_p is the e-beam plasma frequency, σ_B is the area of the cross-section of the e-beam, $\dot{v} > 0$ is stationary velocity of electrons in the e-beam and \dot{n} is the density of the number of electrons. The constant R_{sc} is the plasma frequency reduction factor that accounts phenomenologically for finite dimensions of the e-beam cylinder as well as geometric features of the slow-wave structure, [BraMih], [Gilm1, 9.2], [Nusi, 3.3.3]. The frequency

$$\omega_{rp} = R_{sc} \omega_p \quad (2.2)$$

is known as reduced plasma frequency, [Gilm1, 9.2].

Assume the Gaussian system of units of the physical dimensions of a complete set of the e-beam parameters, as in Tables 1 and 2.

Frequency	Plasma frequency	$\omega_p = \sqrt{\frac{4\pi \dot{n} e^2}{m}}$
Velocity	e-beam velocity	\dot{v}
Wavenumber		$k_q = \frac{\omega_{rp}}{\dot{v}} = \frac{R_{sc} \omega_p}{\dot{v}}$
Length	Wavelength for k_q	$\lambda_{rp} = \frac{2\pi \dot{v}}{\omega_{rp}}, \omega_{rp} = R_{sc} \omega_p$
Time	Wave time period	$\dot{\tau} = \frac{2\pi}{\omega_p}$

TABLE 1. Natural units relevant to the e-beam.

i	current	$\frac{[\text{charge}]}{[\text{time}]}$
q	charge	[charge]
\dot{n}	number of electrons p/u of volume	$\frac{[1]}{[\text{length}]^3}$
$\lambda_{rp} = \frac{2\pi \dot{v}}{\omega_{rp}}, \omega_{rp} = R_{sc} \omega_p$	the electron plasma wavelength	[length]
$g_B = \frac{\sigma_B}{4\lambda_{rp}}$	the e-beam spatial scale	[length]
$\beta = \frac{\sigma_B}{4\pi} R_{sc}^2 \omega_p^2 = \frac{e^2}{m} R_{sc}^2 \sigma_B \dot{n}$	e-beam intensity	$\frac{[\text{length}]^2}{[\text{time}]^2}$
$\beta' = \frac{\beta}{\dot{v}^2} = \frac{\pi \sigma_B}{\lambda_{rp}^2} = \frac{4\pi g_B}{\lambda_{rp}}$	dimensionless e-beam intensity	[dim-less]

TABLE 2. Physical dimensions of the e-beam parameters. Abbreviations: dimensionless – dim-less, p/u – per unit.

We would like to point to an important spatial scale related to the e-beam, namely

$$\lambda_{rp} = \frac{2\pi\dot{v}}{R_{sc}\omega_p}, \quad \omega_{rp} = R_{sc}\omega_p, \quad (2.3)$$

which is the distance passed by an electron for the time period $\frac{2\pi}{\omega_{rp}}$ associated with the plasma oscillations at the reduced plasma frequency ω_{rp} . This scale is well known in the theory of klystrons and is referred to as *the electron plasma wavelength*, [Gilm1, 9.2]. Another spatial scale related to the e-beam that arises in our analysis later on is

$$g_B = \frac{\sigma_B}{4\lambda_{rp}}, \quad (2.4)$$

and we will refer to it as *e-beam spatial scale*. Using these spatial scales we obtain the following representation for the dimensionless form β' of the e-beam intensity

$$\beta' = \frac{\beta}{\dot{v}^2} = \frac{\pi\sigma_B}{\lambda_{rp}^2} = \frac{4\pi g_B}{\lambda_{rp}}. \quad (2.5)$$

As for the single transmission line, its shunt capacitance per unit of length is a real number $C > 0$ and its inductance per unit of length is another real number $L > 0$. The coupling constant $0 < b \leq 1$ is also a number, see [FigTWTbk, 3] for more details. The TL single characteristic velocity w and the single *TL principal coefficient* θ are defined by

$$w = \frac{1}{\sqrt{CL}}, \quad \theta = \frac{b^2}{C}. \quad (2.6)$$

Following [FigTWTbk, 3], we assume that

$$0 < \dot{v} < w. \quad (2.7)$$

2.1. TWT Lagrangian and evolution equations. Following the developments in [FigTWTbk], we introduce the *TWT principal parameter* $\bar{\gamma} = \theta\beta$. This parameter in view of equations (2.1) and (2.6) can be represented as follows

$$\gamma = \theta\beta = \frac{b^2}{C} \frac{\sigma_B}{4\pi} R_{sc}^2 \omega_p^2 = \frac{b^2}{C} \frac{e^2}{m} R_{sc}^2 \sigma_B \dot{n}, \quad \theta = \frac{b^2}{C}, \quad \beta = \frac{e^2}{m} R_{sc}^2 \sigma_B \dot{n}. \quad (2.8)$$

The TWT Lagrangian \mathcal{L}_{TB} in the simplest case of a single transmission line and one stream e-beam is of the following form, [FigTWTbk, 4, 24]:

$$\mathcal{L}(\{Q\}, \{q\}) = \mathcal{L}_{Tb}(\{Q\}, \{q\}) + \mathcal{L}_B(\{q\}), \quad (2.9)$$

$$\mathcal{L}_{Tb} = \frac{L}{2} (\partial_t Q)^2 - \frac{1}{2C} (\partial_z Q + b\partial_z q)^2, \quad \mathcal{L}_B = \frac{1}{2\beta} (\partial_t q + \dot{v}\partial_z q)^2 - \frac{2\pi}{\sigma_B} q^2,$$

where where $b > 0$ is a coupling coefficient and

$$\{Q\} = Q, \partial_z Q, \partial_t Q, \quad Q = Q(z, t); \quad \{q\} = q, \partial_z q, \partial_t q, \quad q = q(z, t), \quad (2.10)$$

where $q(z, t)$ and $Q(z, t)$ are *charges* associated respectively with the e-beam and the TL. The charges defined as time integrals of the corresponding e-beam currents $i(z, t)$ and TL current $I(z, t)$, that is

$$q(z, t) = \int^t q(z, t') dt', \quad Q(z, t) = \int^t I(z, t') dt'. \quad (2.11)$$

Note that the term $-\frac{2\pi}{\sigma_B} q^2$ in the Lagrangian \mathcal{L}_B defined in equations (2.9) represents space-charge effects including the so-called debunching (electron-to-electron repulsion). The corresponding Euler-Lagrange equations is represented by the following system of second-order differential

equations

$$L\partial_t^2 Q - \partial_z [C^{-1}(\partial_z Q + b\partial_z q)] = 0, \quad (2.12)$$

$$\frac{1}{\beta}(\partial_t + \dot{v}\partial_z)^2 q + \frac{4\pi}{\sigma_B}q - b\partial_z [C^{-1}(\partial_z Q + b\partial_z q)] = 0, \quad (2.13)$$

where \dot{v} is the stationary velocity of electrons in the e-beam, σ_B is the area of the cross-section of the e-beam and β is the e-beam intensity defined by equations (2.8).

2.2. Space-charge wave velocity and electron density fields. Following to the field theory constructions in [FigTWTbk, 22] we consider the total electron density $N = \dot{n} + n$ and $V = \dot{v} + v$ where \dot{n} and \dot{v} are respectively densities of the electron number and the electron velocity of the stationary dc electron flow, and $n = n(z, t)$ and $v = v(z, t)$ are respectively position and time dependent ac densities of the electron number and the electron velocity of the space-charge wave field $q = q(z, t)$ and the electric field $E = E(z, t)$. To comply with the linear theory approximation we assume that n and v to be relatively small:

$$|n| \ll \dot{n}, \quad |v| \ll \dot{v}. \quad (2.14)$$

We consider also the ac current density field $j = j(z, t)$ that satisfies

$$j = j(z, t) = -e(\dot{n}v + \dot{v}n), \quad \partial_t(-en) + \partial_z j = 0. \quad (2.15)$$

Then the following relations between charge density field $q = q(z, t)$ and fields $n = n(z, t)$ and $v = v(z, t)$ hold, [FigTWTbk, 22.2]:

$$\partial_z q = \sigma_B en, \quad \partial_t q = \sigma_B j = J, \quad (2.16)$$

where J is the e-beam current. The first equation (2.16) readily implies

$$n = \frac{1}{\sigma_B e} \partial_z q. \quad (2.17)$$

The relations between charge variable $q = q(z, t)$ defined in Section 2.1, the velocity $v = v(z, t)$ and associated with it current $J_v = J_v(z, t)$ are as follows, [FigTWTbk, 22.2]:

$$e\sigma_B \dot{n}v = -D_t q, \quad J_v = -e\sigma_B \dot{n}v = D_t q, \quad D_t = \partial_t + \dot{v}\partial_z \quad (2.18)$$

where D_t is the so-called *material time derivative*. The second equation in (2.18) implies evidently that current J_v is exactly $D_t q$, whereas the first equation in (2.18) yields the following representations of the velocity v

$$v = -\frac{1}{e\sigma_B \dot{n}} D_t q = -\frac{J_v}{e\sigma_B \dot{n}}. \quad (2.19)$$

The electric field $E = E(z, t)$ associated with the space-charge wave satisfies the Poisson equation, [FigTWTbk, 22.2]:

$$\partial_z E = -\frac{4\pi}{\sigma_B} \partial_z q = -4\pi en. \quad (2.20)$$

Under the additional natural assumption “if there is no charges there is no electric field”, that is, $\bar{q} = 0$ must imply $E = 0$, the above equation yields

$$E = -\frac{4\pi}{\sigma_B} \bar{q}. \quad (2.21)$$

If we introduce the e-beam voltage $V_b = V_b(z, t) = -\partial_z E$ then the Poisson equation (2.20) can be recast as

$$\partial_z^2 V_b = 4\pi en. \quad (2.22)$$

3. ANALYTIC MODEL OF COUPLED-CAVITY TRAVELING WAVE TUBE

When integrating into the mathematical model significant features of the CCTWT, we make a number of simplifying assumptions. In particular, we use the following basic assumptions of one-dimensional model of space-charge waves in velocity-modulated beams, [Tsim, 7.6.1]: (i) all quantities of interest depend only on a single space variable z ; (ii) the electric field has only an z -component; (iii) there are no transverse velocities of electrons; (iv) ac values are small compared with dc values; (v) electrons have a constant dc velocity which is much smaller than the speed of light, and (vi) electron beams are nondense. The list of preliminary assumptions of our ideal model for the CCTWT is as follows.

Assumption 1. (*ideal model of the e-beam and the TL interaction*).

- (i) *E-beam is represented by a cylinder of infinitesimally small radius having as its axis the z -axis (see Fig. 1).*
- (ii) *Coupled-cavity structure (CCS) is represented mathematically by a periodic array of adjacent segments of a transmission line (TL) of length $a > 0$ connected by cavities at points $a\ell$, $\ell \in \mathbb{Z}$ by cavities.*
- (iii) *Every cavity carries shunt capacitance c_0 . The e-beam interacts with the CCS exclusively through the cavities located at a discrete set of equidistant points, that is the lattice*

$$a\mathbb{Z} : \mathbb{Z} = \{\dots, -2, -1, 0, 1, 2, \dots\}, \quad (3.1)$$

where $a > 0$ and we refer to this parameter as the CCS period or just period. The cavity width l_g and the corresponding transit time τ_g are assumed to be zero, see equations (1.4) and comments above it.

The CCTWT state is described by charges $q = q(z, t)$ and $Q = Q(z, t)$ for respectively the e-beam and the TL defined as the time integrals of the corresponding currents

$$Q = Q(z, t) = \int^t I(z, t') dt', \quad q = q(z, t) = \int^t i(z, t') dt'. \quad (3.2)$$

Since according to the formulated above assumptions the interaction should occur only at the discrete set $a\mathbb{Z}$ (lattice) of points embedded into one-dimensional continuum of real numbers \mathbb{R} some degree of singularity of functions $Q(z, t)$ and $q(z, t)$ is expected. As the analysis shows it is appropriate to impose the following *jump and continuity conditions* on charge functions $Q(z, t)$ and $q(z, t)$.

Assumption 2. (*jump-continuity of charge functions*).

- (i) *Functions $Q(z, t)$ and $q(z, t)$ and their time derivatives $\partial_t^j Q(z, t)$ and $\partial_t^j q(z, t)$ for $j = 1, 2$ are continuous for all real t and z .*
- (ii) *Derivatives $\partial_t^j Q(z, t)$, $\partial_t^j q(z, t)$, $\partial_z^j Q(z, t)$, $\partial_z^j q(z, t)$ for $j = 1, 2$, and the mixed derivatives $\partial_z \partial_t Q(z, t) = \partial_t \partial_z Q(z, t)$, $\partial_z \partial_t q(z, t) = \partial_t \partial_z q(z, t)$ exist and continuous for all real t and z except for the interaction points in the lattice $a\mathbb{Z}$.*
- (iii) *Let for a function $F(z)$ and a real number b symbols $F(b-0)$ and $F(b+0)$ stand for its left and right limit at b assuming their existence, that is*

$$F(b \pm 0) = \lim_{z \rightarrow b \pm 0} F(z). \quad (3.3)$$

Let us also denote by $[F](b)$ the jump of function $F(z)$ at b , that is

$$[F](b) = F(b+0) - F(b-0). \quad (3.4)$$

The following right and left limits exist

$$\partial_z^j Q(a\ell \pm 0, t), \quad \partial_z^j q(a\ell \pm 0, t), \quad j = 1, 2; \quad \ell \in \mathbb{Z}, \quad (3.5)$$

I	Current	$\frac{[\text{charge}]}{[\text{time}]}$
Q	Charge	[charge]
c_0	Cavity capacitance	[length]
l_0	Cavity inductance	$\frac{[\text{time}]^2}{[\text{length}]}$
b	Coupling parameter	[dim-less]

TABLE 3. Physical dimensions of cavity related quantities. Abbreviations: dimensionless – dim-less

I	Current	$\frac{[\text{charge}]}{[\text{time}]}$
Q	Charge	[charge]
C	Shunt capacitance p/u of length	[dim-less]
L	Series inductance p/u of length	$\frac{[\text{time}]^2}{[\text{length}]^2}$

TABLE 4. Physical dimensions of the TL related quantities. Abbreviations: dimensionless – dim-less, p/u – per unit.

and these limits are continuously differentiable functions of t . The values $\partial_z Q(al \pm 0, t)$ as well as $\partial_z q(al \pm 0, t)$ can be different and consequently the jumps $[\partial_z Q](al, t)$ and $[\partial_z q](al, t)$ can be nonzero.

Remark 1 (physical significance of jumps). Though according to Assumption 1 we neglect the widths of the EM cavities their interaction with the electron flow is represented through jumps $[\partial_z q](al, t)$ which are of the direct physical significance. Indeed, the field interpretation of the kinetic properties of the electron flow in Section 10.2, namely equations (10.3), imply

$$[\partial_z q](al, t) = \sigma_B e [n](al, t). \quad (3.6)$$

Equation (3.6) shows that jump $[\partial_z q](al, t)$ up to a multiplicative constant $\frac{1}{\sigma_B e}$ represents jump $[n](al, t) = \frac{[\partial_z q](al, t)}{\sigma_B e}$ in the number of electron density *manifesting the electron bunching* that occurs in the EM cavity centered at al . In view of equations (10.4) we also have $[v](al, t) = -\frac{\dot{v}[\partial_z q](al, t)}{e\sigma_B \dot{n}}$ manifesting the ac electron velocity modulation in the EM cavity centered at al .

The physical dimensions of quantities related to the cavities and the TL are summarized respectively in Tables 3 and 4.

3.1. CCTWT Lagrangian and the Euler-Lagrange equations. To simplify expressions we use the following notations:

$$\{Q\} = Q, \partial_z Q, \partial_t Q, \quad Q = Q(z, t); \quad \{q\} = q, \partial_z q, \partial_t q, \quad q = q(z, t), \quad (3.7)$$

$$x = \begin{bmatrix} Q \\ q \end{bmatrix}, \quad \{x\} = \begin{bmatrix} Q \\ q \end{bmatrix}, \quad \begin{bmatrix} \partial_z Q \\ \partial_z q \end{bmatrix}, \quad \begin{bmatrix} \partial_t Q \\ \partial_t q \end{bmatrix}. \quad (3.8)$$

The CCTWT Lagrangian \mathcal{L} is defined as the sum of its three components: (i) \mathcal{L}_T is the TL Lagrangian, (ii) \mathcal{L}_B is the e-beam Lagrangian; (iii) \mathcal{L}_{TB} represent the TL and e-beam interaction Lagrangian. That is,

$$\mathcal{L}(\{x\}) = \mathcal{L}_T(\{Q\}) + \mathcal{L}_B(\{q\}) + \mathcal{L}_{TB}(x), \quad (3.9)$$

where we used notations (3.7) and (3.8). The expressions for \mathcal{L}_T and \mathcal{L}_B are similar to the TWT Lagrangian components in equations (2.9), (2.10), namely

$$\mathcal{L}_T(\{Q\}) = \mathcal{L}_{Tb}|_{b=0} = \frac{L}{2} (\partial_t Q)^2 - \frac{1}{2C} (\partial_z Q)^2, \quad \mathcal{L}_B(\{q\}) = \frac{1}{2\beta} (\partial_t q + \dot{v} \partial_z q)^2 - \frac{2\pi}{\sigma_B} q^2, \quad (3.10)$$

where \mathcal{L}_{Tb} is defined by equation (2.9) and the interaction Lagrangian \mathcal{L}_{TB} is defined by

$$\mathcal{L}_{TB}(x) = \sum_{\ell=-\infty}^{\infty} \delta(z - a\ell) \left\{ \frac{l_0}{2} (\partial_t Q(a\ell))^2 - \frac{1}{2c_0} [Q(a\ell) + bq(a\ell)]^2 \right\}. \quad (3.11)$$

Parameters C and L are respectively distributed shunt capacitance and inductance of the TL, σ_B is the area of the cross-section and β is the e-beam intensity defined in Section 2. Lagrangian \mathcal{L}_B in equations (2.10) represents the e-beam and the term $-\frac{2\pi}{\sigma_B} q^2$ models the space-charge effects including the so-called debunching (electron-to-electron repulsion). Lagrangian \mathcal{L}_{Tb} in equations (2.9) integrates into it the interactions between the TL and the e-beam whereas for the CCTWT the Lagrangian \mathcal{L}_T corresponds to the decoupled TL. This is why we set \mathcal{L}_T to be \mathcal{L}_{Tb} for $b = 0$. Note also that (i) expression (3.11) for the interaction Lagrangian \mathcal{L}_{TB} is limited by design to the interaction points $a\ell$ as indicated by delta functions $\delta(z - a\ell)$ and (ii) the factors before delta functions $\delta(z - a\ell)$ are expressions similar to density \mathcal{L}_{Tb} in equations (2.9) adapted to lattice $a\mathbb{Z}$ of discrete interaction points $a\ell$; (iii) capacitance c_0 is of the most significance for the interaction between the TL and the e-beam and we refer to it as the *cavity capacitance*. *It follows from equations (3.9), (3.10) and (3.11) that \mathcal{L} is a periodic Lagrangian of the period a .*

As we derive in Section 11 the Euler-Lagrange (EL) equations for points z outside the lattice $a\mathbb{Z}$ are

$$L\partial_t^2 Q - C^{-1}\partial_z^2 Q = 0, \quad \frac{1}{\beta} (\partial_t + \dot{v}\partial_z)^2 q + \frac{4\pi}{\sigma_B} q = 0, \quad z \neq a\ell, \quad \ell \in \mathbb{Z}, \quad (3.12)$$

or equivalently

$$\partial_z^2 Q - \frac{1}{w^2} \partial_t^2 Q = 0, \quad \left(\frac{1}{v} \partial_t + \partial_z \right)^2 q + \frac{4\pi\beta}{\sigma_B \dot{v}^2} q = 0, \quad z \neq a\ell, \quad \ell \in \mathbb{Z}. \quad (3.13)$$

The EL equations at the interaction points $a\ell$ are

$$[Q](a\ell) = 0, \quad [q](a\ell) = 0, \quad (3.14)$$

$$[\partial_z Q](a\ell) = C_0 \left[\left(\frac{\partial_t^2}{\omega_0^2} + 1 \right) Q(a\ell) + bq(a\ell) \right], \quad [\partial_z q](a\ell) = -\frac{b\beta_0}{\dot{v}^2} [Q(a\ell) + bq(a\ell)], \quad (3.15)$$

where we make use of parameters

$$C_0 = \frac{C}{c_0}, \quad \omega_0 = \frac{1}{\sqrt{l_0 c_0}}, \quad \beta_0 = \frac{\beta}{c_0}, \quad (3.16)$$

and jumps $[Q](a\ell)$, $[q](a\ell)$, $[\partial_z Q](a\ell)$ and $[\partial_z q](a\ell)$ are defined by equation (3.4). We refer to β_0 as *nodal e-beam interaction parameter*. Note that equations (3.14) is just an acknowledgment of the continuity of charges $Q(z, t)$ and $q(z, t)$ at the interaction points in consistency with Assumption 2. Equations (3.14), (3.15) can be viewed as the boundary conditions at the interaction points that are complementary to the differential equations (3.12) and (3.13).

The Euler-Lagrange differential equations (3.12), (3.13) together with the boundary conditions (3.14), (3.15) form the complete set of equation describing the CCTWT evolution. Boundary conditions (3.14), (3.15) can be recast into the following matrix form:

$$[\partial_z x](al) = P_{\text{TB}} x(al), \quad x = \begin{bmatrix} Q \\ q \end{bmatrix}, \quad P_{\text{TB}} = \begin{bmatrix} C_0 \left(\frac{\partial_t^2}{\omega_0^2} + 1 \right) & C_0 b \\ -\frac{b\beta_0}{\dot{v}^2} & -\frac{b^2\beta_0}{\dot{v}^2} \end{bmatrix}, \quad (3.17)$$

where parameters C_0 and β_0 are defined by equations (3.16). Hence, the complete set of the boundary conditions at interaction points al can be concisely written as

$$x(+al) = x(-al), \quad \partial_z x(+al) = \partial_z x(-al) + P_{\text{TB}} x. \quad (3.18)$$

Consequently

$$X(al+0) = S_b X(al-0), \quad S_b = \begin{bmatrix} \mathbb{I} & 0 \\ P_{\text{TB}} & \mathbb{I} \end{bmatrix}, \quad X = \begin{bmatrix} x \\ \partial_z x \end{bmatrix}, \quad x = \begin{bmatrix} Q \\ q \end{bmatrix}, \quad (3.19)$$

where \mathbb{I} is 2×2 identity matrix and in view of equations (3.17) we have

$$S_b = \begin{bmatrix} \mathbb{I} & 0 \\ P_{\text{TB}} & \mathbb{I} \end{bmatrix} = \begin{bmatrix} 1 & 0 & 0 & 0 \\ 0 & 1 & 0 & 0 \\ C_0 \left(\frac{\partial_t^2}{\omega_0^2} + 1 \right) & C_0 b & 1 & 0 \\ -\frac{b\beta_0}{\dot{v}^2} & -\frac{b^2\beta_0}{\dot{v}^2} & 0 & 1 \end{bmatrix}, \quad C_0 = \frac{C}{c_0}, \quad \beta_0 = \frac{\beta}{c_0}. \quad (3.20)$$

3.2. Natural units and dimensionless parameters. The natural units relevant to the e-beam in CCTWT are shown in Table 5.

Velocity	e-beam velocity	\dot{v}
Length	period	a
Length	Wavelength	$\lambda = \frac{1}{k} = \frac{\dot{v}}{\omega_p}$
Frequency	Period frequency	$\omega_a = \frac{\dot{v}}{a}$
Frequency	Plasma frequency	$\omega_p = \sqrt{\frac{4\pi\hbar e^2}{m}}$
Time	Time of passing the period a	$\frac{1}{\omega_a} = \frac{a}{\dot{v}}$
Time	Plasma oscillation time period	$\tau = \frac{1}{\omega_p}$

TABLE 5. Natural units relevant to the e-beam in CCTWT.

Another variables that arise in our analysis are

$$\lambda_{\text{rp}} = \frac{2\pi\dot{v}}{\omega_{\text{rp}}}, \quad \omega_{\text{rp}} = R_{\text{sc}}\omega_p, \quad \chi = \frac{w}{\dot{v}} = \frac{1}{\dot{v}\sqrt{CL}}, \quad (3.21)$$

$$f_B = \sqrt{\frac{4\pi\beta}{\sigma_B\dot{v}^2}} = \frac{\omega_{\text{rp}}}{\dot{v}} = \frac{2\pi}{\lambda_{\text{rp}}}, \quad C_0 = \frac{C}{c_0}, \quad \beta_0 = \frac{\beta}{c_0},$$

where ω_{rp} and λ_{rp} are respectively the *reduced plasma frequency* and the *electron plasma wavelength*.

The dimensionless variables of importance are

$$z' = \frac{z}{a}, \quad \partial_{z'} = a\partial_z, \quad t' = \frac{\dot{v}}{a}t, \quad \partial_{t'} = \frac{a}{\dot{v}}\partial_t, \quad \omega' = \frac{\omega}{\omega_a} = \frac{a}{2\pi\dot{v}}\omega, \quad \omega'_0 = \frac{\omega_0}{\omega_a} = \frac{a}{2\pi\dot{v}}\omega_0, \quad (3.22)$$

a	the MCK period	[length]
\mathring{v}	the e-beam stationary velocity	$\frac{[\text{length}]}{[\text{time}]}$
$\omega_a = \frac{2\pi\mathring{v}}{a}$	the period frequency	$\frac{[1]}{[\text{time}]}$
$\omega_p = \sqrt{\frac{4\pi\mathring{n}e^2}{m}}$	the plasma frequency	$\frac{[1]}{[\text{time}]}$
$\lambda_{rp} = \frac{2\pi\mathring{v}}{\omega_{rp}}, \omega_{rp} = R_{sc}\omega_p$	the electron plasma wavelength	[length]
$g_B = \frac{\sigma_B}{4\lambda_{rp}}$	the e-beam spatial scale	[length]
$f' = af = \frac{2\pi\omega_{rp}}{\omega_a} = \frac{2\pi a}{\lambda_{rp}}$	normalized period in units of $\frac{\lambda_{rp}}{2\pi}$	[dim-less]
\mathring{n}	the number of electrons p/u of volume	$\frac{[1]}{[\text{length}]^3}$
c_0, l_0	the cavity capacitance, inductance	[length], $\frac{[\text{time}]^2}{[\text{length}]}$
$\omega_0 = \frac{1}{\sqrt{l_0 c_0}}$	the cavity resonant frequency	$\frac{[1]}{[\text{time}]}$
$\beta = \frac{\sigma_B R_{sc}^2 \omega_p^2}{4\pi} = \frac{e^2 R_{sc}^2 \sigma_B \mathring{n}}{m} = \frac{\pi \sigma_B \mathring{v}^2}{\lambda_{rp}^2}$	the e-beam intensity	$\frac{[\text{length}]^2}{[\text{time}]^2}$
$\beta' = \frac{\beta}{\mathring{v}^2} = \frac{\pi \sigma_B}{\lambda_{rp}^2} = \frac{4\pi g_B}{\lambda_{rp}}$	dim-less e-beam intensity	[dim-less]
$\beta'_0 = \frac{\beta'}{c'_0} = \frac{a\beta}{c_0 \mathring{v}^2}$	the first interaction par.	[dim-less]
$B(\omega) = B_0 \frac{\omega^2}{\omega^2 - \omega_0^2}, \quad B_0 = b^2 \beta'_0$	the second interaction par.	[dim-less]
$K_0 = \frac{B_0}{2f} = \frac{b^2 \beta'_0}{2f} = \frac{b^2 \sigma_B}{4\lambda_{rp} c_0} = \frac{b^2 g_B}{c_0}$	the gain coefficient	[dim-less]
$K(\omega) = \frac{B(\omega)}{2f} = K_0 \frac{\omega^2}{\omega^2 - \omega_0^2}$	the gain parameter	[dim-less]
$C'_0 = \frac{C'}{c'_0} = \frac{aC}{c_0} = aC_0$	the capacitance parameter	[dim-less]

TABLE 6. The CCTWT significant parameters. Abbreviations: dimensionless: dim-less, p/u: per unit, par.: parameter. For the sake of simplicity of the notation, we often omit “prime” super-index indicating that the dimensionless version of the relevant parameter is involved when it is clear from the context.

$$L' = \mathring{v}^2 L, \quad C' = C, \quad \beta' = \frac{\beta}{\mathring{v}^2}, \quad \sigma'_B = \frac{\sigma_B}{a^2}, \quad c'_0 = \frac{c_0}{a}, \quad l'_0 = \frac{\mathring{v}^2}{a} l_0, \quad (3.23)$$

$$C'_0 = \frac{C'}{c'_0} = \frac{aC}{c_0} = aC_0, \quad \beta'_0 = \frac{\beta'}{c'_0} = \frac{a\beta}{c_0 \mathring{v}^2}, \quad f'_B = af_B = \sqrt{\frac{4\pi\beta'}{\sigma'_B}} = \frac{a\omega_{rp}}{\mathring{v}} = \frac{2\pi\omega_{rp}}{\omega_a} = \frac{2\pi a}{\lambda_{rp}}. \quad (3.24)$$

Notice also that since $w = \chi v$

$$L'C' = \frac{\mathring{v}^2}{w^2} = \frac{1}{\chi^2}, \quad a\delta(z) = \delta(z'), \quad z = az'. \quad (3.25)$$

For the reader convenience we collected in Table 6 all significant parameters associated with CCTWT.

3.3. Euler-Lagrange equations in dimensionless variables. The component Lagrangians represented in dimensionless variables are as follows:

$$\mathcal{L}'_{\text{T}} = \frac{L'}{2} (\partial_{t'} Q)^2 - \frac{1}{2C'} (\partial_{z'} Q)^2, \quad \mathcal{L}'_{\text{B}} = \frac{1}{2\beta'} (\partial_{t'} q + \partial_{z'} q)^2 - \frac{2\pi}{\sigma'_{\text{B}}} q^2, \quad \ell \in \mathbb{Z}, \quad (3.26)$$

$$\mathcal{L}'_{\text{TB}} = -\frac{1}{2c'_0} \sum_{\ell=-\infty}^{\infty} \delta(z' - \ell) [Q(\ell) + bq(\ell)]^2, \quad (3.27)$$

The corresponding EL equations are

$$\partial_{t'}^2 Q - \frac{1}{\chi^2} \partial_{z'}^2 Q = 0, \quad (\partial_{t'} + \partial_{z'})^2 q + f_{\text{B}}'^2 q = 0, \quad z' \neq \ell; \quad f'_{\text{B}} = \sqrt{\frac{4\pi\beta'}{\sigma'_{\text{B}}}} = \frac{R_{\text{sc}}\omega_{\text{p}}}{\omega_a}, \quad (3.28)$$

$$[\partial_{z'} Q](\ell) = C'_0 \left[\left(\frac{\partial_{t'}^2}{\omega_0'^2} + 1 \right) Q(\ell) + bq(\ell) \right], \quad [\partial_{z'} q](\ell) = -b\beta'_0 [Q(\ell) + bq(\ell)], \quad \ell \in \mathbb{Z}. \quad (3.29)$$

To simplify notations, we will omit the prime symbol identifying the dimensionless variables in equations but rather simply will acknowledge their dimensionless form. Hence, we will use from now on the following dimensionless form of the EL equations (3.28) and (3.24):

$$\partial_t^2 Q - \frac{1}{\chi^2} \partial_z^2 Q = 0, \quad (\partial_t + \partial_z)^2 q + f^2 q = 0, \quad z \neq \ell, \quad \ell \in \mathbb{Z}; \quad f = \frac{R_{\text{sc}}\omega_{\text{p}}}{\omega_a}, \quad (3.30)$$

$$[\partial_z Q](\ell) = C_0 \left[\left(\frac{\partial_t^2}{\omega_0^2} + 1 \right) Q(\ell) + bq(\ell) \right], \quad [\partial_z q](\ell) = -b\beta_0 [Q(\ell) + bq(\ell)], \quad \ell \in \mathbb{Z}. \quad (3.31)$$

Equations (3.30), (3.31) are linear partial differential equations in time and space variables. Their analysis is simplified considerably if we recast them as equations in frequency and space variable. With that in mind we apply the Fourier transform in t (see Appendix A) to equations (3.30), (3.31) and obtain the following equations

$$\partial_z^2 \check{Q} + \frac{\omega^2}{\chi^2} \check{Q} = 0, \quad (\partial_z - i\omega)^2 \check{q} + f^2 \check{q} = 0, \quad z \neq \ell, \quad (3.32)$$

$$[\partial_z Q](\ell) = C_0 \left[\frac{\omega_0^2 - \omega^2}{\omega_0^2} Q(\ell) + bq(\ell) \right], \quad [\partial_z q](\ell) = -b\beta_0 [Q(\ell) + bq(\ell)], \quad \ell \in \mathbb{Z}, \quad (3.33)$$

where \check{Q} and \check{q} are the time Fourier transform of the corresponding quantities. Equations (3.32) and (3.33) are ODE equations in space variable z with frequency dependent coefficients.

To apply the constructions of the Floquet theory reviewed in Appendix F we recast system of equations (3.32), (3.33) yet another time into the following manifestly spatially periodic vector ODE:

$$\partial_z^2 x + A_1 \partial_z x + A_0 x + \sum_{\ell=-\infty}^{\infty} \delta(z - \ell) P_{\text{TB}} x = 0, \quad x = \begin{bmatrix} \check{Q} \\ \check{q} \end{bmatrix}, \quad (3.34)$$

where 2×2 matrices A_j and P_{TB} are defined by

$$A_1 = A_1(\omega) = \begin{bmatrix} 0 & 0 \\ 0 & -2i\omega \end{bmatrix}, \quad A_0 = A_0(\omega) = \begin{bmatrix} \frac{\omega^2}{\chi^2} & 0 \\ 0 & f^2 - \omega^2 \end{bmatrix}, \quad (3.35)$$

$$P_{\text{TB}} = P_{\text{TB}}(\omega) = \begin{bmatrix} C_0 \frac{\omega_0^2 - \omega^2}{\omega_0^2} & C_0 b \\ -b\beta_0 & -b^2\beta_0 \end{bmatrix}. \quad (3.36)$$

Equations (3.34)-(3.36) are evidently the second-order vector ODE with spatially periodic frequency dependent singular matrix potential $\sum_{\ell=-\infty}^{\infty} \delta(z - \ell) P_{\text{TB}}(\omega)$. These equations becomes is the object of our studies below.

According to Appendix E the second-order differential equation (3.34)-(3.36) is equivalent to the first-order spatially periodic differential equation of the form:

$$\partial_z X = A(z) X, \quad A(z) = A(z, \omega) = \begin{bmatrix} 0 & \mathbb{I} \\ -A_0 - P(z) & -A_1 \end{bmatrix}, \quad X = \begin{bmatrix} x \\ \partial_z x \end{bmatrix}, \quad (3.37)$$

$$P(z) = P(z, \omega) = \sum_{\ell=-\infty}^{\infty} \delta(z - \ell) P_{\text{TB}}(\omega),$$

where frequency dependent matrices A_0 , A_1 and P_{TB} satisfy equations (3.35) and (3.36).

Using results of Appendix G.2 we find that the spatially periodic vector ODE (3.37) is Hamiltonian with the following choice of nonsingular Hermitian matrix $G = G(\omega)$:

$$G = G^* = \begin{bmatrix} 0 & 0 & i & 0 \\ 0 & -\frac{2\omega C_0}{\beta_0} & 0 & -i\frac{C_0}{\beta_0} \\ -i & 0 & 0 & 0 \\ 0 & i\frac{C_0}{\beta_0} & 0 & 0 \end{bmatrix}, \quad \det \{G\} = \frac{C_0^2}{\beta_0^2}. \quad (3.38)$$

Indeed, it is an elementary exercise to verify that for each value of z matrix $A(z)$ is G -skew-Hermitian, that is

$$GA(z) + A^*(z)G = 0. \quad (3.39)$$

Then if $\Phi(z)$ is the matrizant of the Hamiltonian equation (3.37) then according to results of Appendix G $\Phi(z)$ is G -unitary matrix satisfying

$$\Phi^*(z)G\Phi(z) = G. \quad (3.40)$$

Consequently its spectrum $\sigma\{\Phi(z)\}$ is invariant with respect to the inversion transformation $\zeta \rightarrow \frac{1}{\zeta}$, that is it is symmetric with respect to the unit circle:

$$\zeta \in \sigma\{\Phi(z)\} \Rightarrow \frac{1}{\zeta} \in \sigma\{\Phi(z)\}. \quad (3.41)$$

3.4. CCTWT subsystems: the coupled cavity structure and the e-beam. It is instructive to take a view on the CCTWT system as a composition of its integral components which are the *coupled cavity structure (CCS)* and the *electron beam (e-beam)*. It comes at no surprise that special features of the CCS and the e-beam are manifested in fundamental properties of the CCTWT justifying their thorough analysis. This section provides the initial steps of the analysis whereas more detailed studies of the CCS features are pursued in Section 9.

One way to identify the CCS and the e-beam components of the CCTWT is to use its analysis carried out in previous sections setting there the coupling coefficient b to be zero. With that in mind we consider monodromy matrix matrix \mathcal{T} defined by equations (4.16)-(4.18) and set there $b = 0$. To separate variables relevant to the CCS and the e-beam we use permutation matrix P_{23} defined by equation (4.10) and transform $\mathcal{T}|_{b=0}$ as follows:

$$P_{23} \mathcal{T}|_{b=0} P_{23}^{-1} = \begin{bmatrix} \mathcal{T}_C & 0 \\ 0 & \mathcal{T}_B \end{bmatrix}, \quad (3.42)$$

where \mathcal{T}_C and \mathcal{T}_B are 2×2 matrices defined by

$$\mathcal{T}_C = \begin{bmatrix} \cos\left(\frac{\omega}{\chi}\right) & \frac{\chi}{\omega} \sin\left(\frac{\omega}{\chi}\right) \\ \left(1 - \frac{\omega^2}{\omega_0^2}\right) C_0 \cos\left(\frac{\omega}{\chi}\right) - \frac{\omega}{\chi} \sin\left(\frac{\omega}{\chi}\right) & \left(1 - \frac{\omega^2}{\omega_0^2}\right) \frac{C_0 \chi}{\omega} \sin\left(\frac{\omega}{\chi}\right) + \cos\left(\frac{\omega}{\chi}\right) \end{bmatrix}, \quad (3.43)$$

$$\mathcal{T}_B = e^{i\omega} \begin{bmatrix} \cos(f) - i \frac{\sin(f)}{f} \omega & \frac{\sin(f) e^{i\omega}}{f} \\ \frac{(\omega^2 - f^2) \sin(f)}{f} & \left(\cos(f) + i \frac{\sin(f)}{f} \omega \right) e^{i\omega} \end{bmatrix}. \quad (3.44)$$

Evidently \mathcal{T}_C defined by equation (3.43) is the CCS monodromy matrix and \mathcal{T}_B defined by equation (3.44) is the e-beam monodromy matrix.

It follows from equation (3.43) for matrix \mathcal{T}_C that the corresponding characteristic equation $\det \{ \mathcal{T}_C - s\mathbb{I} \} = 0$ for the Floquet multipliers s (see Appendix F) is

$$\det \{ \mathcal{T}_C - s\mathbb{I} \} = s^2 + 2W_C(\omega) s + 1 = 0, \quad s = \exp \{ ik \}, \quad (3.45)$$

$$W_C(\omega) = \frac{C_0}{2} \left(\frac{\omega}{\omega_0^2} - \frac{1}{\omega} \right) \chi \sin \left(\frac{\omega}{\chi} \right) - \cos(\omega).$$

Real-valued function $W_C(\omega)$ in the second equation in (3.45) plays an important role in the analysis of the CCS and its plot is depicted in Fig. 16(b). We refer to $W_C(\omega)$ as the *CCS instability parameter* for as we will find that it completely determines if the Floquet multipliers satisfy the instability criterion $|s| > 1$.

It also follows from equation (3.44) for matrix \mathcal{T}_B that the corresponding characteristic equation $\det \{ \mathcal{T}_B - s\mathbb{I} \} = 0$ for the Floquet multipliers s is

$$\det \{ \mathcal{T}_B - s\mathbb{I} \} = s^2 - 2 \cos(f) e^{i\omega} s + e^{2i\omega} = 0, \quad s = \exp \{ ik \}. \quad (3.46)$$

In view of equations (3.42), (3.45) and (3.46) the following factorization holds for the characteristic function of the monodromy matrix $\mathcal{T}|_{b=0}$ of the decoupled system

$$\det \{ \mathcal{T}|_{b=0} - s\mathbb{I} \} = (s^2 + 2W_C(\omega) s + 1) (s^2 - 2 \cos(f) e^{i\omega} s + e^{2i\omega}). \quad (3.47)$$

4. SOLUTIONS TO THE COUPLED-CAVITY TWT EQUATIONS

Dimensionless form of the EL equations (3.34)-(3.36) and their solutions can be analyzed by applying the Floquet theory reviewed in Appendix F. To use the Floquet theory we recast first the second-order vector ODE as the first-order vector ODE following to our review on subject in Appendix E.

4.1. Solutions to the Euler-Lagrange equation inside the period. We begin with introducing expressions for (i) the characteristic scalar polynomial $A_T(s)$ associated with the first equation in (3.32) for the TL; and (ii) the characteristic scalar polynomial $A_B(s)$ associated with the second equation in (3.32) for the e-beam:

$$A_T(s) = \frac{\omega^2}{\chi^2} + s^2, \quad A_B = s^2 - 2i\omega s + f^2 - \omega^2. \quad (4.1)$$

Note that in the accordance with the general theory of differential equations (see Appendices C, D and E) the spectral parameter s in expressions for the characteristic polynomials $A_T(s)$ and $A_B(s)$ represents symbolically the differential operator ∂_z .

The 2×2 companion matrix \mathcal{C}_T of the scalar characteristic polynomial $A_T(s)$ (see Appendices C, D and E) is

$$\mathcal{C}_T = \begin{bmatrix} 0 & 1 \\ -\frac{\omega^2}{\chi^2} & 0 \end{bmatrix} = \mathcal{Z}_T \begin{bmatrix} i\frac{\omega}{\chi} & 0 \\ 0 & -i\frac{\omega}{\chi} \end{bmatrix} \mathcal{Z}_T^{-1}, \quad \mathcal{Z}_T = \begin{bmatrix} -i\frac{\chi}{\omega} & i\frac{\chi}{\omega} \\ 1 & 1 \end{bmatrix}, \quad x = \begin{bmatrix} Q \\ \partial_z Q \end{bmatrix}, \quad (4.2)$$

where the columns of matrix \mathcal{Z}_T are eigenvectors of the companion matrix \mathcal{C}_T with the corresponding eigenvalues being the relevant entries of the diagonal matrix in equations (4.2). Expression

of vector x in equations (4.2) clarifies the meaning of the entries of relevant matrices. Consequently, the exponent $\exp\{z\mathcal{C}_T\}$ which is the fundamental matrix solution to the first-order ODE associated with first equation in (3.32) satisfies

$$\exp\{z\mathcal{C}_T\} = \begin{bmatrix} \cos\left(\frac{\omega z}{\chi}\right) & \frac{\chi}{\omega} \sin\left(\frac{\omega z}{\chi}\right) \\ -\frac{\omega}{\chi} \sin\left(\frac{\omega z}{\chi}\right) & \cos\left(\frac{\omega z}{\chi}\right) \end{bmatrix} = \mathcal{Z}_T \exp\left\{\begin{bmatrix} i\frac{\omega z}{\chi} & 0 \\ 0 & -i\frac{\omega z}{\chi} \end{bmatrix}\right\} \mathcal{Z}_T^{-1}. \quad (4.3)$$

The 2×2 companion matrix \mathcal{C}_B of the scalar characteristic polynomial $A_B(s)$

$$\mathcal{C}_B = \begin{bmatrix} 0 & 1 \\ \omega^2 - f^2 & 2i\omega \end{bmatrix} = \mathcal{Z}_B \begin{bmatrix} i(\omega - f) & 0 \\ 0 & i(\omega + f) \end{bmatrix} \mathcal{Z}_B^{-1}, \quad \mathcal{Z}_B = \begin{bmatrix} -\frac{i}{\omega - f} & -\frac{i}{\omega + f} \\ 1 & 1 \end{bmatrix}, \quad (4.4)$$

$$x = \begin{bmatrix} q \\ \partial_z q \end{bmatrix},$$

where the columns of matrix \mathcal{Z}_B are eigenvectors of the companion matrix \mathcal{C}_B with the corresponding eigenvalues being the relevant entries of the diagonal matrix in equations (4.4). Expression of vector x in equations (4.4) clarifies the meaning of the entries of relevant matrices. Consequently, the exponent $\exp\{z\mathcal{C}_B\}$ which is the fundamental matrix solution to the first-order ODE associated with the second equation in (3.32) satisfies

$$\begin{aligned} \exp\{z\mathcal{C}_B\} &= \frac{1}{f} \exp\{i\omega z\} \begin{bmatrix} f \cos(fz) - i\omega \sin(fz) & \sin(fz) \\ (\omega^2 - f^2) \sin(fz) & f \cos(fz) + i\omega \sin(fz) \end{bmatrix} = \\ &= \mathcal{Z}_B \exp\left\{\begin{bmatrix} i(\omega - f)z & 0 \\ 0 & i(\omega + f)z \end{bmatrix}\right\} \mathcal{Z}_B^{-1}. \end{aligned} \quad (4.5)$$

The 2×2 matrix characteristic polynomial $A_{TB}(s)$ of *non-interacting TL* and the e-beam is the following diagonal matrix polynomial

$$A_{TB}(s) = \begin{bmatrix} A_T(s) & 0 \\ 0 & A_B(s) \end{bmatrix} = \begin{bmatrix} \frac{\omega^2}{\chi^2} + s^2 & 0 \\ 0 & s^2 - 2i\omega s + f^2 - \omega^2 \end{bmatrix}. \quad (4.6)$$

The 4×4 companion matrix of the matrix polynomial $A_{TB}(s)$ 4×4 is (see Appendices C, D and E)

$$\mathcal{C}_{TB} = \begin{bmatrix} 0 & 0 & 1 & 0 \\ 0 & 0 & 0 & 1 \\ -\frac{\omega^2}{\chi^2} & 0 & 0 & 0 \\ 0 & \omega^2 - f^2 & 0 & 2i\omega \end{bmatrix}, \quad X = \begin{bmatrix} Q \\ q \\ \partial_z Q \\ \partial_z q \end{bmatrix}, \quad (4.7)$$

where vector X clarifies the meaning of the entries of matrix \mathcal{C}_{TB} .

The exponential $\exp\{z\mathcal{C}_{TB}\}$ of the component matrix \mathcal{C}_{TB} is the fundamental matrix solution to the first-order ODE associated with the system of equations (3.32) and it satisfies

$$\begin{aligned} \exp\{z\mathcal{C}_{TB}\} &= \\ &\begin{bmatrix} \cos\left(\frac{\omega z}{\chi}\right) & 0 & \frac{\chi}{\omega} \sin\left(\frac{\omega z}{\chi}\right) & 0 \\ 0 & e^{i\omega z} \left[\cos(fz) - i\frac{\omega}{f} \sin(fz) \right] & 0 & \frac{1}{f} e^{i\omega z} \sin(fz) \\ -\frac{\omega}{\chi} \sin\left(\frac{\omega z}{\chi}\right) & 0 & \cos\left(\frac{\omega z}{\chi}\right) & 0 \\ 0 & \frac{1}{f} e^{i\omega z} (\omega^2 - f^2) \sin(zf) & 0 & e^{i\omega z} \left[\cos(fz) - i\frac{\omega}{f} \sin(fz) \right] \end{bmatrix}. \end{aligned} \quad (4.8)$$

In particular for $z = 1$, which is the period in dimensionless variables, we get

$$\exp \{ \mathcal{C}_{\text{TB}} \} = \begin{bmatrix} \cos \left(\frac{\omega}{\chi} \right) & 0 & \frac{\chi}{\omega} \sin \left(\frac{\omega}{\chi} \right) & 0 \\ 0 & e^{i\omega} \left[\cos(f) - i \frac{\omega}{f} \sin(f) \right] & 0 & \frac{1}{f} e^{i\omega} \sin(f) \\ -\frac{\omega}{\chi} \sin \left(\frac{\omega}{\chi} \right) & 0 & \cos \left(\frac{\omega}{\chi} \right) & 0 \\ 0 & \frac{1}{f} e^{i\omega} (\omega^2 - f^2) \sin(f) & 0 & e^{i\omega} \left[\cos(f) - i \frac{\omega}{f} \sin(f) \right] \end{bmatrix} \quad (4.9)$$

Using 4×4 matrix P_{23} that permutes the second and the third coordinates, that is

$$P_{23} = \begin{bmatrix} 1 & 0 & 0 & 0 \\ 0 & 0 & 1 & 0 \\ 0 & 1 & 0 & 0 \\ 0 & 0 & 0 & 1 \end{bmatrix} = P_{23}^{-1}, \quad (4.10)$$

we get the following representation of $\exp \{ z \mathcal{C}_{\text{TB}} \}$ in terms of $\exp \{ z \mathcal{C}_{\text{T}} \}$ and $\exp \{ z \mathcal{C}_{\text{B}} \}$:

$$\exp \{ z \mathcal{C}_{\text{TB}} \} = P_{23} \begin{bmatrix} \exp \{ z \mathcal{C}_{\text{T}} \} & 0 \\ 0 & \exp \{ z \mathcal{C}_{\text{B}} \} \end{bmatrix} P_{23}^{-1}. \quad (4.11)$$

One can also verify the correctness of the identity (4.11) by tedious but straightforward evaluation.

4.2. The boundary conditions and the monodromy matrix in dimensionless variables.

The fundamental matrix solution $\exp \{ z \mathcal{C}_{\text{TB}} \}$ represented by equation (4.11) provides the solution of the relevant first-order vector ODE strictly inside the period $(0, 1)$. The complete solution on the interval $(0, 1]$ that includes the boundary 1 has to account for the boundary jump conditions represented by equations (3.31). These boundary conditions are equivalent to

$$X(\ell + 0) = S_{\text{b}} X(\ell - 0), \quad S_{\text{b}} = \begin{bmatrix} \mathbb{I} & 0 \\ P_{\text{TB}} & \mathbb{I} \end{bmatrix}, \quad X = \begin{bmatrix} x \\ \partial_z x \end{bmatrix}, \quad x = \begin{bmatrix} \check{Q} \\ \check{q} \end{bmatrix}, \quad (4.12)$$

where the *boundary matrix* S_{b} satisfies

$$S_{\text{b}} = \begin{bmatrix} \mathbb{I} & 0 \\ P_{\text{TB}} & \mathbb{I} \end{bmatrix} = \begin{bmatrix} 1 & 0 & 0 & 0 \\ 0 & 1 & 0 & 0 \\ \left(1 - \frac{\omega^2}{\omega_0^2}\right) C_0 & C_0 b & 1 & 0 \\ -b\beta_0 & -b^2\beta_0 & 0 & 1 \end{bmatrix}. \quad (4.13)$$

The Floquet theory (see Appendix F) when applied to the first-order ODE equivalent to the EL equations (3.34)-(3.36) yields the the following equations for the fundamental 4×4 matrix solution $\Phi(z)$:

$$\begin{aligned} \Phi(z) &= \exp \{ (z - \ell) \mathcal{C}_{\text{TB}} \} \Phi(\ell + 0), \quad \ell < z < \ell + 1, \\ \Phi(0 + 0) &= \mathbb{I}, \quad \Phi(\ell + 0) = S_{\text{b}} \Phi(\ell - 0), \quad \ell \in \mathbb{Z}, \end{aligned} \quad (4.14)$$

where $\exp \{ z \mathcal{C}_{\text{TB}} \}$ is defined by equation (4.8). In particular, according to the Floquet theorem 22 the monodromy matrix is $\mathcal{T} = \Phi(1 + 0)$ and in view of equations (4.13) and (4.14) we have

$$\mathcal{T} = \Phi(1 + 0) = S_{\text{b}} \exp \{ \mathcal{C}_{\text{TB}} \} = \begin{bmatrix} \mathcal{T}_{11} & \mathcal{T}_{12} \\ \mathcal{T}_{21} & \mathcal{T}_{22} \end{bmatrix}, \quad (4.15)$$

where $\exp \{\mathcal{C}_{\text{TB}}\}$ is defined by equation (4.9) and 2×2 matrix blocks of \mathcal{T} are as follows

$$\mathcal{T}_{11} = \begin{bmatrix} \cos\left(\frac{\omega}{\chi}\right) & 0 \\ 0 & \left(\cos(f) - i\frac{\sin(f)}{f}\omega\right)e^{i\omega} \end{bmatrix}, \quad \mathcal{T}_{12} = \begin{bmatrix} \frac{\chi}{\omega} \sin\left(\frac{\omega}{\chi}\right) & 0 \\ 0 & \frac{\sin(f)e^{i\omega}}{f} \end{bmatrix}, \quad (4.16)$$

$$\mathcal{T}_{21} = \begin{bmatrix} \left(1 - \frac{\omega^2}{\omega_0^2}\right) C_0 \cos\left(\frac{\omega}{\chi}\right) - \frac{\omega}{\chi} \sin\left(\frac{\omega}{\chi}\right) & C_0 b \left(\cos(f) - i\frac{\sin(f)}{f}\omega\right)e^{i\omega} \\ -\beta_0 b \cos\left(\frac{\omega}{\chi}\right) & \left[\beta_0 b^2 \left(i\frac{\sin(f)}{f}\omega - \cos(f)\right) + \frac{(\omega^2 - f^2)\sin(f)}{f}\right]e^{i\omega} \end{bmatrix}, \quad (4.17)$$

$$\mathcal{T}_{22} = \begin{bmatrix} \left(1 - \frac{\omega^2}{\omega_0^2}\right) \frac{C_0 \chi}{\omega} \sin\left(\frac{\omega}{\chi}\right) + \cos\left(\frac{\omega}{\chi}\right) & \frac{C_0 b \sin(f)e^{i\omega}}{f} \\ -\frac{\beta_0 b \chi}{\omega} \sin\left(\frac{\omega}{\chi}\right) & \left[\left(i\frac{\sin(f)}{f}\omega + \cos(f)\right) - \frac{\beta_0 b^2 \sin(f)}{f}\right]e^{i\omega} \end{bmatrix}, \quad (4.18)$$

and the involved above dimensionless constants satisfy (see Section 3.2)

$$\chi = \frac{w}{\dot{v}} = \frac{1}{\dot{v}\sqrt{CL}}, \quad C_0 = \frac{aC}{c_0}, \quad \beta_0 = \frac{a\beta}{c_0\dot{v}^2}, \quad f = \frac{aR_{\text{sc}}\omega_p}{\dot{v}} = \frac{R_{\text{sc}}\omega_p}{\omega_a}. \quad (4.19)$$

An important special and simpler case of the monodromy matrix \mathcal{T} defined by equations (4.16)-(4.18) is when the following equations hold

$$\chi = 1, \quad b = 1. \quad (4.20)$$

The condition $\chi = 1$ according to equations (3.21) is equivalent to the equality of the phase velocity w associated with TL and the e-beam stationary flow velocity \dot{v} . Equation $b = 1$ signifies the maximal coupling between the TL and e-beam at interaction points. In this case the monodromy matrix \mathcal{T} turns into

$$\mathcal{T}_1 = \begin{bmatrix} \mathcal{T}_{11} & \mathcal{T}_{12} \\ \mathcal{T}_{21} & \mathcal{T}_{22} \end{bmatrix}, \quad \chi = 1, \quad b = 1, \quad (4.21)$$

where

$$\mathcal{T}_{11} = \begin{bmatrix} \cos(\omega) & 0 \\ 0 & \left(\cos(f) - i\frac{\sin(f)}{f}\omega\right)e^{i\omega} \end{bmatrix}, \quad \mathcal{T}_{12} = \begin{bmatrix} \frac{\sin(\omega)}{\omega} & 0 \\ 0 & \frac{\sin(f)e^{i\omega}}{f} \end{bmatrix}, \quad (4.22)$$

$$\mathcal{T}_{21} = \begin{bmatrix} \left(1 - \frac{\omega^2}{\omega_0^2}\right) C_0 \cos(\omega) - \omega \sin(\omega) & C_0 \left(\cos(f) - i\frac{\sin(f)}{f}\omega\right)e^{i\omega} \\ -\beta_0 \cos(\omega) & \left[\beta_0 \left(i\frac{\sin(f)}{f}\omega - \cos(f)\right) + \frac{(\omega^2 - f^2)\sin(f)}{f}\right]e^{i\omega} \end{bmatrix}, \quad (4.23)$$

$$\mathcal{T}_{22} = \begin{bmatrix} \left(1 - \frac{\omega^2}{\omega_0^2}\right) \frac{C_0 \sin(\omega)}{\omega} + \cos(\omega) & \frac{C_0 \sin(f)e^{i\omega}}{f} \\ -\frac{\beta_0 \sin(\omega)}{\omega} & \left[\left(i\frac{\sin(f)}{f}\omega + \cos(f)\right) - \frac{\beta_0 \sin(f)}{f}\right]e^{i\omega} \end{bmatrix}, \quad (4.24)$$

where dimensionless constants C_0 , β_0 and f satisfy equations (4.19).

5. CHARACTERISTIC EQUATION, THE FLOQUET MULTIPLIERS AND THE DISPERSION RELATION

We turn now to the four *Floquet multipliers* s which are the eigenvalues of the CCTWT monodromy matrix \mathcal{T} defined by equations (4.15)-(4.18). Consequently, s are solutions to *characteristic equation* $\det \{\mathcal{T} - s\mathbb{I}\} = 0$ which is the following polynomial equation of the order 4:

$$S^4 + c_3 S^3 + c_2 S^2 + \bar{c}_3 S + 1 = 0, \quad s = \exp\{ik\}, \quad S = se^{-i\frac{\omega}{2}} = \exp\left\{i\left(k - \frac{\omega}{2}\right)\right\}, \quad (5.1)$$

where k is the wavenumber that can be real or complex-valued and coefficients c_3 and c_2 satisfy

$$c_3 = 2e^{\frac{i}{2}\omega} b_f^\infty + e^{-\frac{i}{2}\omega} \left[C_0 \frac{\chi}{\omega} \sin\left(\frac{\omega}{\chi}\right) \left(\frac{\omega^2}{\omega_0^2} - 1\right) - 2 \cos\left(\frac{\omega}{\chi}\right) \right], \quad (5.2)$$

$$c_2 = 2b_f^\infty \left[C_0 \frac{\chi}{\omega} \sin\left(\frac{\omega}{\chi}\right) \frac{\omega^2}{\omega_0^2} - 2 \cos\left(\frac{\omega}{\chi}\right) \right] + 2 \cos(f) C_0 \frac{\chi}{\omega} \sin\left(\frac{\omega}{\chi}\right) + 2 \cos(\omega), \quad (5.3)$$

where

$$b_f^\infty = K_0 \sin(f) - \cos(f), \quad K_0 = \frac{b^2 \beta_0}{2f} = \frac{b^2 g_B}{c_0}, \quad g_B = \frac{\sigma_B}{4\lambda_{rp}}. \quad (5.4)$$

Note that the quantity b_f^∞ in equation (5.4) arises also in the theory of the MCK reviewed in Section 8 (see equation 8.21). Note also that coefficient c_2 defined by equation (5.3) is manifestly real. The utility of representing the Floquet multipliers s in the form $s = S e^{i\frac{\omega}{2}}$ is explained by the fact that equation (5.1) for S possesses a manifest symmetry: if S is a solution to equation (5.1) then $\frac{1}{S}$ is its solution as well. The forth-order polynomials carrying this special symmetry are considered in Section 12.

It what follows to simplify analytical evaluations we make the following assumption.

Assumption 3. (*exact synchronism*) . To assure efficient cavity coupling we assume the so-called exact synchronism condition, that is $\chi = 1$ meaning that TL velocity w equals exactly to the e-beam stationary velocity \hat{v} , namely $w = \hat{v}$. It is also convenient to choose frequency units so that $\omega_0 = 1$. Combining these two conditions we assume

$$\chi = 1, \quad \omega_0 = 1. \quad (5.5)$$

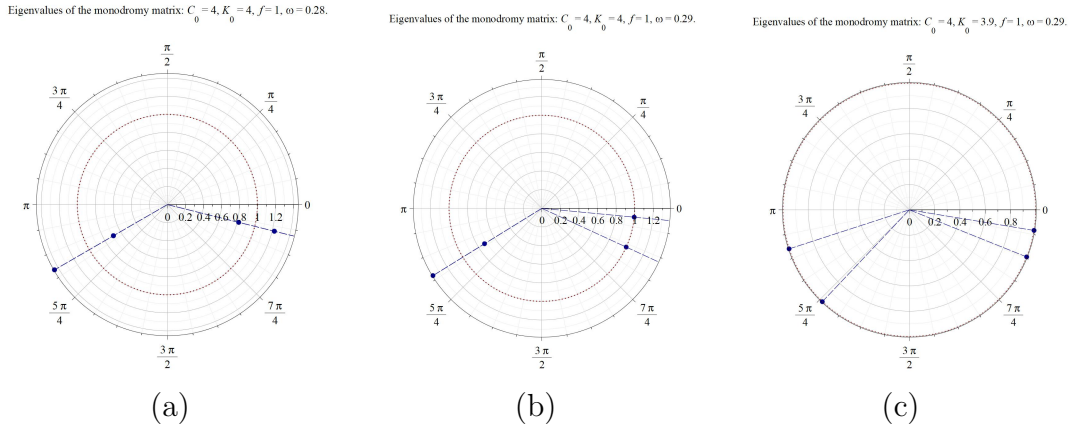


FIGURE 3. The plots of the four complex eigenvalues (the Floquet multipliers) $s = S e^{i\frac{\omega}{2}}$ that solve the characteristic equation (5.1) for the monodromy matrix \mathcal{T}_1 defined by equations (4.21)-(4.24) in case when $\chi = 1$, $\omega_0 = 1$, $f = 1$, and $C_0 = 4$: (a) $K_0 = 4$, $\omega = 0.28$; (b) $K_0 = 4$, $\omega = 0.29$; (c) $K_0 = 3.9$, $\omega = 0.29$. The horizontal and vertical axes represent respectively $\Re\{s\}$ and $\Im\{s\}$. The eigenvalues are shown by solid (blue) dots.

6. DISPERSION RELATIONS

The CCTWT evolution is governed by spatially periodic ODE (3.34)-(3.37) implying that the dispersion relations as the relations between frequency ω and wavenumber k is constructed based on the Floquet theory reviewed in Appendix F. Specifically in view of the relation $s = \exp\{ik\}$ between the Floquet multiplier s and the wave number k (see Section F and Remark 25) the characteristic

equation (5.1)- (5.4) can be viewed as an expression of the dispersion relations between the frequency ω and the wavenumber k and we will refer to it as the CCTWT dispersion relations or just the dispersion relations.

Under simplifying exact synchronism Assumption 3, that is $\chi = 1$ and $\omega_0 = 1$, the dispersion relations described by equations (5.1)-(5.4) turn into

$$S^4 + c_3 S^3 + c_2 S^2 + \bar{c}_3 S + 1 = 0, \quad s = \exp \{ik\}, \quad S = \exp \left\{ i \left(k - \frac{\omega}{2} \right) \right\}, \quad (6.1)$$

$$c_3 = 2e^{\frac{i}{2}\omega} b_f^\infty + e^{-\frac{i}{2}\omega} \left[C_0 \frac{\omega^2 - 1}{\omega} \sin(\omega) - 2 \cos(\omega) \right], \quad (6.2)$$

$$c_2 = 2b_f^\infty [C_0 \omega \sin(\omega) - 2 \cos(\omega)] + 2 \cos(f) C_0 \frac{\sin(\omega)}{\omega} + 2 \cos(\omega). \quad (6.3)$$

where

$$b_f^\infty = K_0 \sin(f) - \cos(f), \quad K_0 = \frac{b^2 \beta_0}{2f} = \frac{b^2 g_B}{c_0}, \quad g_B = \frac{\sigma_B}{4\lambda_{rp}}. \quad (6.4)$$

Yet another form of the dispersion relations (6.1), under the same exact synchronism assumption $\chi = 1$ and $\omega_0 = 1$, is its high-frequency form, namely

$$D(\omega, k) = D^{(0)}(\omega, k) + \frac{D^{(1)}(\omega, k)}{\omega} + \frac{D^{(2)}(\omega, k)}{\omega^2} = 0, \quad (6.5)$$

where

$$D^{(0)}(\omega, k) = C_0 \sin(\omega) (b_f^\infty + \cos(\omega - k)), \quad (6.6)$$

$$D^{(1)}(\omega, k) = 2(\cos(k) - \cos(\omega)) b_f^\infty + \cos(2k - \omega) - \cos(k - 2\omega) + \cos(\omega) - \cos(k), \quad (6.7)$$

$$D^{(2)}(\omega, k) = (\cos(f) - \cos(k - \omega)) \sin(\omega) C_0, \quad (6.8)$$

where b_f^∞ is defined by equations (6.4). We refer to function $D(\omega, k)$ in equation (6.5) as *the CCTWT dispersion function*.

There exists a remarkable in its simplicity relations between the CCTWT dispersion function $D(\omega, k)$ and the dispersion functions $D_C(\omega, k)$ and $D_K(\omega, k)$ for respectively the CCS and the MCK systems. These relations can be verified by tedious but elementary algebraic evaluations and they are subjects of the following theorem.

Theorem 2 (dispersion function factorization). *Let us assume that $\chi = \omega_0 = 1$. Let the CCTWT, the CCS and the MCK dispersion functions $D(\omega, k)$, $D_C(\omega, k)$ and $D_K(\omega, k)$ be defined by respectively equations (6.1), (9.17) and (8.36). Then the following identity hold:*

$$D(\omega, k) - D_C(\omega, k) D_K(\omega, k) = \frac{K_0}{\omega} \left[\frac{2(\cos(\omega) - \cos(k))}{\omega^2 - 1} - \frac{C_0 \sin(\omega) (1 - \sin(f))}{\omega} \right], \quad (6.9)$$

$$K_0 = \frac{b^2 \beta_0}{2f} = \frac{b^2 g_B}{c_0}, \quad g_B = \frac{\sigma_B}{4\lambda_{rp}}. \quad (6.10)$$

In the case of the high-frequency approximation the following identity holds:

$$D^{(0)}(\omega, k) = D_C^{(0)}(\omega, k) D_K^{(0)}(\omega, k) = C_0 \sin(\omega) (b_f^\infty + \cos(\omega - k)). \quad (6.11)$$

The dispersion function identities (6.9) and (6.11) signify a very particular way the CCS and the MCK subsystems are coupled and integrated into the CCTWT system. The right-hand side of the identity (6.9) can be naturally viewed as a measure of coupling between the CCS and the MCK subsystems

Remark 3 (graphical confirmation of the dispersion factorization). The statements of the Theorem 2 are well illustrated by Figs. 4(f), 5(f), 6(f) and 7 when compared with Figure 16 for the CCS and Figure 15 for the MCK. One can confidently identify in the CCTWT dispersion-instability graphs the patterns of the dispersion-instability graphs of its integral components - the CCS and the MCK.

Let us consider now the conventional dispersion relation assuming that k and ω must be real numbers. Then dividing equation (6.1) by S^2 and carrying elementary transformations we arrive at the following trigonometric form of the conventional dispersion relation:

$$\begin{aligned} \cos(2k - \omega) + |c_3| \cos\left(k - \frac{\omega}{2} + \alpha\right) &= -\frac{c_2}{2}, \\ c_3 &= |c_3| \exp\{i\alpha\}, \quad S = \exp\left\{i\left(k - \frac{\omega}{2}\right)\right\}, \quad k, \omega \in \mathbb{R}, \end{aligned} \quad (6.12)$$

where $c_3 = c_3(\omega)$, $c_2 = c_2(\omega)$ and $\alpha = \arg\{c_3(\omega)\}$ are frequency dependent parameters satisfying equations (6.2)-(6.4).

6.1. Graphical representation of the dispersion relations. As to the graphical representation of the dispersion relation recall that the conventional dispersion relations are defined as the relations between real-valued frequency ω and real-valued wavenumber k associated with the relevant eigenmodes. In the case of interest k can be complex-valued and to represent all system modes geometrically we follow to [FigTWTbk, 7]. First, we parametrize every mode of the system uniquely by the pair $(k(\omega), \omega)$ where ω is its frequency and $k(\omega)$ is its wavenumber. If $k(\omega)$ is degenerate, it is counted a number of times according to its multiplicity. In view of the importance to us of the mode instability, that is, when $\Im\{k(\omega)\} \neq 0$, we partition all the system modes represented by pairs $(k(\omega), \omega)$ into two distinct classes – oscillatory modes and unstable ones – based on whether the wavenumber $k(\omega)$ is real- or complex-valued with $\Im\{k(\omega)\} \neq 0$. We refer to a mode (eigenmode) of the system as an *oscillatory mode* if its wavenumber $k(\omega)$ is real-valued. We associate with such an oscillatory mode point $(k(\omega), \omega)$ in the $k\omega$ -plane with k being the horizontal axis and ω being the vertical one. Similarly, we refer to a mode (eigenmode) of the system as a (*convective*) *unstable mode* if its wavenumber k is complex-valued with a nonzero imaginary part, that is, $\Im\{k(\omega)\} \neq 0$. We associate with such an unstable mode point $(\Re\{k(\omega)\}, \omega)$ in the $k\omega$ -plane. Since we consider here only *convective unstable modes*, we refer to them shortly as *unstable modes*. Notice that every point $(\Re\{k(\omega)\}, \omega)$ is in fact associated with two complex conjugate system modes with $\pm\Im\{k(\omega)\}$.

Based on the above discussion, we represent the set of all oscillatory and unstable modes of the system geometrically by the set of the corresponding modal points $(k(\omega), \omega)$ and $(\Re\{k(\omega)\}, \omega)$ in the $k\omega$ -plane. We name this set the *dispersion-instability graph*. To distinguish graphically points $(k(\omega), \omega)$ associated oscillatory modes when $k(\omega)$ is real-valued from points $(\Re\{k(\omega)\}, \omega)$ associated unstable modes when $k(\omega)$ is complex-valued with $\Im\{k(\omega)\} \neq 0$ we show points $\Im\{k(\omega)\} = 0$ in blue color whereas points with $\Im\{k(\omega)\} \neq 0$ are shown in brown color. We remind once again that every point $(\omega, \Re\{k(\omega)\})$ with $\Im\{k(\omega)\} \neq 0$ represents exactly two complex conjugate unstable modes associated with $\pm\Im\{k(\omega)\}$.

When $\Im\{k_{\pm}(\omega)\} \neq 0$ and $\Re\{k_+(\omega)\} = \Re\{k_-(\omega)\}$ and consequently the corresponding branches overlap with each point on the segments representing two modes with complex-conjugate wave numbers k_{\pm} . These branches represent exponentially growing or decaying in the space modes and shown in plot (c) in brown color.

We generated three sets of dispersion-instability graphs for the CCTWT shown in Figs. 4, 5 and 6 to demonstrate their dependence on the gain coefficient K_0 , the capacitance parameter C_0 and the normalized period f as they vary in indicated ranges. Figs. 4(f), 5(f), 6(f) and 7

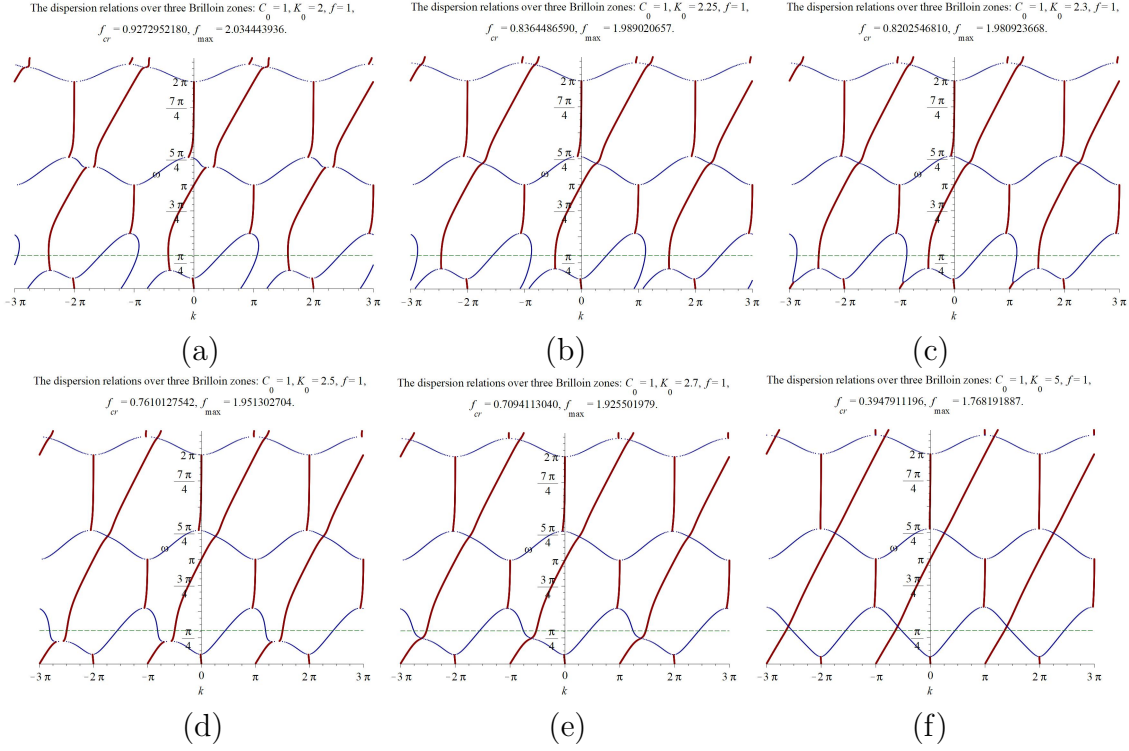


FIGURE 4. The dispersion-instability graphs for the CCTWT as the gain coefficient K_0 varies. In all plots the horizontal and vertical axes represent respectively $\Re\{k\}$ and ω . Each of the plots shows 3 bands of the dispersion of the CCTWT described by equations (5.1)-(5.4) over 3 Brillouin zones $\Re\{k\} \in [-3\pi, 3\pi]$ for $\chi = 1$, $\omega_0 = 1$, $f = 1$, and $C_0 = 1$: (a) $K_0 = 2$, $f_{cr} \cong 0.927292180$ and $f_{max} \cong 2.034$; (b) $K_0 = 2.25$, $f_{cr} \cong 0.837$ and $f_{max} \cong 1.99$; (c) $K_0 = 2.3$, $f_{cr} \cong 0.820$ and $f_{max} \cong 1.981$; (d) $K_0 = 2.5$, $f_{cr} \cong 0.761$ and $f_{max} \cong 1.951$; (e) $K_0 = 2.7$, $f_{cr} \cong 0.709$ and $f_{max} \cong 1.926$; (f) $K_0 = 5$, $f_{cr} \cong 0.395$ and $f_{max} \cong 1.768$ (see Theorem 2). When $\Im\{k_{\pm}(\omega)\} = 0$, that is the case of oscillatory modes, and $\Re\{k(\omega)\} = k(\omega)$ the corresponding branches are shown as solid (blue) curves. When $\Im\{k_{\pm}(\omega)\} \neq 0$, that is there is an instability, and $\Re\{k_+(\omega)\} = \Re\{k_-(\omega)\}$ then the corresponding branches overlap, they are shown as bold solid curves in brown color, and each point of these branches represents exactly two modes with complex-conjugate wave numbers k_{\pm} .

when compared with Figure 16 for the CCS and Figure 15 for the MCK clearly indicate that the CCTWT dispersion-instability graph is composed of the dispersion-instability graphs of its integral components - the CCS and the MCK. The later is important since the CCS and the MCK are significantly simpler systems compare to the original CCTWT.

6.2. Exceptional points of degeneracy. Jordan eigenvector degeneracy, which is a degeneracy of the system evolution matrix when not only some eigenvalues coincide but the corresponding eigenvectors coincide also, is sometimes referred to as exceptional point of degeneracy (EPD), [Kato, II.1]. Our prior studies of traveling wave tubes (TWT) in [FigTWTbk, 4, 7, 13, 14, 54, 55] demonstrate that TWTs always have EPDs. A particularly important class of applications of EPDs is sensing, [CheN], [KNAC], [OGC], [Wie], [Wie1]. For applications of EPDs for traveling wave tubes see [FigtwTEPD], [OTC], [OVFC], [OVFC1], [VOFC].

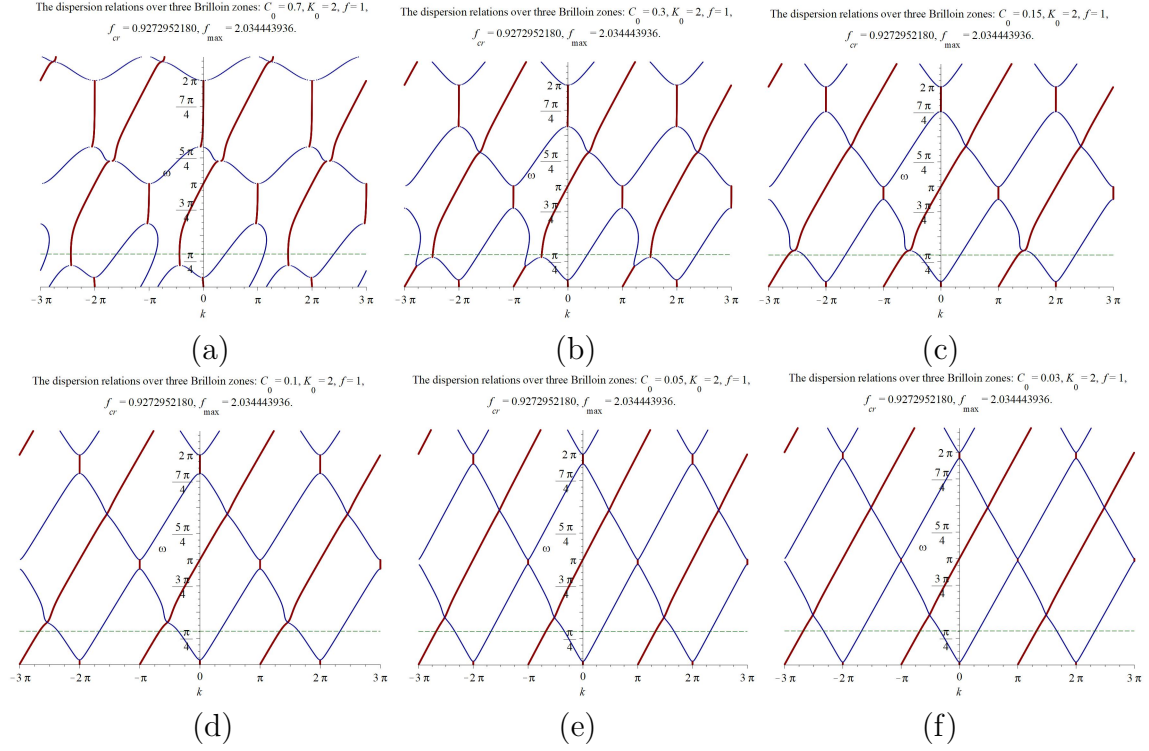


FIGURE 5. The dispersion-instability graphs for the CCTWT as the capacitance parameter C_0 varies. In all plots the horizontal and vertical axes represent respectively $\Re\{k\}$ and ω . Each of the plots shows 3 bands of the dispersion of the CCTWT described by equations (5.1)-(5.4) over 3 Brillouin zones $\Re\{k\} \in [-3\pi, 3\pi]$ for $\chi = 1$, $\omega_0 = 1$, $f = 1$, and $K_0 = 2$, $f_{cr} \cong 0.927292180$ and $f_{max} \cong 2.034$: (a) $C_0 = 0.7$; (b) $C_0 = 0.3$; (c) $C_0 = 0.15$; (d) $C_0 = 0.1$; (e) $C_0 = 0.05$; (f) $C_0 = 0.03$ (see Theorem 2). When $\Im\{k_{\pm}(\omega)\} = 0$, that is the case of oscillatory modes, and $\Re\{k(\omega)\} = k(\omega)$ the corresponding branches are shown as solid (blue) curves. When $\Im\{k_{\pm}(\omega)\} \neq 0$, that is there is an instability, and $\Re\{k_+(\omega)\} = \Re\{k_-(\omega)\}$ then the corresponding branches overlap, they are shown as bold solid (brown) curves in brown color, and each point of these branches represents exactly two modes with complex-conjugate wave numbers k_{\pm} .

Applying the results of Appendix 12 particularly the system of equations (12.4) we obtain the following trigonometric form of equations for *exceptional points of degeneracy (EPDs)*:

$$\cos(2k - \omega) + |c_3| \cos\left(k - \frac{\omega}{2} + \alpha\right) = -\frac{c_2}{2}, \quad 2\sin(2k - \omega) + |c_3| \sin\left(k - \frac{\omega}{2} + \alpha\right) = 0, \quad (6.13)$$

$$c_3 = |c_3| \exp\{i\alpha\} \quad S = \exp\left\{i\left(k - \frac{\omega}{2}\right)\right\}, \quad k, \omega \in \mathbb{R}.$$

Note that the first equation in (6.13) is identical to the trigonometric form (6.12) of the CCTWT dispersion relations.

Figure 8 shows examples of the dispersion-instability graphs with EPDs as points which are the points of the transition to instability. In particular, Figure 8(c) when compared with Figure 16 for the CCS and Figure 15 for the MCK indicates convincingly that the components of the CCTWT dispersion-instability graph can be attributed to the dispersion-instability graphs of its integral components - the CCS and the MCK (see Theorem 2 and Remark 3).

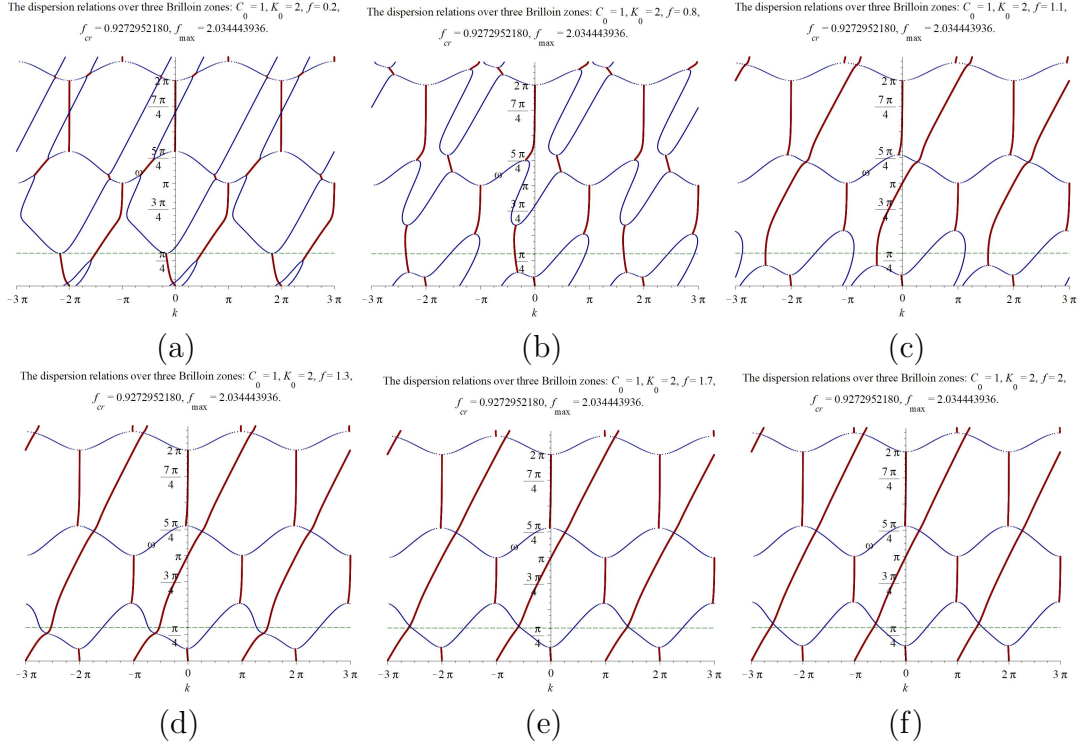


FIGURE 6. The dispersion-instability graphs for the CCTWT as the normalized period f varies. In all plots the horizontal and vertical axes represent respectively $\Re\{k\}$ and ω . Each of the plots shows 3 bands of the dispersion of the CCTWT described by equations (5.1)-(5.4) over 3 Brillouin zones $\Re\{k\} \in [-3\pi, 3\pi]$ for $\chi = 1$, $\omega_0 = 1$, $C_0 = 1$, $K_0 = 2$, $f_{cr} \cong 0.927292180$ and $f_{max} \cong 2.034443936$: (a) $f = 0.2$; (b) $f = 0.8$; (c) $f = 1.1$; (d) $f = 1.3$; (e) $f = 1.7$; (f) $f = 2$ (see Theorem 2). When $\Im\{k_{\pm}(\omega)\} = 0$, that is the case of oscillatory modes, and $\Re\{k(\omega)\} = k(\omega)$ the corresponding branches are shown as solid (blue) curves. When $\Im\{k_{\pm}(\omega)\} \neq 0$, that is there is an instability, and $\Re\{k_+(\omega)\} = \Re\{k_-(\omega)\}$ then the corresponding branches overlap, they are shown as bold solid (brown) curves in brown color, and each point of these branches represents exactly two modes with complex-conjugate wave numbers k_{\pm} .

7. GAIN EXPRESSION IN TERMS OF THE FLOQUET MULTIPLIERS

Based on the prior analysis we introduce the CCTWT gain G in dB per one period as the rate of the exponential growth of the CCTWT eigenmodes associated with the Floquet multipliers s which are the solutions to the characteristic equations (5.1)-(5.4), namely

$$G = G(f, \omega, K_0) = 20 |\log(|s(f, \omega, K_0)|)|. \quad (7.1)$$

Consequently, to analyze the gain expression (7.1) we have to turn to the indicated characteristic equations.

It turns out that the gain expression (7.1) can be significantly simplified under exact synchronism Assumption 3, that is $\chi = 1$ and $\omega_0 = 1$. Under these conditions the CCTWT characteristic equations (5.1)-(5.4) can be recast into the following form:

$$P = P(f, \omega, K_0) = s^4 + p_3 s^3 + p_2 s^2 + p_1 s + 1 = 0, \quad (7.2)$$

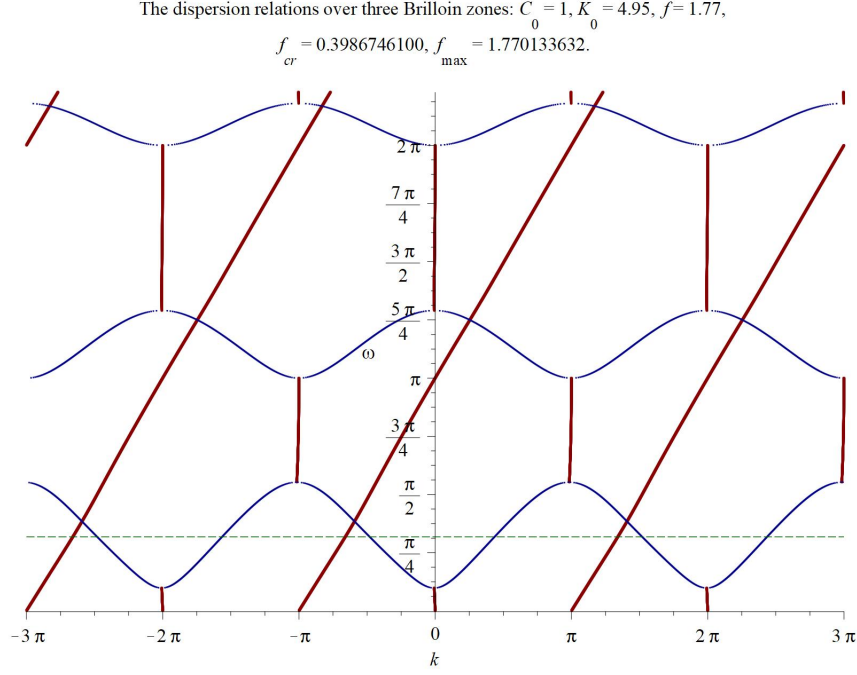


FIGURE 7. The dispersion-instability graphs for the CCTWT as the normalized period f varies (see Theorem 2 and Remark 3). The horizontal and vertical axes represent respectively $\Re\{k\}$ and ω . The plot shows 3 bands of the dispersion of the CCTWT described by equations (5.1)-(5.4) over 3 Brillouin zones $\Re\{k\} \in [-3\pi, 3\pi]$ for $\chi = 1, \omega_0 = 1, C_0 = 1, f \cong 1.77, K_0 = K_{0T} = 4.95$ (typical value) and consequently $f_{cr} \cong 0.397, f_{max} \cong 1.770$. When $\Im\{k_{\pm}(\omega)\} = 0$, that is the case of oscillatory modes, and $\Re\{k(\omega)\} = k(\omega)$ the corresponding branches are shown as solid (blue) curves. When $\Im\{k_{\pm}(\omega)\} \neq 0$, that is there is an instability, and $\Re\{k_+(\omega)\} = \Re\{k_-(\omega)\}$ then the corresponding branches overlap, they are shown as bold solid (brown) curves in brown color, and each point of these branches represents exactly two modes with complex-conjugate wave numbers k_{\pm} . (see Theorem 2 and Remark 3)

where the coefficients of the *CCTWT characteristic polynomial* P have the following expressions:

$$p_3 = 2e^{i\omega}b_f^{\infty} + C_0\frac{\omega^2 - 1}{\omega}\sin(\omega) - 2\cos(\omega), \quad (7.3)$$

$$p_2 = e^{i\omega} \left\{ 2b_f^{\infty} [C_0\omega\sin(\omega) - 2\cos(\omega)] + 2\cos(f)C_0\frac{\sin(\omega)}{\omega} + 2\cos(\omega) \right\}, \quad (7.4)$$

$$p_1 = e^{2i\omega} \left[C_0\frac{\omega^2 - 1}{\omega}\sin(\omega) - 2\cos(\omega) \right] + 2e^{i\omega}b_f^{\infty} = e^{2i\omega}\bar{p}_3, \quad (7.5)$$

where

$$b_f^{\infty} = K_0\sin(f) - \cos(f), \quad K_0 = \frac{b^2\beta_0}{2f} = \frac{b^2g_B}{c_0}, \quad g_B = \frac{\sigma_B}{4\lambda_{rp}}. \quad (7.6)$$

According to equations (9.13) the CCS characteristic polynomial P_C has the following expression:

$$P_C(\omega, s) = s^2 + \left[C_0 \left(\omega - \frac{1}{\omega} \right) \sin(\omega) - 2\cos(\omega) \right] s + 1 = 0. \quad (7.7)$$

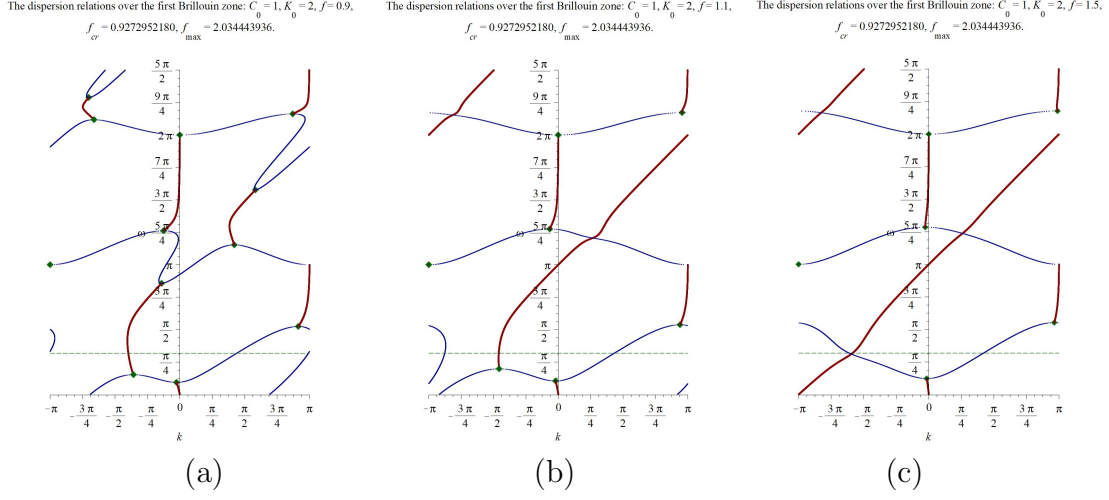


FIGURE 8. The dispersion-instability graphs for the CCTWT showing the degeneracy (transition to instability) points as diamond (green) dots for $C_0 = 1$, $K_0 = 2$ and consequently $f_{\text{cr}} \cong 0.927$, $f_{\text{max}} \cong 1.770$: (a) $f = 0.9 < f_{\text{cr}}$; (b) $f = 1.1 > f_{\text{cr}}$; (c) $f = 1.5 > f_{\text{cr}}$ (see Theorem 2 and Remark 3). In all plots the horizontal and vertical axes represent respectively $\Re\{k\}$ and ω . Solid (green) diamond dots identify points of the transition from the instability to the stability which are also EPD points

The MCK characteristic equation (8.26) can be recast as follows:

$$P_K(\omega, s) = s^2 + 2e^{i\omega} \left(\frac{2K_0 \sin(f) \omega^2}{\omega^2 - 1} - \cos(f) \right) s + e^{2i\omega} = 0, \quad (7.8)$$

and we refer to P_K as the *MCK characteristic polynomial*.

Using the definitions (7.2)-(7.2), (7.7) and (7.8) for respectively the characteristic polynomials $P(f, \omega, K_0)$, $P_C(\omega, s)$ and $P_K(\omega, s)$ one can identify their leading terms $P^{(0)}$, $P_C^{(0)}(\omega, s)$ and $P_K^{(0)}$ as $\omega \rightarrow \infty$ which are:

$$P^{(0)}(\omega, s) = C_0 \sin(\omega) s (s^2 + 2b_f^\infty e^{i\omega} s + e^{2i\omega}), \quad (7.9)$$

$$P_C^{(0)}(\omega, s) = C_0 \sin(\omega) s, \quad P_K^{(0)}(\omega, s) = s^2 + 2b_f^\infty e^{i\omega} s + e^{2i\omega}, \quad (7.10)$$

where b_f^∞ is defined by equations (7.6).

Just as in the case of the dispersion relations that we analyzed in Section 6 there are simple relations between the CCTWT characteristic function $P(\omega, s)$ and the characteristic polynomials $P_C(\omega, s)$ and $P_K(\omega, s)$ for respectively the CCS and MCK systems. These relations can be verified by tedious but elementary algebraic evaluations and they are subjects of the following theorem that relates the characteristic polynomials for CCTTX, CCS and MCK systems.

Theorem 4 (characteristic polynomial factorization). *Let us assume that $\chi = \omega_0 = 1$. Let the CCTWT, the CCS and the MCK dispersion functions $P(\omega, s)$, $P_C(\omega, s)$ and $P_K(\omega, s)$ be defined by respectively equations (7.2)-(7.2), (7.7) and (7.8). Then the following identity hold:*

$$P(\omega, s) - P_C(\omega, s) P_K(\omega, s) = -\frac{2K_0 \sin(f) e^{i\omega} s (s^2 - 2 \cos(\omega) s + 1)}{\omega (\omega^2 - 1)}, \quad (7.11)$$

$$K_0 = \frac{b^2 \beta_0}{2f} = \frac{b^2 g_B}{c_0}, \quad g_B = \frac{\sigma_B}{4\lambda_{\text{rp}}}. \quad (7.12)$$

In the case of the high-frequency approximation the following identity holds:

$$P^{(0)}(\omega, s) = P_C^{(0)}(\omega, s) P_K^{(0)}(\omega, s) = C_0 \sin(\omega) s (s^2 + 2b_f^\infty e^{i\omega} s + e^{2i\omega}). \quad (7.13)$$

The identities (7.11) and (7.13) represent a particular way the CCS and the MCK subsystems are coupled and integrated into the CCTWT system. The right-hand side of the identity (7.11) can be naturally viewed as a measure of coupling between the CCS and the MCK subsystems

Remark 5 (graphical confirmation of the characteristic polynomial factorization). The statements of the Theorem 4 are well illustrated by Figures 9 and 10 when compared with Figure 17 for the CCS and Figure 12 for the MCK. One can confidently recognize in components of the graph of the gain CCTWT the patents of the graphs for the gain of the CCS and the MCK.

Let us consider now the convent

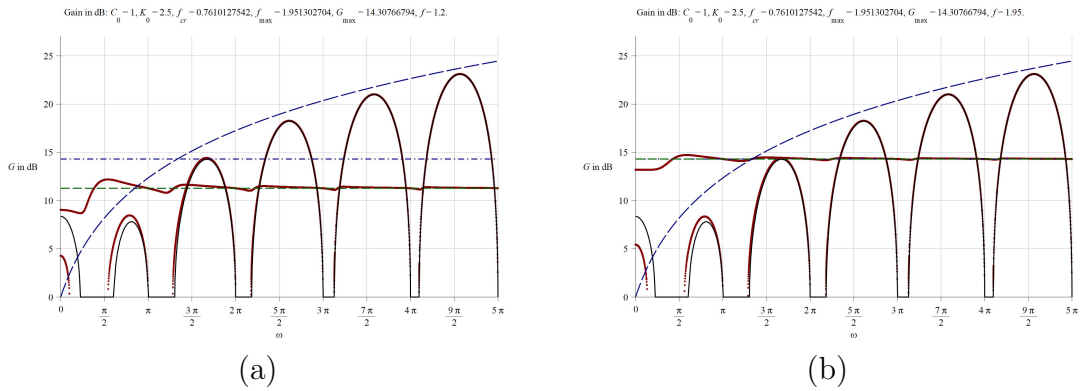


FIGURE 9. Plots of gain G per one period in dB as a function of frequency ω defined by equations (7.1) for $\omega_0 = 1$, $K_0 = 2.5$ and consequently $f_{\text{cr}} \cong 0.7610127542$, $f_{\text{max}} \cong 1.951302704$, $G_{\text{max}} = 14.30766794$ (see Section 8.2 for the definition of the MCK quantities f_{cr} , f_{max} and G_{max}) and: (a) $f = 1.2 > f_{\text{cr}}$; (b) $f = 1.95 \approx f_{\text{max}}$. In all plots the horizontal and vertical axes represent respectively frequency ω and gain G in dB. The solid (brown) curves represent gain G as a function of frequency ω ; the dashed horizontal (blue) line $G = G_{\text{max}}$ represents the maximal G_{max} value of G in the high frequency limit (see Section 8.2); the dashed horizontal (green) line represents the value of G in the high frequency limit for given value of f (see Section 8.2). The envelope of the local maxima of the gain for large values of frequency ω behaves as $20 |\log(C_0 \omega)|$ (see captions to Fig. 17) and it is shown as dashed (blue) curve.

Remark 6 (amplification in stopbands). E-beam interactions in periodic slow-wave structures were studied by V. Solntsev in [Solnt]. Under the condition of exact synchronism as in our Assumption 3 the amplification was observed in *stopbands*, known also as spectral gaps in the system (oscillatory) spectrum. Our theory accounts for this general spectral phenomenon too as indicated by growing in magnitude “bumps” in Figures 9 and 10. One can also see similar bumps in Figure 17 for the CCS.

It is instructive to relate and compare the frequency dependent gain G per one period in dB for CCTWT defined by equations (7.1), (5.1)-(5.4) with its expressions by equation (8.19) for MCK gain in Section 8.2 and equations (9.24) for CCS gain $G_C = G_C(\omega, C_0)$.

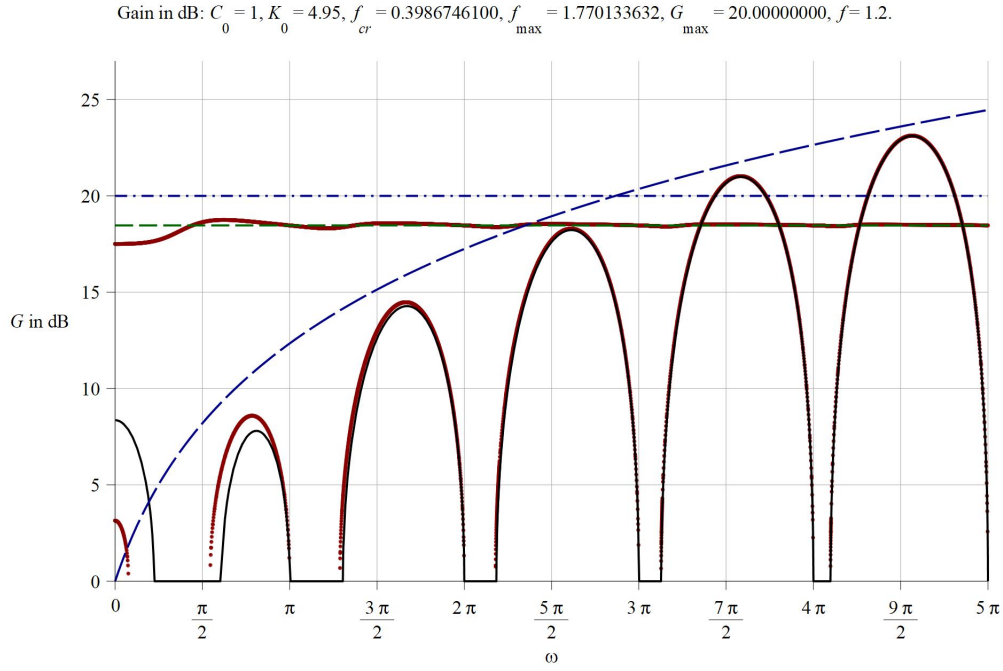


FIGURE 10. Plot of gain G per one period in dB as a function of frequency ω defined by equations (9.24) for $\omega_0 = 1$, $K_0 = K_{0T} = 4.95$ and consequently $f_{cr} \cong 0.3986746100$, $f_{max} \cong 1.770133632$, $G_{max} = 20$ (see Section 8.2 for the definition of the MCK quantities f_{cr} , f_{max} and G_{max}) and $f = 1.2 > f_{cr}$. The horizontal and vertical axes represent respectively frequency ω and gain G in dB. The solid (brown) curves represent gain G as a function of frequency ω ; the dashed horizontal (blue) line $G = G_{max}$ represents the maximal G_{max} value of G in the high frequency limit (see Section 8.2); the dashed horizontal (green) line represents the value of G in the high frequency limit for $f = f_{cr}$ (see Section 8.2). The envelope of the local maxima of the gain for large values of frequency ω behaves as $20 |\log(C_0 \omega)|$ (see captions to Fig. 17) and it is shown as dashed (blue) curve.

8. SKETCH OF THE MULTICAVITY KLYSTRON ANALYTICAL MODEL

Usage of cavity resonators in the klystron was a revolutionary idea of Hansen and the Varians, [Tsim, 7.1]. In the pursuit of higher power and efficiency the original design of Vairan klystrons evolve significantly over years featuring today multiple cavities and multiple electron beam, [Tsim, 7.7]. The advantages of klystrons are their high power and efficiency, potentially wide bandwidth, phase and amplitude stability, [BenSweScha, 9.1].

The construction of an analytic model for the multicavity klystron (MCK) in [FigKly] utilizes elements of the analytic model of the traveling wave tube (TWT) introduced and studied in our monograph [FigTWTbk, 4, 24], see Section 2. Multicavity klystron, known also as cascade amplifier, [Werne, IIb], is composed of the e-beam interacting with a periodic array of electromagnetic cavities, see Fig. 11. Consequently the MCK can be naturally viewed as a subsystem of the CCTWT that contributes to the properties of CCTWT.

8.1. The Euler-Lagrange equations in dimensionless variables. As to basic variables related to the e-beam and the klystron cavities we refer the reader to Sections 2, Section 3.2 and

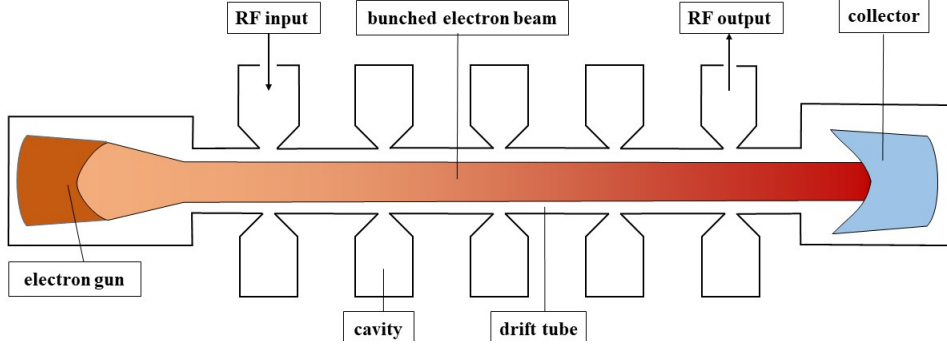


FIGURE 11. A schematic representation of a multicavity klystron (MCK) that exploits constructive interaction between the pencil-like electron beam and an array of electromagnetic cavities (often of toroidal shape). The interaction causes the electron bunching and consequent amplification of the RF signal.

Tables 2, 3Table 6 . The dimensionless form of the \mathcal{L}' of the Lagrangians is as follows:

$$\mathcal{L}' = \mathcal{L}'_B + \mathcal{L}'_{CB}; \quad \mathcal{L}'_B = \frac{1}{2\beta'} (\partial_{t'} q + \partial_{z'} q)^2 - \frac{2\pi}{\sigma'_B} q^2, \quad \ell \in \mathbb{Z}, \quad (8.1)$$

$$\mathcal{L}'_{CB} = \sum_{\ell=-\infty}^{\infty} \delta(z' - \ell) \left\{ \frac{l'_0}{2} (\partial_t Q(al))^2 - \frac{1}{2c'_0} [Q(al) + bq(al)]^2 \right\}. \quad (8.2)$$

Just as we did before to simplify notations we will omit prime symbol in equations but rather will simply acknowledge their dimensionless form. The dimensionless form of the EL equations for the MCK is

$$(\partial_t + \partial_z)^2 q + f^2 q = 0, \quad z \neq \ell, \quad \ell \in \mathbb{Z}; \quad f = \frac{2\pi R_{sc} \omega_p}{\omega_a} = \frac{2\pi a}{\lambda_{rp}}, \quad (8.3)$$

$$\begin{aligned} \partial_t^2 Q(al) + \omega_0^2 [Q(al) + bq(al)] &= 0, \quad \omega_0 = \frac{1}{\sqrt{l_0 c_0}}, \quad \beta_0 = \frac{\beta}{c_0}, \\ [\partial_z q](al) &= -b\beta_0 [Q(al) + bq(al)], \quad \ell \in \mathbb{Z}. \end{aligned} \quad (8.4)$$

Note that term $-\frac{2\pi}{\sigma'_B} q^2$ in the Lagrangian \mathcal{L}'_B defined in equations (8.1) represents space-charge effects including the so-called debunching (electron-to-electron repulsion).

The Fourier transform in t (see Appendix A) of equations (8.3), (8.4) is

$$(\partial_z - i\omega)^2 \tilde{q} + f^2 \tilde{q} = 0, \quad z \neq \ell, \quad (8.5)$$

subjects to the boundary conditions at the interaction points

$$[\tilde{q}](al) = 0, \quad [\partial_z \tilde{q}](al) = -B(\omega) \tilde{q}(al) \quad \ell \in \mathbb{Z}, \quad (8.6)$$

where \tilde{q} is the time Fourier transform of q and $B(\omega)$ is an important parameter defined by

$$B = B(\omega) = \frac{b^2 \beta_0 \omega^2}{\omega^2 - \omega_0^2} = B_0 \frac{\omega^2}{\omega^2 - \omega_0^2}, \quad B_0 = b^2 \beta_0 = \frac{b^2 \beta}{c_0}, \quad (8.7)$$

we refer to it as *cavity e-beam interaction parameter*. The Fourier transform in time of equation (8.4) yields

$$\check{Q}(a\ell) = \frac{\omega_0^2}{\omega^2 - \omega_0^2} b\check{q}(a\ell), \quad \ell \in \mathbb{Z}, \quad (8.8)$$

where \check{Q} is the time Fourier transform of Q , and equation (8.8) was used to obtain the second equation in (8.6).

Boundary conditions (8.6) can be recast into the matrix form as follows

$$X(a\ell + 0) = S_b X(a\ell - 0), \quad S_b = \begin{bmatrix} 1 & 0 \\ -B(\omega) & 1 \end{bmatrix}, \quad X = \begin{bmatrix} \check{q} \\ \partial_z \check{q} \end{bmatrix}, \quad B(\omega) = \frac{b^2 \beta_0 \omega^2}{\omega^2 - \omega_0^2}. \quad (8.9)$$

In order to use the standard form of the Floquet theory reviewed in Appendix F we recast the ordinary differential equations (8.5) with boundary (interface) conditions (8.6) as the following single second-order ordinary differential equation with singular, frequency dependent, periodic potential:

$$\partial_z^2 \check{q} - 2i\omega \partial_z \check{q} + (f^2 - \omega^2) \check{q} - B(\omega) p(z) \check{q} = 0, \quad p(z) = \sum_{\ell=-\infty}^{\infty} \delta(z - \ell), \quad \check{q} = \check{q}(z), \quad (8.10)$$

where the second interaction parameter $B(\omega)$ is defined by equation (8.7).

Analysis of equations (8.10) based on the Floquet theory (see Appendix F) becomes now the primary subject of studies. The second-order ordinary differential equation (8.10) can in turn be recast into the following matrix ordinary differential equation

$$\partial_z X = A_K(z) X, \quad A_K(z) = A_K(z, \omega) = \begin{bmatrix} 0 & 1 \\ \omega^2 - f^2 + B(\omega) p(z) & 2i\omega \end{bmatrix}, \quad X = \begin{bmatrix} q \\ \partial_z q \end{bmatrix}, \quad (8.11)$$

$$B(\omega) = \frac{b^2 \beta_0 \omega^2}{\omega^2 - \omega_0^2} = 2f K_0 \frac{\omega^2}{\omega^2 - \omega_0^2}, \quad p(z) = \sum_{\ell=-\infty}^{\infty} \delta(z - \ell).$$

Note that normalized period $f = \frac{2\pi a}{\lambda_{rp}}$ and the MCK gain coefficient $K_0 = \frac{b^2 g_B}{c_0}$ play particularly significant roles for the MCK properties.

One can verify by straightforward evaluation that equation (8.10) has the Hamiltonian structure (see Appendix G) with the following selection for the metric matrix

$$G_K = G_K^* = \begin{bmatrix} 2\omega & i \\ -i & 0 \end{bmatrix}, \quad G_K^{-1} = \begin{bmatrix} 0 & i \\ -i & -2\omega \end{bmatrix}, \quad \det[G_K] = -1. \quad (8.12)$$

The eigenvalues are eigenvectors of metric matrix G_K are as follows:

$$\omega + \sqrt{\omega^2 + 1}, \quad \begin{bmatrix} i \\ -\omega + \sqrt{\omega^2 + 1} \\ 1 \end{bmatrix}; \quad \omega - \sqrt{\omega^2 + 1}, \quad \begin{bmatrix} -i \\ \omega + \sqrt{\omega^2 + 1} \\ 1 \end{bmatrix}. \quad (8.13)$$

Using expressions (8.11) and (8.12) for respectively matrices $A(z)$ and G one can readily verify that $A(z)$ is G -skew-Hermitian matrix, that is

$$G_K A_K(z) + A_K^*(z) G_K = 0, \quad (8.14)$$

and that according to Appendix G implies that the system (8.11) is Hamiltonian. Consequently, according to Appendix G the matrizant $\Phi_K(z)$ of the Hamiltonian system (8.11) is G_K -unitary and its spectrum $\sigma\{\Phi_K(z)\}$ is symmetric with respect to the unit circle, that is

$$\Phi_K^*(z) G_K \Phi_K(z) = G, \quad \zeta \in \sigma\{\Phi_K(z)\} \Rightarrow \frac{1}{\zeta} \in \sigma\{\Phi_K(z)\}. \quad (8.15)$$

8.2. The monodromy matrix, the dispersion-instability relations and the gain. The MCK monodromy matrix \mathcal{T}_K (see Appendix F) is as follows:

$$\mathcal{T}_K = e^{i\omega} \begin{bmatrix} \cos(f) - i\omega \operatorname{sinc}(f) & \operatorname{sinc}(f) \\ \operatorname{sinc}(f) \omega^2 + 2i\omega (\cos(f) + b_f) - \frac{2b_f \cos(f) + \cos^2(f) + 1}{\operatorname{sinc}(f)} & i\omega \operatorname{sinc}(f) - \cos(f) - 2b_f \end{bmatrix}, \quad (8.16)$$

where

$$b_f = \frac{B(\omega)}{2} \operatorname{sinc}(f) - \cos(f), \quad \operatorname{sinc}(f) = \frac{\sin(f)}{f}, \quad B(\omega) = \frac{b^2 \beta_0 \omega^2}{\omega^2 - \omega_0^2}. \quad (8.17)$$

We assume that the MCK normalized period $f = \frac{2\pi a}{\lambda_{rp}}$, an important parameter that effects the instability, satisfies the following inequalities.

Assumption 4. (*smaller MCK period*). The MCK normalized period f satisfies the following bounds:

$$0 < f = \frac{2\pi a}{\lambda_{rp}} < \pi. \quad (8.18)$$

The MCK gain is defined by the following expression:

$$G = G(f, \omega, K_0) = \begin{cases} 20 \left| \log \left(\left| |b_f| + \sqrt{b_f^2 - 1} \right| \right) \right| & \text{if } |b_f| > 1 \\ 0 & \text{if } |b_f| \leq 1 \end{cases}, \quad (8.19)$$

$$b_f = b_f(\omega) = K(\omega) \sin(f) - \cos(f), \quad K(\omega) = K_0 \frac{\omega^2}{\omega^2 - \omega_0^2}, \quad K_0 = \frac{b^2 \beta_0}{2f} = \frac{b^2 g_B}{c_0}.$$

Note that the following high-frequency decomposition holds for the instability parameter b_f :

$$b_f(\omega) = b_f^\infty + K_0 \frac{\omega_0^2}{\omega^2 - \omega_0^2}, \quad (8.20)$$

where

$$b_f^\infty = \lim_{\omega \rightarrow \infty} b_f(\omega) = K_0 \sin(f) - \cos(f), \quad K_0 = \frac{b^2 g_B}{c_0}, \quad (8.21)$$

It turns out that the high-frequency limit b_f^∞ of instability parameter b_f defined by equation (8.21) plays significant role in the analysis of the MCK instability and its gain. In particular, there exists a unique value f_{cr} on interval $(0, \pi)$ of the normalized period f such that

$$b_{f_{cr}}^\infty = 1, \quad 0 < f_{cr} < \pi, \quad (8.22)$$

and we refer to it as the *critical value* and the following representation holds

$$f_{cr} = 2 \arctan \left(\frac{1}{K_0} \right), \quad \text{where } K_0 = \frac{b^2 g_B}{c_0}, \quad g_B = \frac{\sigma_B}{4\lambda_{rp}}, \quad |\arctan(*)| < \frac{\pi}{2}. \quad (8.23)$$

The significance of the critical value f_{cr} is that for $f_{cr} < f < \pi$ any $\omega > \omega_0$ is an instability frequency. One can see that in Figure 12 showing the frequency dependence of the gain G and its asymptotic behavior as $\omega \rightarrow +\infty$.

The maximal value

$$G_{\max} = 20 \left| \log \left(\left| K_0 + \sqrt{K_0^2 + 1} \right| \right) \right| = 20 \frac{\ln \left(K_0 + \sqrt{K_0^2 + 1} \right)}{\ln(10)}. \quad (8.24)$$

of gain G is attained at $f = f_{\max}$ that satisfies

$$f_{\max} = \pi - \arctan(K_0), \quad f_{\text{cr}} < f_{\max} < \pi. \quad (8.25)$$

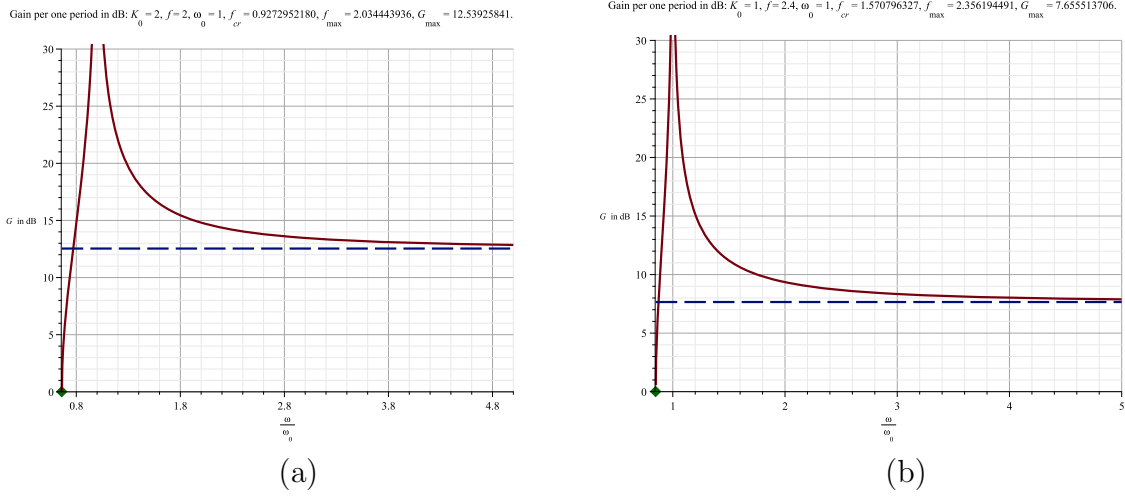


FIGURE 12. Plots of gain G as a function of frequency ω defined by equations (8.19) for $\omega_0 = 1$ and (a) $K_0 = 2, f = 2 > f_{\text{cr}}$ with $f_{\text{cr}} \cong 0.9272952180, f_{\max} \cong 2.034443936$ and $G_{\max} \cong 12.53925841$; (b) $K_0 = 1, f = 2.4 > f_{\text{cr}}$ with $f_{\text{cr}} \cong 1.570796327, f_{\max} \cong 2.356194491$ and $G_{\max} \cong 7.655513706$. In all plots the horizontal and vertical axes represent respectively frequency ω and gain G in dB. The solid (brown) curves represent gain G as a function of frequency ω , the dashed (blue) line $G = G_{\max}$ represents the maximal G_{\max} value of G in the high frequency limit. The diamond solid (green) dots mark the values of Ω_f^- which is the lower frequency boundary of the instability interval.

$$\text{Functions } f_{\text{cr}} = 2 \arctan\left(\frac{1}{K_0}\right), f_{\max} = \pi - \arctan(K_0).$$

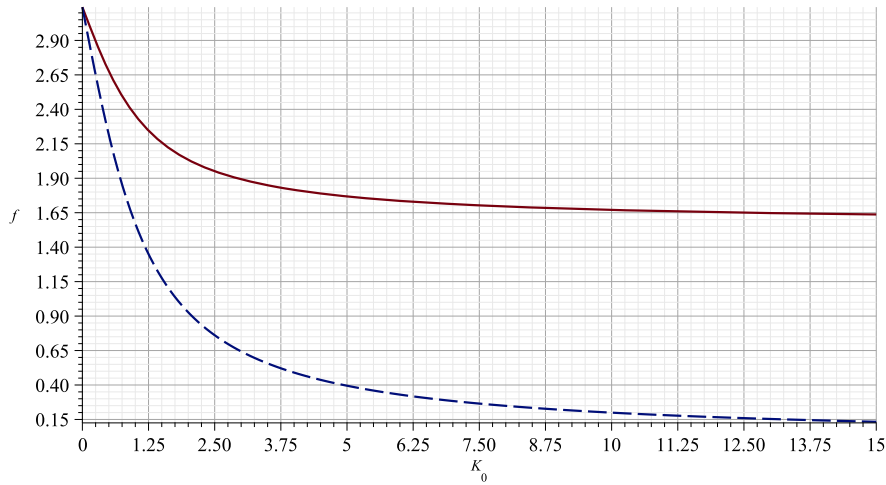


FIGURE 13. Plots of $f_{\max} = \pi - \arctan(K_0)$ as solid (brown) curve and $f_{\text{cr}} = 2 \arctan\left(\frac{1}{K_0}\right)$ as dashed (blue) curve. The horizontal and vertical axes represent respectively K_0 and f .

Let $s = \exp \{ik\}$ where k is the wave number be the Floquet multiplier of the monodromy matrix \mathcal{T}_K defined by equations (8.16), (8.17), (see Section F and Remark 25). Then the two Floquet multipliers s_{\pm} are solutions to the characteristic equation $\det \{\mathcal{T}_K - s\mathbb{I}\} = 0$ which is, [FigKly]:

$$s = e^{ik} = e^{i\omega} S : S^2 + 2b_f S + 1 = 0; \quad S = S_{\pm} = -b_f \pm \sqrt{b_f^2 - 1}, \quad (8.26)$$

readily implying

$$s_{\pm} = e^{ik_{\pm}} = e^{i\omega} S_{\pm} = e^{i\omega} \left(-b_f \pm \sqrt{b_f^2 - 1} \right), \quad b_f = b_f(\omega) = K(\omega) \sin(f) - \cos(f), \quad (8.27)$$

$$K(\omega) = K_0 \frac{\omega^2}{\omega^2 - \omega_0^2}, \quad K_0 = \frac{b^2 \beta_0}{2f} = \frac{b^2 g_B}{c_0},$$

Equations (8.26) show that *parameter b_f completely determines the two Floquet multipliers s_{\pm} justifying its its name the instability parameter. Importantly, the characteristic equation (8.26) can be viewed as an expression of the dispersion relations between the frequency ω and the wavenumber k as we discuss in Section 6. Equation (8.26) can be readily recast as*

$$S + 2b_f + S^{-1} = 0, \quad S = s \exp \{-i\omega\} = \exp \{i(k - \omega)\}, \quad s = \exp \{ik\}, \quad (8.28)$$

or, equivalently, a

$$\cos(k - \omega) + b_f(\omega) = 0, \quad b_f(\omega) = K(\omega) \sin(f) - \cos(f), \quad (8.29)$$

Equations (8.28) and (8.29) can be viewed as expressions of the dispersion relations between the frequency ω and the wavenumber k and we will refer to it as the MCK dispersion relations. Dispersion relation (8.29) can be readily recast as

$$k_{\pm}(\omega) = \omega \pm \arccos(-b_f(\omega)), \quad b_f(\omega) = K(\omega) \sin(f) - \cos(f), \quad (8.30)$$

$$K(\omega) = K_0 \frac{\omega^2}{\omega^2 - \omega_0^2}, \quad K_0 = \frac{b^2 \beta_0}{2f} = \frac{b^2 g_B}{c_0}.$$

Equation (8.30) in turn can recast into even more explicit form as stated in the following theorem, [FigKly].

Theorem 7 (MCK dispersion relations). *Let s_{\pm} be the MCK Floquet multipliers, that is solutions to equations (8.28), and let $k_{\pm}(\omega)$ be the corresponding complex-valued wave numbers satisfying*

$$s_{\pm} = s_{\pm}(\omega) = \exp \{ik_{\pm}(\omega)\}, \quad (8.31)$$

Then the following representation for $k_{\pm}(\omega)$ holds

$$k_{\pm}(\omega) = \begin{cases} -\frac{1+\text{sign}\{b_f(\omega)\}}{2}\pi + \omega + 2\pi m \pm i \ln \left[\left(|b_f(\omega)| + \sqrt{b_f^2(\omega) - 1} \right) \right] & \text{if } b_f^2 > 1 \\ -\frac{1+\text{sign}\{b_f(\omega)\}}{2}\pi + \omega + 2\pi m \pm \arccos(|b_f(\omega)|) & \text{if } b_f^2 \leq 1 \end{cases}, \quad m \in \mathbb{Z}, \quad (8.32)$$

where $0 < f < \pi$ and

$$b_f(\omega) = K_0 \frac{\omega^2}{\omega^2 - \omega_0^2} \sin(f) - \cos(f), \quad K_0 = \frac{b^2 \beta_0}{2} = \frac{b^2 g_B}{c_0}, \quad g_B = \frac{\sigma_B}{4\lambda_{rp}}. \quad (8.33)$$

Requirement for $\Re \{k_{\pm}(\omega)\}$ to be in the first (main) Brillouin zone $(-\pi, \pi]$ effectively selects the band number m that depend on ω as follows. For any given $\omega > 0$ and $0 < f < \pi$ the band number $m \in \mathbb{Z}$ is determined by the requirement to satisfy the following inequalities:

$$\begin{aligned} -\pi &< -\frac{1+\text{sign}\{b_f(\omega)\}}{2}\pi + \omega + 2\pi m \leq \pi, & \text{if } b_f^2(\omega) > 1 \\ -\pi &< -\frac{1+\text{sign}\{b_f(\omega)\}}{2}\pi \pm \arccos(-b_f(\omega)) + \omega + 2\pi m \leq \pi, & \text{if } b_f^2(\omega) < 1 \end{aligned} \quad (8.34)$$

The equations (8.32) for the complex-valued wave numbers $k_{\pm}(\omega)$ represent the dispersion relations of the MCK.

Remark 8. Note that according to expression (8.32) in Theorem 7 we have

$$\Re\{k_{\pm}(\omega)\} = \pi + \omega + 2\pi m, \quad \omega_0 < \omega < \Omega_f^+, \quad (8.35)$$

where Ω_f^+ is the upper boundary of instability frequencies. Figure 15 illustrates graphically equation (8.35) by perfect straight lines parallel to $\Re\{k\} = \omega$ in the shadowed area.

There is yet another form of the dispersion relation (8.28) and (8.29) which is the high-frequency form:

$$D_K(\omega, k) = D_K^{(0)}(\omega, k) + \frac{K_0 \omega_0^2}{\omega^2 - \omega_0^2} = 0, \quad (8.36)$$

$$D_K^{(0)}(\omega, k) = \cos(\omega - k) + b_f^\infty, \quad b_f^\infty = K_0 \sin(f) - \cos(f). \quad (8.37)$$

We refer to function $D_K(\omega, k)$ as the *MCK dispersion function*.

This form readily yields the following high-frequency approximation to the MCK dispersion relations

$$\cos(\omega - k) + b_f^\infty = 0, \quad b_f^\infty = K_0 \sin(f) - \cos(f), \quad |b_f^\infty| \leq 1, \quad (8.38)$$

or, equivalently

$$\omega = k \pm \arccos(-b_f^\infty) + 2\pi m, \quad b_f^\infty = K_0 \sin(f) - \cos(f), \quad |b_f^\infty| \leq 1, \quad m \in \mathbb{Z}, \quad (8.39)$$

where inequality $|b_f^\infty| \leq 1$ is necessary and sufficient for the existence of real-valued ω and k satisfying the dispersion relation.

Theorem 2 shows how the MCK dispersion function $D_K(\omega, k)$ and its high-frequency approximation $D_K^{(0)}(\omega, k)$ are integrated into the relevant dispersion functions associated with the CCTWT.

Figures 14 and 15 illustrate graphically the dispersion relations $k_{\pm}(\omega)$ described by equations (8.32). The pairs of nearly straight lines above the shadowed instability zone depicted in Figure 14 are consistent with the high-frequency approximation (8.39) to the MCK dispersion relation.

Interestingly, there is an empirical formula due to Tsimring that shows the dependence of the maximum power gain $G_T(N)$ on the number N of cavities in the klystron, [Tsim, 7.7.1], [Grigo, 7.2.6], [ValMid, 16]:

$$G_T(N) = 15 + 20(N - 2) \text{ dB}. \quad (8.40)$$

Realistically achievable maximum amplification values though are smaller and are of the order of 50 dB to 70 dB. The main limiting factors are noise and self-excitation of the klystron because of parasitic feedback between cavities.

9. COUPLED CAVITY STRUCTURE

We introduce and study here basic properties of the *coupled cavity structure (CCS)*. Since CCS is naturally an integral part of CCTWT the knowledge of its properties would allow to find out its contribution to the properties of CCTWT. As to particular designs of coupled cavities and the way they interact with TWTs see [BenSweScha, 9.1, 9.3.3].

The Lagrangian $\mathcal{L}_C(\{Q\})$ of the CCS system can be readily obtained from the Lagrangian \mathcal{L} of CCTWT defined by equations (3.9), (3.10) and (3.11) by assuming $b = 0$ and omitting component \mathcal{L}_B , that is

$$\mathcal{L}_C(\{Q\}) = \frac{L}{2} (\partial_t Q)^2 - \frac{1}{2C} (\partial_z Q)^2 - \frac{1}{2c_0} \sum_{\ell=-\infty}^{\infty} \delta(z - a\ell) [Q(a\ell)]^2. \quad (9.1)$$

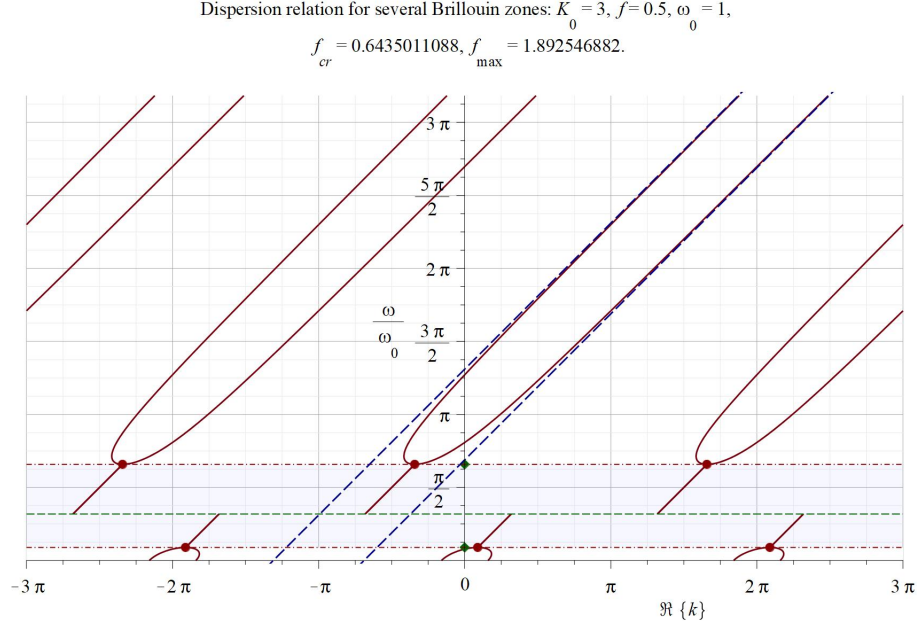


FIGURE 14. The MCK dispersion-instability plot (solid brown curves and lines) over 3 Brillouin zones $3[-\pi, \pi]$ for $K_0 = 3, \omega_0 = 1$ for which $f_{cr} \cong 0.6435011088$, $f_{max} \cong 1.892546882$ and $f = 0.5 < f_{cr} \cong 0.6435011088$. The horizontal and vertical axes represent respectively $\Re\{k\}$ and $\frac{\omega}{\omega_0}$. Two solid (green) diamond dots identify the values of Ω_f^- and Ω_f^+ which are the frequency boundaries of the instability. Solid (brown) disk dots identify points of the transition from the instability to the stability which are also EPD points. Two horizontal (brown) dash-dot lines $\omega = \Omega_f^\pm$ identify the frequency boundaries of the instability and the shaded (light blue) region between the lines identify points $(\Re\{k\}, \omega)$ of instability. Dashed horizontal (green) line $\omega = \omega_0$ identifies the resonance frequency ω_0 . Note the plot has a jump-discontinuity along the dashed (green) line, namely $\Re\{k_\pm(\omega)\}$ jumps by π according to equations (8.32) as the frequency ω passes through the resonance frequency ω_0 and the sign of $b_f(\omega)$ changes. The shadowed area marks points $(\Re\{k\}, \omega)$ associated with the instability. The dashed (blue) straight lines correspond to the high frequency approximation defined by equations (8.39).

Then the corresponding EL equations (3.12) and (3.14) are reduced to

$$L\partial_t^2 Q - C^{-1}\partial_z^2 Q = 0, \quad [\partial_z Q](al) = C_0 \left(\frac{\partial_t^2}{\omega_0^2} + 1 \right) Q(al), \quad C_0 = \frac{C}{c_0}, \quad al \in \mathbb{Z}, \quad (9.2)$$

where jumps $[Q](al)$ and $[\partial_z Q](al)$ are defined by equation (3.4), and consequently

$$X(al + 0) = S_b X(al - 0), \quad S_b = \begin{bmatrix} 1 & 0 \\ C_0 \left(\frac{\partial_t^2}{\omega_0^2} + 1 \right) & 1 \end{bmatrix}, \quad X = \begin{bmatrix} Q \\ \partial_z Q \end{bmatrix} \quad (9.3)$$

Using the same set of dimensionless variables as in Section 3.2 and omitting prime symbol for notation simplicity we obtain the following dimensionless form of the EL equations (9.2)

$$\partial_t^2 Q - \frac{1}{\chi^2} \partial_z^2 Q = 0, \quad z \neq \ell; \quad [\partial_z Q](\ell) = C_0 \left(\frac{\partial_t^2}{\omega_0^2} + 1 \right) Q(\ell), \quad \ell \in \mathbb{Z}. \quad (9.4)$$

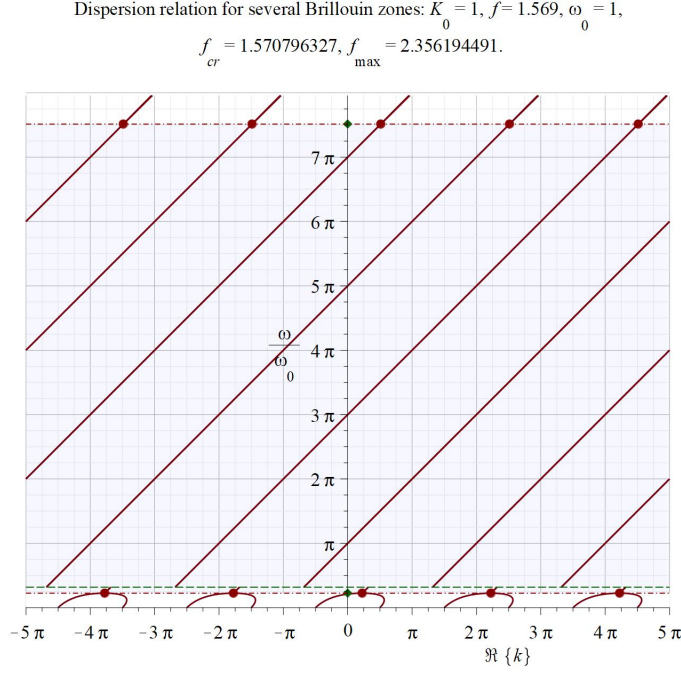


FIGURE 15. The MCK dispersion-instability plot (solid brown curves and lines) over 3 Brillouin zones $3[-\pi, \pi]$ for $K_0 = 1, \omega_0 = 1$ for which $f_{cr} \cong 1.570796327$, $f_{max} \cong 1.892546882$ and $f = 1.569 \cong f_{cr} \cong 1.570796327$. The horizontal and vertical axes represent respectively $\Re\{k\}$ and $\frac{\omega}{\omega_0}$. Two solid (green) diamond dots identify the values of Ω_f^- and Ω_f^+ which are the frequency boundaries of the instability. Solid (brown) disk dots identify points of the transition from the instability to the stability which are also EPD points. Two horizontal (brown) dash-dot lines $\omega = \Omega_f^\pm$ identify the frequency boundaries of the instability and the shaded (light blue) region between the lines identify points $(\Re\{k\}, \omega)$ of instability. Dashed horizontal (green) line $\omega = \omega_0$ identifies the resonance frequency ω_0 . Note the plot has a jump-discontinuity along the dashed (green) line, namely $\Re\{k_\pm(\omega)\}$ jumps by π according to equations (8.32) as the frequency ω passes through the resonance frequency ω_0 and the sign of $b_f(\omega)$ changes. The shadowed area marks points $(\Re\{k\}, \omega)$ associated with the instability.

The Fourier transform in t (see Appendix A) of equations (9.4) yields

$$\partial_z^2 \check{Q} + \frac{\omega^2}{\chi^2} \check{Q} = 0, \quad z \neq \ell; \quad [\partial_z Q](\ell) = C_0 \left(1 - \frac{\omega^2}{\omega_0^2}\right) Q(\ell), \quad \ell \in \mathbb{Z} \quad (9.5)$$

where \check{Q} and \check{q} are the time Fourier transform of the corresponding quantities.

An alternative form the system of equations (9.5) is the following second-order vector ODE with the periodic singular potential:

$$\partial_z^2 \check{Q} + \frac{\omega^2}{\chi^2} \check{Q} + C_0 \left(1 - \frac{\omega^2}{\omega_0^2}\right) \sum_{\ell=-\infty}^{\infty} \delta(z - \ell) \check{Q} = 0. \quad (9.6)$$

According to Appendix E second-order differential equation (9.6) is equivalent to the first-order differential equation of the form:

$$\partial_z X = A_C(z) X, \quad A_C(z) = \begin{bmatrix} 0 & 1 \\ -\frac{\omega^2}{\chi^2} - p(z) & 0 \end{bmatrix}, \quad X = \begin{bmatrix} \tilde{Q} \\ \partial_z \tilde{Q} \end{bmatrix}, \quad (9.7)$$

$$p(z) = C_0 \left(1 - \frac{\omega^2}{\omega_0^2}\right) \sum_{\ell=-\infty}^{\infty} \delta(z - \ell).$$

Using results of Appendix G.2 we find that system (9.7) is Hamiltonian for the following choice of nonsingular Hermitian matrix G :

$$G_C = G_C^* = \begin{bmatrix} 0 & i \\ -i & 0 \end{bmatrix}, \quad \det \{G_C\} = -1 \quad (9.8)$$

In particular, it is an elementary exercise to verify that for each value of z matrix $A_C(z)$ is G_C -skew-Hermitian, that is

$$G_C A_C(z) + A_C^*(z) G_C = 0. \quad (9.9)$$

Then if $\Phi(z)$ is the matrizant of Hamiltonian equation (9.7) then according to results of Appendix G $\Phi_C(z)$ is G_C -unitary matrix

$$\Phi_C^*(z) G_C \Phi_C(z) = G_C, \quad (9.10)$$

and consequently its spectrum $\sigma \{\Phi_C(z)\}$ is invariant with respect to the inversion transformation $\zeta \rightarrow \frac{1}{\zeta}$, that is it symmetric with respect to the unit circle:

$$\zeta \in \sigma \{\Phi_C(z)\} \Rightarrow \frac{1}{\zeta} \in \sigma \{\Phi_C(z)\}. \quad (9.11)$$

To simplify analytic evaluations we assume as before that Assumption 3 holds.

9.1. Monodromy matrix and the dispersion-instability relations. Under simplifying Assumption 3 ($\chi = \omega_0 = 1$) the monodromy matrix matrix \mathcal{T}_C defined by equation (3.43) takes the form

$$\mathcal{T}_C = \begin{bmatrix} \cos(\omega) & \omega^{-1} \sin(\omega) \\ (1 - \omega^2) C_0 \cos(\omega) - \omega \sin(\omega) & \cos(\omega) - C_0(\omega - \omega^{-1}) \sin(\omega) \end{bmatrix}. \quad (9.12)$$

The corresponding characteristic equation (3.45) turns into

$$P_C(\omega, s) = s^2 + 2W_C(\omega)s + 1 = 0, \quad W_C(\omega) = \frac{C_0}{2} \left(\omega - \frac{1}{\omega}\right) \sin(\omega) - \cos(\omega), \quad (9.13)$$

$$s = \exp \{ik\},$$

where quadratic polynomial P_C is referred to as the *CCS characteristic polynomial* and quantity $W_C(\omega)$ is the CCS instability parameter which is depicted in Fig. 16(b).

The two Floquet multipliers s_{\pm} which are the eigenvalues of the monodromy matrix \mathcal{T}_C defined by equation (9.12) and consequently are the solutions to its characteristic equation (9.13) can be represented as follows

$$s_{\pm} = e^{ik_{\pm}} = W_C \pm \sqrt{W_C^2 - 1}, \quad W_C = W_C(\omega) = \frac{C_0}{2} \left(\omega - \frac{1}{\omega}\right) \sin(\omega) - \cos(\omega). \quad (9.14)$$

Equations (9.14) imply that *instability parameter* $W_C(\omega)$ *there completely determines the two Floquet multipliers* s_{\pm} justifying its its name.

Importantly, the characteristic equation (9.13) can be viewed as an expression of the dispersion relations between the frequency ω and the wavenumber k . To obtain an explicit form of the

dispersion relations for the CCS under simplifying Assumption 3 ($\chi = \omega_0 = 1$) we divide the characteristic equation (9.13) by $2s$, substitute $s = \exp \{ik\}$ obtaining the following equations:

$$\cos(k) + W_C(\omega) = 0, \quad W_C(\omega) = \frac{C_0}{2} \left(\omega - \frac{1}{\omega} \right) \sin(\omega) - \cos(\omega), \quad (9.15)$$

where $W_C(\omega)$ is principle CCS function (see Fig. 16(b)). Alternatively, the dispersion-instability relations (9.14) can be represented in the form

$$k_{\pm} = k_{\pm}(\omega) = -i \ln \left(W_C \pm \sqrt{W_C^2 - 1} \right), \quad (9.16)$$

$$W_C = W_C(\omega) = \frac{C_0}{2} \left(\omega - \frac{1}{\omega} \right) \sin(\omega) - \cos(\omega).$$

Dividing equation (9.15) by ω we obtain the following *high-frequency form of the dispersion relations* for the MCK:

$$D_C(\omega, k) = D_C^{(0)}(\omega, k) + \frac{2(\cos(k) - \cos(\omega))}{\omega} - \frac{C_0 \sin(\omega)}{\omega^2} = 0. \quad (9.17)$$

$$D_C^{(0)}(\omega, k) = C_0 \sin(\omega).$$

We refer to function $D_C(\omega, k)$ as the *CCS dispersion function*.

As to the e-beam transforming characteristic equation (3.46) for the e-beam the same way we obtain the following explicit form of the *dispersion relations for the e-beam*

$$\cos(k - \omega) - \cos(f) = 0; \quad \omega = k \pm f. \quad (9.18)$$

Expression (9.15) for the CCS dispersion relation readily implies that its EPD frequencies are solution to the following *CCS EPD equation*

$$W_C(\omega) = \frac{C_0}{2} \left(\omega - \frac{1}{\omega} \right) \sin(\omega) - \cos(\omega) = \pm 1. \quad (9.19)$$

where $W_C(\omega)$ is principle CCS function defined by the second equation in (9.13) and its plot is depicted in Fig. 16(b). Straightforward evaluations show that $W_C(\omega)$ satisfies the following equations:

$$W_C(\pi n) = (-1)^{n+1}, \quad \partial_{\omega} W_C(\pi n) = (-1)^n, \quad n = 1, 2, \dots \quad (9.20)$$

Consequently πn for positive integers n are CCS EPD points. Remaining set of EPD frequencies ξ_m , $m \geq 1$ are found by solving CCS EPD equation (9.19).

Instability (oscillatory spectrum) bands (intervals)

$$[0, \xi_0], \quad [\xi_m, \pi m], \quad m \geq 1 : 0 < \xi_0 < \xi_1 < \pi, \quad \pi(m-1) < \xi_m < \pi m, \quad m \geq 2 \quad (9.21)$$

where numbers ξ_m satisfy also the following equations:

$$W_C(\xi_0) = -1, \quad W_C(\omega)(\xi_1) = 1, \quad W_C(\xi_m) = (-1)^{m-1}; \quad m \geq 2. \quad (9.22)$$

Stability (oscillatory) spectrum bands (intervals)

$$[\xi_0, \xi_1], \quad [\pi m, \xi_{m+1}], \quad m \geq 1 : 0 < \xi_0 < \xi_1 < \pi, \quad \pi(m-1) < \xi_m < \pi m, \quad m \geq 2 \quad (9.23)$$

Based on the prior analysis we introduce the CCS gain G_C in dB per one period as a the rate of the exponential growth of the CCS eigenmodes associated with Floquet multipliers s_{\pm} defined by equations (9.16). More precisely the definition is as follows.

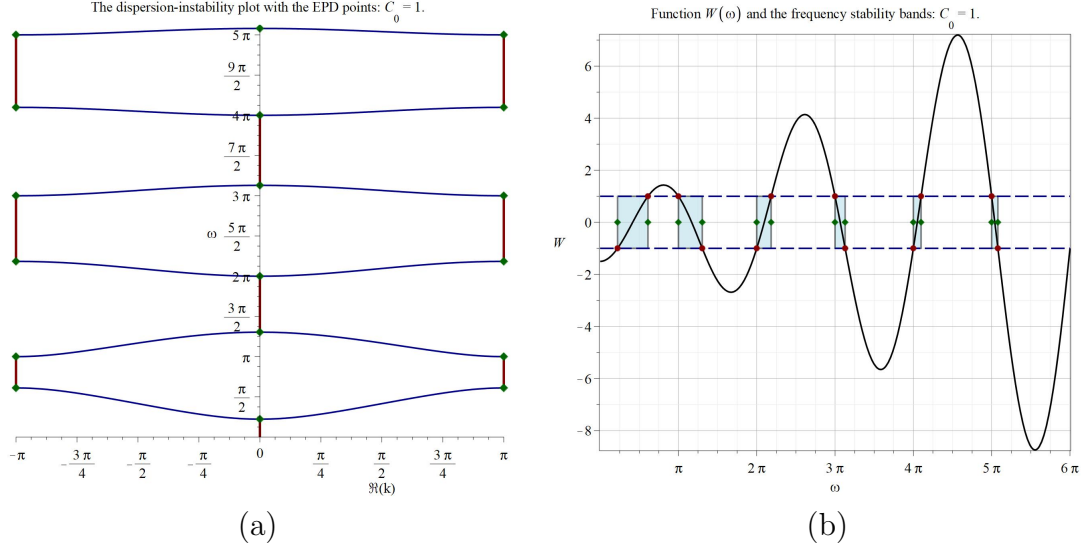


FIGURE 16. The CCS for $C_0 = 1$: (a) dispersion-instability graph, horizontal axis is $\Re\{k\}$ and vertical axis is ω ; (b) the plot of the instability parameter $W_C(\omega)$ defined by the second equation in (9.13). The horizontal axis is $\Re\{k\}$ and the vertical axis is W .

Definition 9 (CCS gain per one period). Let s_{\pm} be the CCS Floquet multipliers defined by equations (9.16). Then the corresponding to them gain G_C in dB per one period is defined by

$$G_C = G_C(\omega, C_0) = \begin{cases} 20 |\log(|s_+|)| = 20 \left| \log \left(|W_C| + \sqrt{W_C^2 - 1} \right) \right| & \text{if } |W_C| > 1 \\ 0 & \text{if } |W_C| \leq 1 \end{cases}, \quad (9.24)$$

$$W_C = W_C(\omega) = \frac{C_0}{2} \left(\omega - \frac{1}{\omega} \right) \sin(\omega) - \cos(\omega).$$

Fig. 17 shows the frequency dependence of the gain G_C per one period. Growing in magnitude “bumps” in Figure 17 indicate the presence of gain/amplification inside of stopbands, known also as spectral gaps in the system (oscillatory) spectrum, of the CCS, see Remark 6.

9.2. Exceptional points of degeneracy. The monodromy matrix \mathcal{T}_C defined by equation (9.12) and its Jordan form at $\omega = \pi n$ are as follows

$$\mathcal{T}_C = \begin{bmatrix} (-1)^n & 0 \\ (1 - \pi^2 n^2) C_0 (-1)^n & (-1)^n \end{bmatrix} = \mathcal{Z}_C \begin{bmatrix} (-1)^n & 1 \\ 0 & (-1)^n \end{bmatrix} \mathcal{Z}_C^{-1}, \quad \omega = \pi n$$

where matrix \mathcal{Z}_C is

$$\mathcal{Z}_C = \begin{bmatrix} 0 & 1 \\ (1 - \pi^2 n^2) C_0 (-1)^n & 0 \end{bmatrix},$$

and columns of the matrix \mathcal{Z}_C is the Jordan basis of the monodromy matrix \mathcal{T}_C

The monodromy matrix expression at EPDs is as follows

$$\mathcal{T}_C = \begin{bmatrix} \cos(\omega) & \omega^{-1} \sin(\omega) \\ \frac{\omega \sin(\omega)(\cos(\omega)-1)}{\cos(\omega)+1} & 2 - \cos(\omega) \end{bmatrix} = \mathcal{Z}_C \begin{bmatrix} 1 & 1 \\ 0 & 1 \end{bmatrix} \mathcal{Z}_C^{-1}, \quad W_C(\omega) = -1, \quad \omega \neq \pi n,$$

where

$$\mathcal{Z}_C = \begin{bmatrix} \cos(\omega) - 1 & 1 \\ \frac{\omega \sin(\omega)(\cos(\omega)-1)}{\cos(\omega)+1} & 0 \end{bmatrix},$$

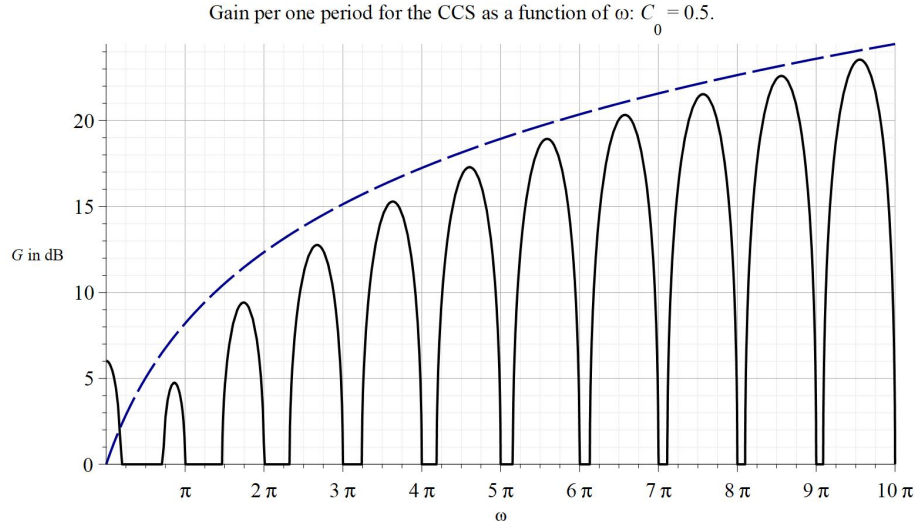


FIGURE 17. The plot of the CCS gain $G_C(\omega, C_0)$ per one period for $C_0 = 0.5$. The horizontal and vertical axes represent respectively frequency ω and gain G in dB. The instability frequencies ω are identified by condition $G_C(\omega, C_0) > 0$. The envelope of the local maxima of the gain $G_C(\omega, C_0)$ behaves asymptotically for large values of frequency ω as $20 |\log(C_0\omega)|$ as it follows from equations (9.24). It is shown as dashed (blue) curve.

and

$$\mathcal{T}_C = \begin{bmatrix} \cos(\omega) & \omega^{-1} \sin(\omega) \\ -\frac{\omega(\cos(\omega)+1)^2}{\sin(\omega)} & -2 - \cos(\omega) \end{bmatrix} = \mathcal{Z}_C \begin{bmatrix} -1 & 1 \\ 0 & -1 \end{bmatrix} \mathcal{Z}_C^{-1}, \quad W_C(\omega) = 1, \quad \omega \neq \pi n,$$

where

$$\mathcal{Z}_C = \begin{bmatrix} \cos(\omega) + 1 & 1 \\ -\frac{\omega(\cos(\omega)+1)^2}{\sin(\omega)} & 0 \end{bmatrix}.$$

10. THE KINETIC AND FIELD POINTS OF VIEW ON THE GAP INTERACTION

We compare here some of the features of our field theory with the relevant features of the kinematic/ballistic theory of the CCTWT operation. Before going into technical details we would like to point out that from the outset our Lagrangian field theory takes into account the space-charge forces, that is the electron-to-electron repulsion, whereas the standard hydrokinetic analysis completely neglects them.

10.1. Some points from the kinetic theory. We briefly review here some points the kinetic/ballistic theory. Kinematic analysis of the CCTWT operation involves: (i) the electron velocity modulation in gaps of the klystron cavities; (ii) consequent electron bunching; (iii) the energy exchange between the e-beam to the EM field; (iv) the energy transfer from the e-beam to the EM field under proper conditions and consequent RF signal amplification. The listed subjects were thoroughly studied by many scholars, see, for instance, [Caryo], [ChoWes], [Gilm1, 15], [Grigo, 7.2], [Tsim, 6.1-6.3; 7.1-7.7], [Shev, II] and references therein. When presenting relevant to us conclusions of the studies we follow mostly to the *hydrokinetic (ballistic) approach* that utilizes *the Eulerian (spatial) and the Lagrangian (material) descriptions (points of view)* as in [Tsim, 7.1-7.7] and [Shev, II]. As to general aspects of the hydrokinetic approach in continua, that includes

in particular the Eulerian and the Lagrangian descriptions, we refer the reader to [Lamb, I.4-I.8], [Redd, 3.1-3.2], [Gran, 1.7].

Our field theory assumes that the cavity width l_g and the corresponding transit time τ_g are zeros, see equations (1.4) and Assumptions 1). Consequently the most sophisticated developments of the kinetic theory dealing with cavity gaps of finite lengths are outside the scope of our studies. In our simpler case when $l_g = 0$ and $\tau_g = 0$ following to [Shev, II.5] we suppose that \mathring{U} is the constant accelerating voltage so the stationary dc electron flow velocity $\mathring{v} = \sqrt{\frac{2e}{m}\mathring{U}}$ where m and $-e$ is respectively the electron mass and its charge. Suppose also that $U_1 \sin(\omega t)$ is the gap voltage. Then based on the elementary energy conservation law one gets

$$\frac{mv^2}{2} = \frac{m\mathring{v}^2}{2} + U_1 \sin(\omega t) \quad (10.1)$$

where v is the modulated velocity. Solving equation (10.1) for v and assuming “small signal” approximation we obtain

$$v \cong \mathring{v} \left(1 + \frac{\xi}{2} \sin(\omega t) \right), \quad \xi = \frac{U_1}{\mathring{U}} \ll 1. \quad (10.2)$$

Then following to [Shev, II.6, II.7] we suppose the velocity-modulated in the cavity electron beam as described by equation (10.2) enters the field-free *drift space* beyond the gap. Then, [Shev, II.6, II.7]:

“Whilst passing through the drift space, some electrons overtake other, slower, electrons which entered the drift space earlier, and the initial distribution of charge in the beam is changed. If the drift space is long enough the initial velocity modulation can lead to substantial density modulation of the electron beam.”

In other words, according the above scenario electron bunching takes place. More precisely, the velocity-modulated, uniformly-dense electron beam, becomes a density-modulated beam with nearly constant dc velocity \mathring{v} .

10.2. Field theory point of view on the kinetic properties of the electron flow. According the CCTWT design all the interactions between the electron flow and the EM field occur in cavity gaps. In what follows to use notations and results from Section 2.2. Let us consider first *the action of the cavity ac EM field on the electron flow*. The cavity ac EM field acts upon the e-beam by accelerating and decelerating its electrons and effectively modulating their velocities by the relatively small compare to \mathring{v} electron velocity field $v = v(z, t)$. So as to this part of the interaction we may view the electron density to be essentially constant \mathring{n} whereas its ac velocity field $v = v(z, t)$ is modulated by ac EM field. Consider now *the action of the e-beam on the cavity ac EM field*. The space charge acts upon the cavity ac EM field essentially quasi electrostatically through relatively small ac electron number density field $n = n(z, t)$. So for this part of the interaction we may view the electron flow to be of nearly constant velocity \mathring{v} perturbed by relatively small ac electron number density $n = n(z, t)$. Following to the results of Section 3 let us take a look at the variation of the ac electron velocity $v = v(z, t)$ and ac electron number density $n = n(z, t)$ in the vicinity of centers al of the cavity gaps.

Note first that the action of the ac cavity EM field on the e-beam is manifested directly through a variation of the electron velocity $v = v(z, t)$ in a vicinity of the gap center al . The action of the e-beam on the cavity EM field is produced by the electron number density $n = n(z, t)$. As to the quantitative assessment of the variations note that equations (2.17) and (2.17) imply that the electron velocity $v = v(z, t)$ and number density $n = n(z, t)$ have the following jumps $[n](al)$ and

$[v](a\ell)$ at the interaction points $a\ell$:

$$[n](a\ell, t) = \frac{[\partial_z q](a\ell, t)}{\sigma_B e}, \quad [v](a\ell, t) = -\frac{\dot{v} [\partial_z q](a\ell, t)}{e \sigma_B \dot{n}} = -\frac{v \dot{n}(a\ell, t)}{\dot{n}}, \quad (10.3)$$

readily implying

$$\frac{[v](a\ell, t)}{\dot{v}} = -\frac{[n](a\ell, t)}{\dot{n}}. \quad (10.4)$$

Equations (2.15) and (10.4) in turn yield

$$[j](a\ell, t) = -e \{ \dot{n} [v, t] + \dot{v} [n] \} (a\ell, t) = 0 \quad (10.5)$$

signifying that the e-beam current density j is continuous in z at the interaction points $a\ell$. In view of the Poisson equation (2.20) and the first equation in (2.15) the following representation holds for the $[\partial_z E](a\ell)$ at the interaction points $a\ell$:

$$[\partial_z E](a\ell, t) = -\frac{4\pi}{\sigma_B} [\partial_z q](a\ell, t) = -4\pi e [n](a\ell, t). \quad (10.6)$$

Note that according to equations (10.4) the jumps in the velocity the number density are in antiphase.

10.3. Relation between the kinetic and the field points of view on the gap interaction.

An insightful comparative analysis of “electron-wave theory” and the kinetic/ballistic theory of bunching is provided in [Shev, II.15]:

“A description of the mechanism of phase focusing as a phenomenon of oscillating space-charge waves, is only a mathematical description of a process the essence of which is as follows. The initial velocity modulation gives rise to periodic concentration and dispersion of electron space charge. The amount of bunching, and the associated alternating current, increase through the bunching region provided there are no repulsive space-charge forces affecting this process. Space-charge forces oppose the initial velocity modulation, and cause additional retardation and acceleration of the electrons. ... Thus the law of conservation of energy is obeyed. On the other hand, the ballistic theory is fundamentally contradictory to this.

In fact, the ballistic theory of bunching assumes that the alternating velocity acquired by the electrons in the modulator remains constant along the whole path. However, the potential energy necessarily increases after electron bunching, and so the total energy of the electron beam constantly varies, and this conflicts with the law of conservation of energy. Despite this contradiction, the ballistic theory is a good enough approximation for many of the cases met with in practice ... In this case, both ballistic and electron-wave theories lead to identical results. “

In agreement with the above quotation our field theory of the space-charge wave can be viewed as an effective mathematical descriptions of the underlying physical complexity involving the electron velocity and the electron number densities.

As to the energy conservation unlike the kinetic theory our Lagrangian field theory surely provides for that. The field theory under some conditions agrees at least with some points of the kinetic/ballistic theory as we discuss below.

Hydrokinetic point of view on our simplifying assumption that the cavity width l_g and the corresponding transit time τ_g are zeros, see equations (1.4) and Assumptions 1), is as follows, [Shev, II.5]:

“Let us assume further that the transit time of electrons between grids 1 and 2 is infinitesimally small, which means a physically small transit time compared with the period of oscillation of the high-frequency field. If the transit time is negligible, electrons can be considered to move through a constant (momentarily) alternating field, i. e. virtually in a static field. The electrons acquire or lose an amount of energy

equal to the product of the electron charge and the momentary value of the voltage. Therefore electrons entering the space between the grids at different moments in time, with equal velocities, pass out of this space at different velocities which are determined by the momentary value of the alternating voltage. The electron beam is thus velocity modulated and has a uniform density of space charge.”

The direct link between our field theory and the hydrokinetic theory is provided by the e-beam Lagrangian \mathcal{L}_B defined by equations (2.9) and (3.10)

$$\mathcal{L}_B(\{q\}) = \frac{1}{2\beta} (D_t q)^2 - \frac{2\pi}{\sigma_B} q^2, \quad D_t = \partial_t + \dot{v} \partial_z. \quad (10.7)$$

Indeed, its first kinetic term $\frac{1}{2\beta} (D_t q)^2$ involves the material time derivative which represents an important concept of “particle” in the hydrokinetic theory. The second term $-\frac{2\pi}{\sigma_B} q^2$ in the e-beam Lagrangian accounts for the electron-to-electron repulsion, a phenomenon neglected by the standard ballistic analysis of the electron bunching.

Another link between the field and the kinetic theories comes from our analysis in Section 10.2. In view of equations (10.3) and (10.4) jumps $[\partial_z q](a\ell, t)$ that are explicitly allowed by the field theory represent jumps $[n](a\ell, t)$ and $[v](a\ell, t)$ related the kinetic properties of the electron flow, see Remark 1. Namely, jump $[n](a\ell, t)$ manifests the electron bunching, jump $[v](a\ell, t)$ manifests the ac electron velocity modulation and equation (10.4) relates the two of them.

11. LAGRANGIAN VARIATIONAL FRAMEWORK

We construct here the Lagrangian variational framework for our model of CCTWT. According to Assumption 1 the model integrates into it quantities associated with continuum of real numbers on one hand and features associated with discrete points on the another hand. The continuum features are represented by Lagrangian densities \mathcal{L}_T and \mathcal{L}_B in equations (3.10) whereas discrete features are represented by Lagrangian \mathcal{L}_{TB} in equations (3.11) with energies concentrated in a set of discrete points $a\mathbb{Z}$. One possibility for constructing the desired Lagrangian variational framework is to apply the general approach developed in [FigRey2] when the “rigidity” condition holds. Another possibility is to directly construct the Lagrangian variational framework using some ideas from [FigRey2] and that is what we actually pursue here.

Following to the standard procedures of the Least Action principle [ArnMech, II.3], [GantM, 3], [GelFom, 7], [GoldM, 8.6] we start with setting up the action integral S based on the Lagrangian \mathcal{L} defined by equations (3.9), (3.10) and (3.11). Using notations (3.7) and (3.8) we define the action integral S as follows:

$$S(\{x\}) = \int_{t_0}^{t_1} dt \int_{z_1}^{z_2} \mathcal{L}(\{x\}) dz = S_T(\{Q\}) + S_B(\{q\}) + S_{TB}(x), \quad t_0 < t_1, \quad z_0 < z_1, \quad (11.1)$$

where

$$S_T(\{Q\}) = \int_{t_0}^{t_1} dt \int_{z_1}^{z_2} \mathcal{L}_T(\{Q\}) dz = \int_{t_0}^{t_1} dt \int_{z_1}^{z_2} \left[\frac{L}{2} (\partial_t Q)^2 - \frac{1}{2C} (\partial_z Q)^2 \right] dz, \quad (11.2)$$

$$S_B(\{q\}) = \int_{t_0}^{t_1} dt \int_{z_1}^{z_2} \mathcal{L}_B(\{q\}) dz = \int_{t_0}^{t_1} dt \int_{z_1}^{z_2} \left[\frac{1}{2\beta} (\partial_t q + \dot{v} \partial_z q)^2 - \frac{2\pi}{\sigma_B} q^2 \right] dz, \quad (11.3)$$

$$\begin{aligned} S_{TB}(\{Q\}) &= \int_{t_0}^{t_1} dt \int_{z_1}^{z_2} \mathcal{L}_{TB}(Q, q) dz = \\ &= \sum_{z_1 < a\ell < z_2} \int_{t_0}^{t_1} dt \left[\frac{l_0}{2} (\partial_t Q(a\ell))^2 - \frac{1}{2c_0} (Q(a\ell) + bq(a\ell))^2 \right]. \end{aligned} \quad (11.4)$$

To make expressions of the action integrals less cluttered we suppress notationally their dependence on intervals (z_0, z_1) and (t_0, t_1) that can be chosen arbitrarily. We consider then variation δS of action S assuming that variations δQ and δq of charges $q = q(z, t)$ and $Q = Q(z, t)$ vanish outside intervals (z_0, z_1) and (t_0, t_1) , that is

$$\delta Q(z, t) = \delta q(z, t) = 0, \quad (z, t) \notin (z_0, z_1) \times (t_0, t_1), \quad (11.5)$$

implying, in particular, that δQ and δq vanish on the boundary of the rectangle $(z_0, z_1) \times (t_0, t_1)$, that is

$$\delta Q(z, t) = \delta q(z, t) = 0, \text{ if } z = z_0, z_1 \text{ or if } t = t_0, t_1. \quad (11.6)$$

We refer to variations δQ and δq satisfying equations (11.5) and hence (11.6) for a rectangle $(z_0, z_1) \times (t_0, t_1)$ as *admissible*.

Following to the least action principle we introduce the functional differential δS of the action by the following formula [GelFom, 7(35)]

$$\delta S = \lim_{\varepsilon \rightarrow 0} \frac{S(\{x + \varepsilon \delta x\}) - S(\{x\})}{\varepsilon}. \quad (11.7)$$

Then the system configurations $x = x(z, t)$ that actually can occur must satisfy

$$\delta S = \lim_{\varepsilon \rightarrow 0} \frac{S(\{x + \varepsilon \delta x\}) - S(\{x\})}{\varepsilon} = 0 \text{ for all admissible variations.} \quad (11.8)$$

Let us choose now any z outside lattice $a\mathbb{Z}$. Then there always exist a sufficiently small $\xi > 0$ and an integer ℓ_0 such that

$$a\ell_0 < z_0 = z - \xi < z < z_1 = z + \xi < a(\ell_0 + 1). \quad (11.9)$$

If we apply now the variational principle (11.9) for all admissible variations δQ and δq such that space interval (z_0, z_1) is compliant with inequalities (11.8) we readily find that

$$\delta S = \delta S_T + \delta S_B = 0, \quad (11.10)$$

where S_T and S_B are defined by expressions (11.2) and (11.3). Using equations (11.6) and carrying out in the standard way the integration by parts transformations we arrive at

$$\delta S_T = - \int_{t_0}^{t_1} dt \int_{z_1}^{z_2} [L \partial_t^2 Q - C^{-1} \partial_z^2 Q] \delta Q dz, \quad (11.11)$$

$$\delta S_B = - \int_{t_0}^{t_1} dt \int_{z_1}^{z_2} \left[\frac{1}{\beta} (\partial_t + \dot{v} \partial_z)^2 q + \frac{4\pi}{\sigma_B} q \right] \delta q dz. \quad (11.12)$$

Combining equations (11.10), (11.11) and (11.12) we arrive at the following EL equations

$$L \partial_t^2 Q - C^{-1} \partial_z^2 Q = 0, \quad \frac{1}{\beta} (\partial_t + \dot{v} \partial_z)^2 q + \frac{4\pi}{\sigma_B} q = 0, \quad z \neq a\ell, \quad \ell \in \mathbb{Z}. \quad (11.13)$$

Consider now the case when $z = a\ell_0$ for an integer ℓ_0 and select space interval (z_0, z_1) as follows

$$a(\ell_0 - 1) < z_0 = a\left(\ell_0 - \frac{1}{2}\right) < z = a\ell_0 < z_1 = a\left(\ell_0 + \frac{1}{2}\right) < a(\ell_0 + 1). \quad (11.14)$$

Notice that in this case all actions S_T , S_T and S_{TB} contribute to the variation δS . In particular, as consequence of the presence of delta functions $\delta(z - a\ell)$ in the expression of the Lagrangian \mathcal{L}_{TB} defined by equation (3.11) the space derivatives $\partial_z Q$ and $\partial_z q$ can have jumps at $z = a\ell_0$ as it was already acknowledged by Assumption 2. Based on this circumstance we proceed as follows:

(i) we split the integral with respect to the space variable z into two integrals:

$$\int_{z_0}^{z_1} = \int_{a(\ell_0 - \frac{1}{2})}^{a\ell_0} + \int_{a\ell_0}^{a(\ell_0 + \frac{1}{2})}; \quad (11.15)$$

(ii) we carry out the integration by parts for each of the two integrals in the right-hand side of equation (11.15); (iii) we use already established EL equations (11.13) to simplify the integral expressions. When that is all done we arrive at the following:

$$\delta S_T = \int_{t_0}^{t_1} \frac{1}{C} [\partial_z Q](a\ell_0, t) \delta Q(a\ell_0, t) dt, \quad \delta S_B = - \int_{t_0}^{t_1} \frac{\dot{v}^2}{\beta} [\partial_z q](a\ell_0, t) \delta q(a\ell_0, t) dt, \quad (11.16)$$

where jumps $[\partial_z Q](a\ell)$ and $[\partial_z q](a\ell)$ are defined by equation (3.4), and

$$\begin{aligned} \delta S_{TB} = & - \int_{t_0}^{t_1} \left\{ l_0 \partial_t^2 Q(a\ell) + \frac{1}{c_0} [Q(a\ell_0, t) + bq(a\ell_0, t)] \right\} \delta Q(a\ell_0, t) dt - \\ & - \int_{t_0}^{t_1} \left\{ \frac{b}{c_0} [Q(a\ell_0, t) + bq(a\ell_0, t)] \right\} \delta q(a\ell_0, t) dt. \end{aligned} \quad (11.17)$$

Using the variational principle (11.8), that is

$$\delta S_T + \delta S_B + \delta S_{TB} = 0, \quad (11.18)$$

and the fact that variations $\delta Q(a\ell_0, t)$ and $\delta q(a\ell_0, t)$ can be chosen arbitrarily we arrive at the following equations

$$\begin{aligned} \frac{1}{C} [\partial_z Q](a\ell_0, t) &= l_0 \partial_t^2 Q(a\ell) + \frac{1}{c_0} [Q(a\ell_0, t) + bq(a\ell_0, t)], \\ \frac{\dot{v}^2}{\beta} [\partial_z q](a\ell_0, t) &= - \frac{b}{c_0} [Q(a\ell_0, t) + bq(a\ell_0, t)], \end{aligned} \quad (11.19)$$

where jumps $[\partial_z Q](a\ell)$ and $[\partial_z q](a\ell)$ are defined by equation (3.4). Equations (11.19) can be ready recast into the following boundary conditions

$$[\partial_z Q](a\ell) = C_0 \left[\left(\frac{\partial_t^2}{\omega_0^2} + 1 \right) Q(a\ell) + bq(a\ell) \right], \quad [\partial_z q](a\ell) = - \frac{b\beta_0}{\dot{v}^2} [Q(a\ell) + bq(a\ell)], \quad (11.20)$$

where

$$C_0 = \frac{C}{c_0}, \quad \omega_0 = \frac{1}{\sqrt{l_0 c_0}}, \quad \beta_0 = \frac{\beta}{c_0}. \quad (11.21)$$

We remind also that as consequence of continuity of Q and q we also have

$$[Q](a\ell_0, t) = 0, \quad [q](a\ell_0, t) = 0. \quad (11.22)$$

Hence equations (11.20) and (11.22) can be viewed as the EL equations at point $a\ell_0$.

Equations (11.20) at an interaction point $a\ell_0$ are perfectly consistent with boundary conditions (2.12) of the general treatment in [FigRey2], which are

$$\begin{aligned} - \frac{\partial L_D}{\partial \psi_D^\ell}(b_1, t) + \frac{\partial L_B}{\partial \psi_B^\ell}(b_1, t) - \partial_0 \left(\frac{\partial L_B}{\partial \partial_0 \psi_B^\ell}(b_1, t) \right) &= 0; \\ \frac{\partial L_D}{\partial \psi_D^\ell}(b_2, t) + \frac{\partial L_B}{\partial \psi_B^\ell}(b_2, t) - \partial_0 \left(\frac{\partial L_B}{\partial (\partial_0 \psi_B^\ell)}(b_2, t) \right) &= 0. \end{aligned} \quad (11.23)$$

where (i) $b_1 = a\ell_0 - 0$ and $b_2 = a\ell_0 + 0$; (ii) L_D corresponds to $\mathcal{L}_T + \mathcal{L}_B$; (iii) L_B corresponds to \mathcal{L}_{TB} ; (iv) fields ψ_D^ℓ correspond to charges Q and q ; (v) boundary fields ψ_B^ℓ correspond to $Q(a\ell_0, t)$ and $q(a\ell_0, t)$. We remind the reader that boundary conditions (2.12) in [FigRey2] is an implementation

of the “rigidity” requirement which is appropriate for Lagrangian \mathcal{L}_{TB} defined by equation (3.11). In fact, the signs of the terms containing L_{D} in equations (11.23) are altered compare to original equations (2.12) in [FigRey2] to correct an unfortunate typo there.

Thus equations (11.20) and (11.22) form a complete set of the EL equations.

12. ROOT DEGENERACY FOR A SPECIAL POLYNOMIAL OF THE FORTH DEGREE

The complex plane transformation $z \rightarrow \frac{1}{\bar{z}}$ is known as the *unit (circle) inversion*, [YagCG, III.13], and if a set is invariant under the transformation we refer to it inversion symmetric set. Let us consider general form of polynomial equation (5.1) of the order 4

$$S^4 + aS^3 + bS^2 + \bar{a}S + 1 = 0, \quad a \in \mathbb{C}, \quad b \in \mathbb{R}. \quad (12.1)$$

If S is a solution to equation (12.1) which is a degenerate one then the following equation must hold also

$$\partial_S (S^4 + aS^3 + bS^2 + \bar{a}S + 1) = 4S^3 + 3aS^2 + 2bS + \bar{a} = 0. \quad (12.2)$$

Subtracting from 2 times equation (12.1) S times equation (12.2) and dividing the result by S^2 we obtain

$$-2S^2 + \frac{2}{S^2} - aS + \frac{\bar{a}}{S^2} = 0. \quad (12.3)$$

If a solution S to the system of equations (12.1) and (12.3) lies on the unit circle, that is $|S| = 1$, then $S^{-1} = \bar{S}$ and the system is equivalent to the following system of equations

$$\Re \left\{ S^2 + aS + \frac{b}{2} \right\} = 0, \quad \Im \{ 2S^2 + aS \} = 0, \quad S = e^{i\varphi}, \quad \varphi \in \mathbb{R}. \quad (12.4)$$

A trigonometric version of the system equations (12.4) is

$$\begin{aligned} \cos(2\varphi) + |a| \cos(\varphi + \alpha) &= -\frac{b}{2}, \quad 2 \sin(2\varphi) + |a| \sin(\varphi + \alpha) = 0, \\ a &= |a| \exp\{i\alpha\}, \quad S = \exp\{i\varphi\}, \quad \varphi, \alpha \in \mathbb{R}. \end{aligned} \quad (12.5)$$

ACKNOWLEDGMENT: This research was supported by AFOSR MURI under Grant No. FA9550-20-1-0409 administered through the University of New Mexico. The author is grateful to E. Schamiloglu for sharing his deep and vast knowledge of high power microwave devices and inspiring discussions.

NOMENCLATURE:

- \mathbb{C} set of complex number.
- \mathbb{C}^n set of n dimensional column vectors with complex complex-valued entries.
- $\mathbb{C}^{n \times m}$ set of $n \times m$ matrices with complex-valued entries.
- $D(\omega, k)$ CCTWT dispersion function.
- $D_{\text{C}}(\omega, k)$ CCS dispersion function.
- $D_{\text{K}}(\omega, k)$ MCK dispersion function.
- $\det\{A\}$ the determinant of matrix A .
- $\text{diag}(A_1, A_2, \dots, A_r)$ block diagonal matrix with indicated blocks.
- $\dim(W)$ dimension of the vector space W .
- EL the Euler-Lagrange (equations).
- \mathbb{I}_{ν} $\nu \times \nu$ identity matrix.
- $\ker(A)$ kernel of matrix A , that is the vector space of vector x such that $Ax = 0$.
- M^{T} matrix transposed to matrix M .
- ODE ordinary differential equations.

- \bar{s} is complex-conjugate to complex number s .
- $\sigma\{A\}$ spectrum of matrix A .
- $\mathbb{R}^{n \times m}$ set of $n \times m$ matrices with real-valued entries.
- $\chi_A(s) = \det \{s\mathbb{I}_\nu - A\}$ characteristic polynomial of a $\nu \times \nu$ matrix A .

APPENDIX A. FOURIER TRANSFORM

Our preferred form of the Fourier transforms as in [Foll, 7.2, 7.5], [ArfWeb, 20.2] is as follows:

$$f(t) = \int_{-\infty}^{\infty} \hat{f}(\omega) e^{-i\omega t} d\omega, \quad \hat{f}(\omega) = \frac{1}{2\pi} \int_{-\infty}^{\infty} f(t) e^{i\omega t} dt, \quad (\text{A.1})$$

$$f(z, t) = \int_{-\infty}^{\infty} \hat{f}(k, \omega) e^{-i(\omega t - kz)} dk d\omega, \quad (\text{A.2})$$

$$\hat{f}(k, \omega) = \frac{1}{(2\pi)^2} \int_{-\infty}^{\infty} f(z, t) e^{i(\omega t - kz)} dz dt.$$

This preference was motivated by the fact that the so-defined Fourier transform of the convolution of two functions has its simplest form. Namely, the convolution $f * g$ of two functions f and g is defined by [Foll, 7.2, 7.5],

$$[f * g](t) = [g * f](t) = \int_{-\infty}^{\infty} f(t - t') g(t') dt', \quad (\text{A.3})$$

$$[f * g](z, t) = [g * f](z, t) = \int_{-\infty}^{\infty} f(z - z', t - t') g(z', t') dz' dt'. \quad (\text{A.4})$$

Then its Fourier transform as defined by equations (A.1) and (A.2) satisfies the following properties:

$$\widehat{f * g}(\omega) = \hat{f}(\omega) \hat{g}(\omega), \quad (\text{A.5})$$

$$\widehat{f * g}(k, \omega) = \hat{f}(k, \omega) \hat{g}(k, \omega). \quad (\text{A.6})$$

APPENDIX B. JORDAN CANONICAL FORM

We provide here very concise review of Jordan canonical forms following mostly to [Hale, III.4], [HorJohn, 3.1, 3.2]. As to a demonstration of how Jordan block arises in the case of a single n -th order differential equation we refer to [ArnODE, 25.4].

Let A be an $n \times n$ matrix and λ be its eigenvalue, and let $r(\lambda)$ be the least integer k such that $\mathcal{N}[(A - \lambda\mathbb{I})^k] = \mathcal{N}[(A - \lambda\mathbb{I})^{k+1}]$, where $\mathcal{N}[C]$ is a null space of a matrix C . Then we refer to $M_\lambda = \mathcal{N}[(A - \lambda\mathbb{I})^{r(\lambda)}]$ is the *generalized eigenspace* of matrix A corresponding to eigenvalue λ . Then the following statements hold, [Hale, III.4].

Proposition 10 (generalized eigenspaces). *Let A be an $n \times n$ matrix and $\lambda_1, \dots, \lambda_p$ be its distinct eigenvalues. Then generalized eigenspaces $M_{\lambda_1}, \dots, M_{\lambda_p}$ are linearly independent, invariant under the matrix A and*

$$\mathbb{C}^n = M_{\lambda_1} \oplus \dots \oplus M_{\lambda_p}. \quad (\text{B.1})$$

Consequently, any vector x_0 in \mathbb{C}^n can be represented uniquely as

$$x_0 = \sum_{j=1}^p x_{0,j}, \quad x_{0,j} \in M_{\lambda_j}, \quad (\text{B.2})$$

and

$$\exp \{At\} x_0 = \sum_{j=1}^p e^{\lambda_j t} p_j(t), \quad (\text{B.3})$$

where column-vector polynomials $p_j(t)$ satisfy

$$p_j(t) = \sum_{k=0}^{r(\lambda_j)-1} (A - \lambda_j \mathbb{I})^k \frac{t^k}{k!} x_{0,j}, \quad x_{0,j} \in M_{\lambda_j}, \quad 1 \leq j \leq p. \quad (\text{B.4})$$

For a complex number λ a Jordan block $J_r(\lambda)$ of size $r \geq 1$ is a $r \times r$ upper triangular matrix of the form

$$J_r(\lambda) = \lambda \mathbb{I}_r + K_r = \begin{bmatrix} \lambda & 1 & \cdots & 0 & 0 \\ 0 & \lambda & 1 & \cdots & 0 \\ 0 & 0 & \ddots & \cdots & \vdots \\ \vdots & \vdots & \ddots & \lambda & 1 \\ 0 & 0 & \cdots & 0 & \lambda \end{bmatrix}, \quad J_1(\lambda) = [\lambda], \quad J_2(\lambda) = \begin{bmatrix} \lambda & 1 \\ 0 & \lambda \end{bmatrix}, \quad (\text{B.5})$$

$$K_r = J_r(0) = \begin{bmatrix} 0 & 1 & \cdots & 0 & 0 \\ 0 & 0 & 1 & \cdots & 0 \\ 0 & 0 & \ddots & \cdots & \vdots \\ \vdots & \vdots & \ddots & 0 & 1 \\ 0 & 0 & \cdots & 0 & 0 \end{bmatrix}. \quad (\text{B.6})$$

The special Jordan block $K_r = J_r(0)$ defined by equation (B.6) is an nilpotent matrix that satisfies the following identities

$$K_r^2 = \begin{bmatrix} 0 & 0 & 1 & \cdots & 0 \\ 0 & 0 & 0 & \cdots & \vdots \\ 0 & 0 & \ddots & \cdots & 1 \\ \vdots & \vdots & \ddots & 0 & 0 \\ 0 & 0 & \cdots & 0 & 0 \end{bmatrix}, \dots, K_r^{r-1} = \begin{bmatrix} 0 & 0 & \cdots & 0 & 1 \\ 0 & 0 & 0 & \cdots & 0 \\ 0 & 0 & \ddots & \cdots & \vdots \\ \vdots & \vdots & \ddots & 0 & 0 \\ 0 & 0 & \cdots & 0 & 0 \end{bmatrix}, \quad K_r^r = 0. \quad (\text{B.7})$$

A general Jordan $n \times n$ matrix J is defined as a direct sum of Jordan blocks, that is

$$J = \begin{bmatrix} J_{n_1}(\lambda_1) & 0 & \cdots & 0 & 0 \\ 0 & J_{n_2}(\lambda_2) & 0 & \cdots & 0 \\ 0 & 0 & \ddots & \cdots & \vdots \\ \vdots & \vdots & \ddots & J_{n_{q-1}}(\lambda_{n_{q-1}}) & 0 \\ 0 & 0 & \cdots & 0 & J_{n_q}(\lambda_{n_q}) \end{bmatrix}, \quad n_1 + n_2 + \cdots + n_q = n, \quad (\text{B.8})$$

where λ_j need not be distinct. Any square matrix A is similar to a Jordan matrix as in equation (B.8) which is called *Jordan canonical form* of A . Namely, the following statement holds, [HorJohn, 3.1].

Proposition 11 (Jordan canonical form). *Let A be an $n \times n$ matrix. Then there exists a non-singular $n \times n$ matrix Q such that the following block-diagonal representation holds*

$$Q^{-1}AQ = J \quad (\text{B.9})$$

where J is the Jordan matrix defined by equation (B.8) and λ_j , $1 \leq j \leq q$ are not necessarily different eigenvalues of matrix A . Representation (B.9) is known as the Jordan canonical form of matrix A , and matrices J_j are called Jordan blocks. The columns of the $n \times n$ matrix Q constitute the Jordan basis providing for the Jordan canonical form (B.9) of matrix A .

A function $f(J_r(s))$ of a Jordan block $J_r(s)$ is represented by the following equation [MeyCD, 7.9], [BernM, 10.5]

$$f(J_r(s)) = \begin{bmatrix} f(s) & \partial f(s) & \frac{\partial^2 f(s)}{2} & \cdots & \frac{\partial^{r-1} f(s)}{(r-1)!} \\ 0 & f(s) & \partial f(s) & \cdots & \frac{\partial^{r-2} f(s)}{(r-2)!} \\ 0 & 0 & \ddots & \cdots & \vdots \\ \vdots & \vdots & \ddots & f(s) & \partial f(s) \\ 0 & 0 & \cdots & 0 & f(s) \end{bmatrix}. \quad (\text{B.10})$$

Note that any function $f(J_r(s))$ of the Jordan block $J_r(s)$ is evidently an upper triangular Toeplitz matrix.

There are two particular cases of formula (B.10), which can also be derived straightforwardly using equations (B.7),

$$\exp\{K_r t\} = \sum_{k=0}^{r-1} \frac{t^k}{k!} K_r^k = \begin{bmatrix} 1 & t & \frac{t^2}{2!} & \cdots & \frac{t^{r-1}}{(r-1)!} \\ 0 & 1 & t & \cdots & \frac{t^{r-2}}{(r-2)!} \\ 0 & 0 & \ddots & \cdots & \vdots \\ \vdots & \vdots & \ddots & 1 & t \\ 0 & 0 & \cdots & 0 & 1 \end{bmatrix}, \quad (\text{B.11})$$

$$[J_r(s)]^{-1} = \sum_{k=0}^{r-1} s^{-k-1} (-K_r)^k = \begin{bmatrix} \frac{1}{s} & -\frac{1}{s^2} & \frac{1}{s^3} & \cdots & \frac{(-1)^{r-1}}{s^r} \\ 0 & \frac{1}{s} & -\frac{1}{s^2} & \cdots & \frac{(-1)^{r-2}}{s^{r-1}} \\ 0 & 0 & \ddots & \cdots & \vdots \\ \vdots & \vdots & \ddots & \frac{1}{s} & -\frac{1}{s^2} \\ 0 & 0 & \cdots & 0 & \frac{1}{s} \end{bmatrix}. \quad (\text{B.12})$$

APPENDIX C. COMPANION MATRIX AND CYCLICITY CONDITION

The companion matrix $C(a)$ for the monic polynomial

$$a(s) = s^\nu + \sum_{1 \leq k \leq \nu} a_{\nu-k} s^{\nu-k} \quad (\text{C.1})$$

where coefficients a_k are complex numbers is defined by [BernM, 5.2]

$$C(a) = \begin{bmatrix} 0 & 1 & \cdots & 0 & 0 \\ 0 & 0 & 1 & \cdots & 0 \\ 0 & 0 & 0 & \cdots & \vdots \\ \vdots & \vdots & \ddots & 0 & 1 \\ -a_0 & -a_1 & \cdots & -a_{\nu-2} & -a_{\nu-1} \end{bmatrix}. \quad (\text{C.2})$$

Note that

$$\det \{C(a)\} = (-1)^\nu a_0. \quad (\text{C.3})$$

An eigenvalue is called *cyclic (nonderogatory)* if its geometric multiplicity is 1. A square matrix is called *cyclic (nonderogatory)* if all its eigenvalues are cyclic [BernM, 5.5]. The following statement provides different equivalent descriptions of a cyclic matrix [BernM, 5.5].

Proposition 12 (criteria for a matrix to be cyclic). *Let $A \in \mathbb{C}^{n \times n}$ be an $n \times n$ matrix with complex-valued entries. Let $\text{spec}(A) = \{\zeta_1, \zeta_2, \dots, \zeta_r\}$ be the set of all distinct eigenvalues and $k_j = \text{ind}_A(\zeta_j)$ is the largest size of Jordan block associated with ζ_j . Then the minimal polynomial $\mu_A(s)$ of the matrix A , that is a monic polynomial of the smallest degree such that $\mu_A(A) = 0$, satisfies*

$$\mu_A(s) = \prod_{j=1}^r (s - \zeta_j)^{k_j}. \quad (\text{C.4})$$

Furthermore, the following statements are equivalent:

- (i) $\mu_A(s) = \chi_A(s) = \det \{s\mathbb{I} - A\}$.
- (ii) A is cyclic.
- (iii) For every ζ_j the Jordan form of A contains exactly one block associated with ζ_j .
- (iv) A is similar to the companion matrix $C(\chi_A)$.

Proposition 13 (companion matrix factorization). *Let $a(s)$ be a monic polynomial having degree ν and $C(a)$ is its $\nu \times \nu$ companion matrix. Then, there exist unimodular $\nu \times \nu$ matrices $S_1(s)$ and $S_2(s)$, that is $\det \{S_m\} = \pm 1$, $m = 1, 2$, such that*

$$s\mathbb{I}_\nu - C(a) = S_1(s) \begin{bmatrix} \mathbb{I}_{\nu-1} & 0_{(\nu-1) \times 1} \\ 0_{1 \times (\nu-1)} & a(s) \end{bmatrix} S_2(s). \quad (\text{C.5})$$

Consequently, $C(a)$ is cyclic and

$$\chi_{C(a)}(s) = \mu_{C(a)}(s) = a(s). \quad (\text{C.6})$$

The following statement summarizes important information on the Jordan form of the companion matrix and the generalized Vandermonde matrix, [BernM, 5.16], [LanTsi, 2.11], [MeyCD, 7.9].

Proposition 14 (Jordan form of the companion matrix). *Let $C(a)$ be an $n \times n$ a companion matrix of the monic polynomial $a(s)$ defined by equation (C.1). Suppose that the set of distinct roots of polynomial $a(s)$ is $\{\zeta_1, \zeta_2, \dots, \zeta_r\}$ and $\{n_1, n_2, \dots, n_r\}$ is the corresponding set of the root multiplicities such that*

$$n_1 + n_2 + \dots + n_r = n. \quad (\text{C.7})$$

Then

$$C(a) = RJR^{-1}, \quad (\text{C.8})$$

where

$$J = \text{diag} \{J_{n_1}(\zeta_1), J_{n_2}(\zeta_2), \dots, J_{n_r}(\zeta_r)\} \quad (\text{C.9})$$

is the the Jordan form of companion matrix $C(a)$ and $n \times n$ matrix R is the so-called generalized Vandermonde matrix defined by

$$R = [R_1 | R_2 | \dots | R_r], \quad (\text{C.10})$$

where R_j is $n \times n_j$ matrix of the form

$$R_j = \begin{bmatrix} 1 & 0 & \cdots & 0 \\ \zeta_j & 1 & \cdots & 0 \\ \vdots & \vdots & \ddots & \vdots \\ \zeta_j^{n-2} & \binom{n-2}{1} \zeta_j^{n-3} & \cdots & \binom{n-2}{n_j-1} \zeta_j^{n-n_j-1} \\ \zeta_j^{n-1} & \binom{n-1}{1} \zeta_j^{n-2} & \cdots & \binom{n-1}{n_j-1} \zeta_j^{n-n_j} \end{bmatrix}. \quad (\text{C.11})$$

As a consequence of representation (C.9) $C(a)$ is a cyclic matrix.

As to the structure of matrix R_j in equation (C.11), if we denote by $Y(\zeta_j)$ its first column then it can be expressed as follows [LanTsi, 2.11]:

$$R_j = [Y^{(0)} | Y^{(1)} | \cdots | Y^{(n_j-1)}], \quad Y^{(m)} = \frac{1}{m!} \partial_{s_j}^m Y(\zeta_j), \quad 0 \leq m \leq n_j - 1. \quad (\text{C.12})$$

In the case when all eigenvalues of a cyclic matrix are distinct then the generalized Vandermonde matrix turns into the standard Vandermonde matrix

$$V = \begin{bmatrix} 1 & 1 & \cdots & 1 \\ \zeta_1 & \zeta_2 & \cdots & \zeta_n \\ \vdots & \vdots & \ddots & \vdots \\ \zeta_1^{n-2} & \zeta_2^{n-2} & \cdots & \zeta_n^{n-2} \\ \zeta_1^{n-1} & \zeta_2^{n-1} & \cdots & \zeta_n^{n-1} \end{bmatrix}. \quad (\text{C.13})$$

APPENDIX D. MATRIX POLYNOMIALS

An important incentive for considering matrix polynomials is that they are relevant to the spectral theory of the differential equations of the order higher than 1, particularly the Euler-Lagrange equations which are the second-order differential equations in time. We provide here selected elements of the theory of matrix polynomials following mostly [GoLaRo, II.7, II.8], [Baum, 9]. The general matrix polynomial eigenvalue problem reads

$$A(s)x = 0, \quad A(s) = \sum_{j=0}^{\nu} A_j s^j, \quad x \neq 0, \quad (\text{D.1})$$

where s is a complex number, A_k are constant $m \times m$ matrices and $x \in \mathbb{C}^m$ is an m -dimensional column-vector. We refer to problem (D.1) of finding complex-valued s and non-zero vector $x \in \mathbb{C}^m$ as the *polynomial eigenvalue problem*.

If a pair of a complex s and non-zero vector x solves problem (D.1) we refer to s as an *eigenvalue* or as a *characteristic value* and to x as the corresponding value to the s *eigenvector*. Evidently the characteristic values of problem (D.1) can be found from polynomial *characteristic equation* as follows:

$$\det \{A(s)\} = 0. \quad (\text{D.2})$$

We refer to matrix polynomial $A(s)$ as *regular* if $\det \{A(s)\}$ is not identically zero. We denote by $m(s_0)$ the *multiplicity* (called also *algebraic multiplicity*) of eigenvalue s_0 as a root of polynomial $\det \{A(s)\}$. In contrast, the *geometric multiplicity* of eigenvalue s_0 is defined as $\dim \{\ker \{A(s_0)\}\}$, where $\ker \{A\}$ defined for any square matrix A stands for the subspace of solutions x to equation $Ax = 0$. Evidently, the geometric multiplicity of eigenvalue does not exceed its algebraic one, see Corollary 17.

It turns out that the matrix polynomial eigenvalue problem (D.1) can be always recast as the standard “linear” eigenvalue problem, namely

$$(s\mathbf{B} - \mathbf{A})\mathbf{x} = 0, \quad (\text{D.3})$$

where $m\nu \times m\nu$ matrices \mathbf{A} and \mathbf{B} are defined by

$$\mathbf{B} = \begin{bmatrix} \mathbb{I} & 0 & \cdots & 0 & 0 \\ 0 & \mathbb{I} & 0 & \cdots & 0 \\ 0 & 0 & \ddots & \cdots & \vdots \\ \vdots & \vdots & \ddots & \mathbb{I} & 0 \\ 0 & 0 & \cdots & 0 & A_\nu \end{bmatrix}, \quad \mathbf{A} = \begin{bmatrix} 0 & \mathbb{I} & \cdots & 0 & 0 \\ 0 & 0 & \mathbb{I} & \cdots & 0 \\ 0 & 0 & 0 & \cdots & \vdots \\ \vdots & \vdots & \ddots & 0 & \mathbb{I} \\ -A_0 & -A_1 & \cdots & -A_{\nu-2} & -A_{\nu-1} \end{bmatrix}, \quad (\text{D.4})$$

with \mathbb{I} being $m \times m$ the identity matrix. Matrix \mathbf{A} , particularly in the monic case, is often referred to as *companion matrix*. In the case of *monic polynomial* $A(\lambda)$, when $A_\nu = \mathbb{I}$ is the $m \times m$ identity matrix, matrix $\mathbf{B} = \mathbf{I}$ is the $m\nu \times m\nu$ identity matrix. The reduction of original polynomial problem (D.1) to an equivalent linear problem (D.3) is called *linearization*.

The linearization is not unique, and one way to accomplish is by introducing the so-called known “companion polynomial”, which is the $m\nu \times m\nu$ matrix

$$\mathbf{C}_A(s) = s\mathbf{B} - \mathbf{A} = \begin{bmatrix} s\mathbb{I} & -\mathbb{I} & \cdots & 0 & 0 \\ 0 & s\mathbb{I} & -\mathbb{I} & \cdots & 0 \\ 0 & 0 & \ddots & \cdots & \vdots \\ \vdots & \vdots & \vdots & s\mathbb{I} & -\mathbb{I} \\ A_0 & A_1 & \cdots & A_{\nu-2} & sA_\nu + A_{\nu-1} \end{bmatrix}. \quad (\text{D.5})$$

Notice that in the case of the EL equations the linearization can be accomplished by the relevant Hamilton equations.

To demonstrate the equivalency between the eigenvalue problems for the $m\nu \times m\nu$ companion polynomial $\mathbf{C}_A(s)$ and the original $m \times m$ matrix polynomial $A(s)$ we introduce two $m\nu \times m\nu$ matrix polynomials $\mathbf{E}(s)$ and $\mathbf{F}(s)$. Namely,

$$\mathbf{E}(s) = \begin{bmatrix} E_1(s) & E_2(s) & \cdots & E_{\nu-1}(s) & \mathbb{I} \\ -\mathbb{I} & 0 & 0 & \cdots & 0 \\ 0 & -\mathbb{I} & \ddots & \cdots & \vdots \\ \vdots & \vdots & \ddots & 0 & 0 \\ 0 & 0 & \cdots & -\mathbb{I} & 0 \end{bmatrix}, \quad (\text{D.6})$$

$$\det \{\mathbf{E}(s)\} = 1,$$

where $m \times m$ matrix polynomials $E_j(s)$ are defined by the following recursive formulas

$$E_\nu(s) = A_\nu, \quad E_{j-1}(s) = A_{j-1} + sE_j(s), \quad j = \nu, \dots, 2. \quad (\text{D.7})$$

Matrix polynomial $\mathbf{F}(s)$ is defined by

$$\mathbf{F}(s) = \begin{bmatrix} \mathbb{I} & 0 & \cdots & 0 & 0 \\ -s\mathbb{I} & \mathbb{I} & 0 & \cdots & 0 \\ 0 & -s\mathbb{I} & \ddots & \cdots & \vdots \\ \vdots & \vdots & \ddots & \mathbb{I} & 0 \\ 0 & 0 & \cdots & -s\mathbb{I} & \mathbb{I} \end{bmatrix}, \quad \det \{\mathbf{F}(s)\} = 1. \quad (\text{D.8})$$

Notice, that both matrix polynomials $E(s)$ and $F(s)$ have constant determinants readily implying that their inverses $E^{-1}(s)$ and $F^{-1}(s)$ are also matrix polynomials. Then, it is straightforward to verify that

$$E(s) C_A(s) F^{-1}(s) = E(s) (sB - A) F^{-1}(s) = \begin{bmatrix} A(s) & 0 & \cdots & 0 & 0 \\ 0 & \mathbb{I} & 0 & \cdots & 0 \\ 0 & 0 & \ddots & \cdots & \vdots \\ \vdots & \vdots & \ddots & \mathbb{I} & 0 \\ 0 & 0 & \cdots & 0 & \mathbb{I} \end{bmatrix}. \quad (D.9)$$

The identity (D.9) where matrix polynomials $E(s)$ and $F(s)$ have constant determinants can be viewed as the definition of equivalency between matrix polynomial $A(s)$ and its companion polynomial $C_A(s)$.

Let us take a look at the eigenvalue problem for eigenvalue s and eigenvector $\mathbf{x} \in \mathbb{C}^{m\nu}$ associated with companion polynomial $C_A(s)$, that is

$$(sB - A)\mathbf{x} = 0, \quad \mathbf{x} = \begin{bmatrix} x_0 \\ x_1 \\ x_2 \\ \vdots \\ x_{\nu-1} \end{bmatrix} \in \mathbb{C}^{m\nu}, \quad x_j \in \mathbb{C}^m, \quad 0 \leq j \leq \nu - 1, \quad (D.10)$$

where

$$(sB - A)\mathbf{x} = \begin{bmatrix} sx_0 - x_1 \\ sx_1 - x_2 \\ \vdots \\ sx_{\nu-2} - x_{\nu-1} \\ \sum_{j=0}^{\nu-2} A_j x_j + (sA_\nu + A_{\nu-1}) x_{\nu-1} \end{bmatrix}. \quad (D.11)$$

With equations (D.10) and (D.11) in mind we introduce the following vector polynomial

$$\mathbf{x}_s = \begin{bmatrix} x_0 \\ sx_0 \\ \vdots \\ s^{\nu-2}x_0 \\ s^{\nu-1}x_0 \end{bmatrix}, \quad x_0 \in \mathbb{C}^m. \quad (D.12)$$

Not accidentally, the components of the vector \mathbf{x}_s in its representation (D.12) are in evident relation with the derivatives $\partial_t^j (x_0 e^{st}) = s^j x_0 e^{st}$. That is just another sign of the intimate relations between the matrix polynomial theory and the theory of systems of ordinary differential equations, see Appendix E.

Theorem 15 (eigenvectors). *Let $A(s)$ as in equations (D.1) be regular, that $\det\{A(s)\}$ is not identically zero, and let $m\nu \times m\nu$ matrices A and B be defined by equations (D.2). Then, the following identities hold*

$$(sB - A)\mathbf{x}_s = \begin{bmatrix} 0 \\ 0 \\ \vdots \\ 0 \\ A(s)x_0 \end{bmatrix}, \quad \mathbf{x}_s = \begin{bmatrix} x_0 \\ sx_0 \\ \vdots \\ s^{\nu-2}x_0 \\ s^{\nu-1}x_0 \end{bmatrix}, \quad (D.13)$$

$$\det \{A(s)\} = \det \{s\mathbf{B} - \mathbf{A}\}, \quad \det \{\mathbf{B}\} = \det \{A_\nu\}, \quad (\text{D.14})$$

where $\det \{A(s)\} = \det \{s\mathbf{B} - \mathbf{A}\}$ is a polynomial of the degree $m\nu$ if $\det \{\mathbf{B}\} = \det \{A_\nu\} \neq 0$. There is one-to-one correspondence between solutions of equations $A(s)x = 0$ and $(s\mathbf{B} - \mathbf{A})x = 0$. Namely, a pair s, x solves eigenvalue problem $(s\mathbf{B} - \mathbf{A})x = 0$ if and only if the following equalities hold

$$x = x_s = \begin{bmatrix} x_0 \\ sx_0 \\ \vdots \\ s^{\nu-2}x_0 \\ s^{\nu-1}x_0 \end{bmatrix}, \quad A(s)x_0 = 0, \quad x_0 \neq 0; \quad \det \{A(s)\} = 0. \quad (\text{D.15})$$

Proof. Polynomial vector identity (D.13) readily follows from equations (D.11) and (D.12). Identities (D.14) for the determinants follow straightforwardly from equations (D.12), (D.15) and (D.9). If $\det \{\mathbf{B}\} = \det \{A_\nu\} \neq 0$ then the degree of the polynomial $\det \{s\mathbf{B} - \mathbf{A}\}$ has to be $m\nu$ since \mathbf{A} and \mathbf{B} are $m\nu \times m\nu$ matrices.

Suppose that equations (D.15) hold. Then combining them with proven identity (D.13) we get $(s\mathbf{B} - \mathbf{A})x_s = 0$ proving that expressions (D.15) define an eigenvalue s and an eigenvector $x = x_s$.

Suppose now that $(s\mathbf{B} - \mathbf{A})x = 0$ where $x \neq 0$. Combining that with equations (D.11) we obtain

$$x_1 = sx_0, \quad x_2 = sx_1 = s^2x_0, \dots, \quad x_{\nu-1} = s^{\nu-1}x_0, \quad (\text{D.16})$$

implying that

$$x = x_s = \begin{bmatrix} x_0 \\ sx_0 \\ \vdots \\ s^{\nu-2}x_0 \\ s^{\nu-1}x_0 \end{bmatrix}, \quad x_0 \neq 0, \quad (\text{D.17})$$

and

$$\sum_{j=0}^{\nu-2} A_j x_j + (sA_\nu + A_{\nu-1})x_{\nu-1} = A(s)x_0. \quad (\text{D.18})$$

Using equations (D.17) and identity (D.13) we obtain

$$0 = (s\mathbf{B} - \mathbf{A})x = (s\mathbf{B} - \mathbf{A})x_s = \begin{bmatrix} 0 \\ 0 \\ \vdots \\ 0 \\ A(s)x_0 \end{bmatrix}. \quad (\text{D.19})$$

Equations (D.19) readily imply $A(s)x_0 = 0$ and $\det \{A(s)\} = 0$ since $x_0 \neq 0$. That completes the proof. \square

Remark 16 (characteristic polynomial degree). Note that according to Theorem 15 the characteristic polynomial $\det \{A(s)\}$ for $m \times m$ matrix polynomial $A(s)$ has the degree $m\nu$, whereas in linear case $s\mathbb{I} - A_0$ for $m \times m$ identity matrix \mathbb{I} and $m \times m$ matrix A_0 the characteristic polynomial $\det \{s\mathbb{I} - A_0\}$ is of the degree m . This can be explained by observing that in the non-linear case of $m \times m$ matrix polynomial $A(s)$ we are dealing effectively with many more $m \times m$ matrices A than just a single matrix A_0 .

Another problem of our particular interest related to the theory of matrix polynomials is eigenvalues and eigenvectors degeneracy and consequently the existence of non-trivial Jordan blocks, that is Jordan blocks of dimensions higher or equal to 2. The general theory addresses this problem by introducing so-called “Jordan chains” which are intimately related to the theory of system of differential equations expressed as $A(\partial_t)x(t) = 0$ and their solutions of the form $x(t) = p(t)e^{st}$ where $p(t)$ is a vector polynomial, see Appendix E and [GoLaRo, I, II], [Baum, 9]. Avoiding the details of Jordan chains developments we simply notice that an important to us point of Theorem 15 is that there is one-to-one correspondence between solutions of equations $A(s)x = 0$ and $(sB - A)x = 0$, and it has the following immediate implication.

Corollary 17 (equality of the dimensions of eigenspaces). *Under the conditions of Theorem 15 for any eigenvalue s_0 , that is, $\det\{A(s_0)\} = 0$, we have*

$$\dim\{\ker\{s_0B - A\}\} = \dim\{\ker\{A(s_0)\}\}. \quad (D.20)$$

In other words, the geometric multiplicities of the eigenvalue s_0 associated with matrices $A(s_0)$ and $s_0B - A$ are equal. In view of identity (D.20) the following inequality holds for the (algebraic) multiplicity $m(s_0)$

$$m(s_0) \geq \dim\{\ker\{A(s_0)\}\}. \quad (D.21)$$

The next statement shows that if the geometric multiplicity of an eigenvalue is strictly less than its algebraic one then there exist non-trivial Jordan blocks, that is Jordan blocks of dimensions higher or equal to 2.

Theorem 18 (non-trivial Jordan block). *Assuming notations introduced in Theorem 15 let us suppose that the multiplicity $m(s_0)$ of eigenvalue s_0 satisfies*

$$m(s_0) > \dim\{\ker\{A(s_0)\}\}. \quad (D.22)$$

Then the Jordan canonical form of companion polynomial $C_A(s) = sB - A$ has a least one nontrivial Jordan block of the dimension exceeding 2.

In particular, if

$$\dim\{\ker\{s_0B - A\}\} = \dim\{\ker\{A(s_0)\}\} = 1, \quad (D.23)$$

and $m(s_0) \geq 2$ then the Jordan canonical form of companion polynomial $C_A(s) = sB - A$ has exactly one Jordan block associated with eigenvalue s_0 and its dimension is $m(s_0)$.

The proof of Theorem 18 follows straightforwardly from the definition of the Jordan canonical form and its basic properties. Note that if equations (D.23) hold, it implies that the eigenvalue 0 is cyclic (nonderogatory) for matrix $A(s_0)$ and eigenvalue s_0 is cyclic (nonderogatory) for matrix $B^{-1}A$ provided B^{-1} exists, see Appendix C.

APPENDIX E. VECTOR DIFFERENTIAL EQUATIONS AND THE JORDAN CANONICAL FORM

In this section we relate the vector ordinary differential equations to the matrix polynomials reviewed in Appendix D following [GoLaRo2, 5.1, 5.7], [GoLaRo, II.8.3], [Hale, III.4], [MeyCD, 7.9].

Equation $A(s)x = 0$ with polynomial matrix $A(s)$ defined by equations (D.1) corresponds to the following m -vector ν -th order ordinary differential

$$A(\partial_t)x(t) = 0, \text{ where } A(\partial_t) = \sum_{j=0}^{\nu} A_j \partial_t^j, \quad (E.1)$$

where $A_j = A_j(t)$ are $m \times m$ matrices. Introducing $m\nu$ -column-vector function

$$Y(t) = \begin{bmatrix} x(t) \\ \partial_t x(t) \\ \vdots \\ \partial_t^{\nu-2} x(t) \\ \partial_t^{\nu-1} x(t) \end{bmatrix} \quad (\text{E.2})$$

and under the assumption that matrix $A_\nu(t)$ is the identity matrix the differential equation (E.1) can be recast and the first order differential equation

$$\partial_t Y(t) = AY(t), \quad (\text{E.3})$$

where A is $m\nu \times m\nu$ matrix defined by

$$A = A(t) = \begin{bmatrix} 0 & \mathbb{I} & \cdots & 0 & 0 \\ 0 & 0 & \mathbb{I} & \cdots & 0 \\ 0 & 0 & 0 & \cdots & \vdots \\ \vdots & \vdots & \ddots & 0 & \mathbb{I} \\ -A_0(t) & -A_1(t) & \cdots & -A_{\nu-2}(t) & -A_{\nu-1}(t) \end{bmatrix}, \quad A_\nu(t) = \mathbb{I}. \quad (\text{E.4})$$

E.1. Constant coefficients case. Let us consider an important special case of equation (E.1) when matrices A_j are $m \times m$ that do not depend on t . Then equation (E.1) can be recast as

$$B\partial_t Y(t) = AY(t), \quad (\text{E.5})$$

where A and B are $m\nu \times m\nu$ companion matrices defined by equations (D.4) and

In the case when A_ν is an invertible $m \times m$ matrix equation (E.5) can be recast further as

$$\partial_t Y(t) = \dot{A}Y(t), \quad (\text{E.6})$$

where

$$\dot{A} = \begin{bmatrix} 0 & \mathbb{I} & \cdots & 0 & 0 \\ 0 & 0 & \mathbb{I} & \cdots & 0 \\ 0 & 0 & 0 & \cdots & \vdots \\ \vdots & \vdots & \ddots & 0 & \mathbb{I} \\ -\dot{A}_0 & -\dot{A}_1 & \cdots & -\dot{A}_{\nu-2} & -\dot{A}_{\nu-1} \end{bmatrix}, \quad \dot{A}_j = A_\nu^{-1}A_j, \quad 0 \leq \nu-1. \quad (\text{E.7})$$

Note that one can interpret equation (E.6) as a particular case of equation (E.5) where matrices A_ν and B are identity matrices of the respective dimensions $m \times m$ and $m\nu \times m\nu$, and that polynomial matrix $A(s)$ defined by equations (D.1) becomes monic matrix polynomial $\dot{A}(s)$, that is

$$\dot{A}(s) = \mathbb{I}s^\nu + \sum_{j=0}^{\nu-1} \dot{A}_j s^j, \quad \dot{A}_j = A_\nu^{-1}A_j, \quad 0 \leq \nu-1. \quad (\text{E.8})$$

Note that in view of equation (E.2), one recovers $x(t)$ from $Y(t)$ by using the following formula:

$$x(t) = P_1 Y(t), \quad P_1 = [\mathbb{I} \ 0 \ \cdots \ 0 \ 0], \quad (\text{E.9})$$

where P_1 evidently is $m \times m\nu$ matrix.

Observe also that, [GoLaRo2, Prop. 5.1.2], [LanTsi, 14]

$$\left[\dot{A}(s) \right]^{-1} = P_1 \left[\mathbb{I}s - \dot{A} \right]^{-1} R_1, \quad P_1 = \begin{bmatrix} \mathbb{I} & 0 & \cdots & 0 & 0 \end{bmatrix}, \quad R_1 = \begin{bmatrix} 0 \\ 0 \\ \vdots \\ 0 \\ \mathbb{I} \end{bmatrix}, \quad (\text{E.10})$$

where P_1 and R_1 evidently respectively $m \times m\nu$ and $m\nu \times m$ matrices.

The general form for the solution to vector differential equation (E.6) is

$$Y(t) = \exp \left\{ \dot{A}t \right\} Y_0, \quad Y_0 \in \mathbb{C}^{m\nu}. \quad (\text{E.11})$$

Then, using formulas (E.9) and (E.11) and Proposition 10, we arrive the following statement.

Proposition 19 (solution to the vector differential equation). *Let \dot{A} be $m\nu \times m\nu$ companion matrix defined by equations (E.7), ζ_1, \dots, ζ_p be its distinct eigenvalues, and $M_{\zeta_1}, \dots, M_{\zeta_p}$ be the corresponding generalized eigenspaces of the corresponding dimensions $r(\zeta_j)$, $1 \leq j \leq p$. Then the $m\nu$ column-vector solution $Y(t)$ to differential equation (E.6) is of the form*

$$Y(t) = \exp \left\{ \dot{A}t \right\} Y_0 = \sum_{j=1}^p e^{\zeta_j t} p_j(t), \quad Y_0 = \sum_{j=1}^p Y_{0,j}, \quad Y_{0,j} \in M_{\zeta_j}, \quad (\text{E.12})$$

where $m\nu$ -column-vector polynomials $p_j(t)$ satisfy

$$p_j(t) = \sum_{k=0}^{r(\zeta_j)-1} \frac{t^k}{k!} \left(\dot{A} - \zeta_j \mathbb{I} \right)^k Y_{0,j}, \quad 1 \leq j \leq p. \quad (\text{E.13})$$

Consequently, the general m -column-vector solution $x(t)$ to differential equation (E.1) is of the form

$$x(t) = \sum_{j=1}^p e^{\zeta_j t} P_1 p_j(t), \quad P_1 = \begin{bmatrix} \mathbb{I} & 0 & \cdots & 0 & 0 \end{bmatrix}. \quad (\text{E.14})$$

Note that $\chi_{\dot{A}}(s) = \det \left\{ s\mathbb{I} - \dot{A} \right\}$ is the characteristic function of the matrix \dot{A} . Then, using notations of Proposition 19, we obtain

$$\chi_{\dot{A}}(s) = \prod_{j=1}^p (s - \zeta_j)^{r(\zeta_j)}. \quad (\text{E.15})$$

Note also that for any values of complex-valued coefficients b_k we have

$$(\partial_t - \zeta_j)^{r(\zeta_j)} \left[e^{\zeta_j t} p_j(t) \right] = 0, \quad p_j(t) = \sum_{k=0}^{r(\zeta_j)-1} b_k t^k, \quad (\text{E.16})$$

implying together with representation (E.15) that

$$\chi_{\dot{A}}(\partial_t) \left[e^{\zeta_j t} p_j(t) \right] = 0, \quad p_j(t) = \sum_{k=0}^{r(\zeta_j)-1} b_k t^k. \quad (\text{E.17})$$

Combining now Proposition 19 with equation (E.17), we obtain the following statement.

Corollary 20 (property of a solution to the vector differential equation). *Let $x(t)$ be the general m -column-vector solution $x(t)$ to differential equation (E.1). Then $x(t)$ satisfies*

$$\chi_{\dot{A}}(\partial_t)x(t) = 0. \quad (\text{E.18})$$

APPENDIX F. FLOQUET THEORY

We provide here a concise review of the Floquet theory following [DalKre, III], [Hale, III.7] and [YakStar, II.2]. The primary subject of the Floquet theory is the general form of solutions to the ordinary differential equations with periodic coefficients. With that in mind suppose that: (i) z is real valued variable, (ii) $x(z)$ is an n -vector valued function of z , (iii) $A(z)$ is an $n \times n$ matrix-valued ς -periodic function of z , and consider the following homogeneous linear periodic system:

$$\partial_z x(z) = A(z)x(z), \quad A(z + \varsigma) = A(z), \quad \varsigma > 0. \quad (\text{F.1})$$

We would like to give a complete characterization of the general structure of the solutions to equation (F.1). We start with the following statement showing how to define the logarithm B of a matrix C so that $C = e^B$.

Lemma 21 (logarithm of a matrix). *Let C be an $n \times n$ matrix with $\det\{C\} \neq 0$. Suppose that $C = Z^{-1}JZ$ where J is the Jordan canonical form of C as described in Proposition 11. Then using the block representation (B.8) for J , that is*

$$J = J = \text{diag}\{J_{n_1}(\zeta_1), J_{n_2}(\zeta_2), \dots, J_{n_r}(\zeta_r)\}, \quad n_1 + n_2 + \dots + n_q = n, \quad (\text{F.2})$$

we decompose J into its diagonal and nilpotent components:

$$J = \text{diag}\{\lambda_1 \mathbb{I}_{n_1}, \lambda_2 \mathbb{I}_{n_2}, \dots, \lambda_q \mathbb{I}_{n_q}\} + K \quad (\text{F.3})$$

where

$$D = \text{diag}\{\lambda_1 \mathbb{I}_{n_1}, \lambda_2 \mathbb{I}_{n_2}, \dots, \lambda_q \mathbb{I}_{n_q}\}, \quad K = \text{diag}\{K_{n_1}, K_{n_2}, \dots, K_{n_q}\}, \quad (\text{F.4})$$

$$K_{n_j} = J_{n_j}(\lambda_j) - \lambda_j \mathbb{I}_{n_j}, \quad 1 \leq j \leq q.$$

Then let $\ln(*)$ be a branch of the logarithm and let

$$H = \ln J = \text{diag}\{\ln(\lambda_1) \mathbb{I}_{n_1}, \ln(\lambda_2) \mathbb{I}_{n_2}, \dots, \ln(\lambda_q) \mathbb{I}_{n_q}\} + S \quad (\text{F.5})$$

where \mathbb{I}_{n_j} are identity matrices of identified dimensions and

$$S = \text{diag}\{S_{n_1}, S_{n_2}, \dots, S_{n_q}\}, \quad S_{n_j} = \sum_{m=1}^{n_j-1} (-1)^{m-1} \frac{1}{m \lambda_j^m} K_{n_j}^m, \quad 1 \leq j \leq q. \quad (\text{F.6})$$

Then

$$C = e^B, \quad B = \ln C = Z^{-1} H Z, \quad (\text{F.7})$$

where matrix H is defined by equation (F.5).

Note that matrix S in equations (F.5) and (F.6) is associated with the nilpotent part of Jordan canonical form J . The expression for S_{n_j} originates in the series

$$\ln(1+s) = \sum_{m=1}^{\infty} (-1)^{m-1} \frac{1}{m} s^m = s - \frac{s^2}{2} + \frac{s^3}{3} + \dots, \quad (\text{F.8})$$

and it is a finite sum since K_{n_j} is a nilpotent matrix such that

$$K_{n_j}^m = 0, \quad m \geq n_j, \quad 1 \leq j \leq q. \quad (\text{F.9})$$

An $n \times n$ matrix $\Phi(z)$ is called *matrizant* (*matriciant*) of equation (F.1) if it satisfies the following equation:

$$\partial_z \Phi(z) = A(z) \Phi(z), \quad \Phi(0) = \mathbb{I}, \quad A(z + \varsigma) = A(z), \quad \varsigma > 0, \quad (\text{F.10})$$

where \mathbb{I} is the $n \times n$ identity matrix. Matrix $\Phi(z)$ is also called *principal fundamental matrix* solution to equation (F.1). Evidently $x(z) = \Phi(z)x_0$ is the a solution to equation (F.1) with the initial condition $x(0) = x_0$. Using the fundamental solution $\Phi(z)$ we can represent any matrix solution $\Psi(z)$ to equation (F.1) based on its initial values as follows

$$\partial_z \Psi(z) = A(z) \Psi(z), \quad \Psi(z) = \Phi(z) \Psi(0). \quad (\text{F.11})$$

In the case of ς -periodic matrix function $A(z)$ the matrix function $\Psi(z) = \Phi(z + \varsigma)$ is evidently a solution to equation (F.11) and consequently

$$\Phi(z + \varsigma) = \Phi(z) \Phi(\varsigma). \quad (\text{F.12})$$

It turns out that matrix $M_\varsigma = \Phi(\varsigma)$ called the *monodromy matrix* is of particular importance for the analysis of solutions to equation (F.10) with ς -periodic matrix function $A(z)$.

The monodromy matrix is integrated into the formulation of the main statement of the Floquet theory describing the structure of solutions to equation (F.11) for ς -periodic matrix function $A(z)$.

Theorem 22 (Floquet). *Suppose that $A(z)$ is a ς -periodic continuous function of z . Let $\Phi(z)$ be the matrizant of equation (F.10) and let $M_\varsigma = \Phi(\varsigma)$ be the corresponding monodromy matrix. Using the statement of Lemma 21 we introduce matrix Γ defined by*

$$\Gamma = \frac{1}{\varsigma} \ln M_\varsigma = \frac{1}{\varsigma} \ln \Phi(\varsigma), \text{ implying } M_\varsigma = \Phi(\varsigma) = e^{\Gamma \varsigma}. \quad (\text{F.13})$$

Then matrizant $\Phi(z)$ satisfies the following equation called *Floquet representation*

$$\Phi(z) = P(z) e^{\Gamma z}, \quad P(z + \varsigma) = P(z), \quad P(0) = \mathbb{I}, \quad (\text{F.14})$$

where $P(z)$ is a differentiable ς -periodic matrix function of z .

Proof. Let us define matrix $P(z)$ by the following equation

$$P(z) = \Phi(z) e^{-\Gamma z}. \quad (\text{F.15})$$

Then combining representation (F.15) for $P(z)$ with equations (F.12) and (F.13) we obtain

$$P(z + \varsigma) = \Phi(z + \varsigma) e^{-\Gamma(z + \varsigma)} = \Phi(z) \Phi(\varsigma) e^{-\Gamma \varsigma} e^{-\Gamma z} = \Phi(z) e^{-\Gamma z} = P(z), \quad (\text{F.16})$$

that is $P(z)$ is a differentiable ς -periodic matrix function of z . Equality $P(0) = \mathbb{I}$ readily follows from equation (F.15) and equality $\Phi(0) = \mathbb{I}$. \square

The eigenvalues of the monodromy matrix $\Phi(\varsigma) = e^{\Gamma \varsigma}$ are called *Floquet (characteristic) multipliers* and their logarithms (not uniquely defined) are called *characteristic exponents*.

Definition 23 (Floquet multipliers, characteristic exponents and eigenmodes). Using notation of Theorem 22 let us consider complex numbers κ , s_κ and vector y_κ satisfying the following equations

$$\Gamma y_\kappa = \kappa y_\kappa, \quad \Phi(\varsigma) y_\kappa = e^{-\Gamma \varsigma} y_\kappa = s_\kappa y_\kappa, \quad s_\kappa = e^{\kappa \varsigma}, \quad (\text{F.17})$$

where evidently κ and y_κ are respectively an eigenvalue and the corresponding eigenvector of matrix Γ . We refer to κ and s_κ respectively as the *Floquet characteristic exponent* and the *Floquet (characteristic) multiplier*.

Using κ and y_κ defined above we introduce the following special solution to the original differential equation (F.1):

$$\psi_\kappa(z) = p_\kappa(z) e^{\kappa z} = \Phi(z) y_\kappa = P(z) e^{\Gamma z} y_\kappa, \quad p_\kappa(z) = P(z) y_\kappa, \quad (\text{F.18})$$

G -unitary	G -skew-Hermitian	G -Hermitian
$\langle Ax, Ay \rangle = \langle x, y \rangle$	$\langle Ax, y \rangle = -\langle x, Ay \rangle$	$\langle Ax, y \rangle = \langle x, Ay \rangle$
$A^\dagger A = G^{-1} A^* G A = \mathbb{I}$,	$A^\dagger = G^{-1} A^* G = -A$,	$A^\dagger = G^{-1} A^* G = A$,
$A^* = G A^{-1} G^{-1}$	$GA + A^* G = 0$	$GA - A^* G = 0$
$A^* G A = G$	$A = iG^{-1}H$, $H = H^*$	$A = G^{-1}H$, $H = H^*$

TABLE 7. G -unitary, G -skew-Hermitian and G -Hermitian matrices.

and we refer to it as the *Floquet eigenmode*. Note that $p_\kappa(z)$ in equations (F.18) is a ς -periodic vector-function of z .

Remark 24 (Floquet eigenmodes). If $\psi_\kappa(z)$ is the Floquet eigenmode defined by equations (F.18) and $\Re\{\kappa\} > 0$ or, equivalently, $|s_\kappa| > 1$ then $\psi_\kappa(z)$ grows exponentially as $z \rightarrow +\infty$, and we refer to such $\psi_\kappa(z)$ as *exponentially growing Floquet eigenmode*. In the case when $\Re\{\kappa\} = 0$ or equivalently $|s_\kappa| = 1$ function $\psi_\kappa(z)$ is bounded and we refer to such $\psi_\kappa(z)$ as an *oscillatory Floquet eigenmode*.

Remark 25 (dispersion relations). In physical applications of the Floquet theory ς -periodic matrix valued function $A(z)$ in differential equation (F.1) depends on the frequency ω , that is $A(z) = A(z, \omega)$. In this case we also have $\kappa = \kappa(\omega)$. If we naturally introduce the wave number k by

$$k = k(\omega) = -i\kappa(\omega), \quad (\text{F.19})$$

then the relation between ω and k provided by equation (F.19) is called the *dispersion relation*.

APPENDIX G. HAMILTONIAN SYSTEM OF LINEAR DIFFERENTIAL EQUATIONS

We follow here to [DalKre, I.8, V.1] and [YakStar, III]. We introduce first *indefinite scalar product* $\langle x, y \rangle$ on the vector space \mathbb{C}^n associated with a nonsingular Hermitian $n \times n$ matrix G , namely

$$\langle x, y \rangle = \overline{\langle y, x \rangle} = x^* G y, \quad G^* = G, \quad \det\{G\} \neq 0, \quad x, y \in \mathbb{C}^n. \quad (\text{G.1})$$

We refer to matrix the G *metric matrix*. We define, then, for any $n \times n$ matrix A another matrix A^\dagger called adjoint by using the following relations:

$$\langle Ax, y \rangle = \langle x, A^\dagger y \rangle \quad \text{or equivalently} \quad A^\dagger = G^{-1} A^* G. \quad (\text{G.2})$$

Note that relations (G.2) readily imply that

$$(AB)^\dagger = B^\dagger A^\dagger. \quad (\text{G.3})$$

Let G and $H(t)$ be Hermitian $n \times n$ matrices and suppose that matrix G is nonsingular. We define the *Hamiltonian system of equations* to be a system of the form.

$$-iG\partial_t x(t) = H(t)x(t), \quad H^*(t) = H(t). \quad (\text{G.4})$$

If based on matrices G and $H(t)$ we introduce G -skew-Hermitian matrix,

$$A(t) = iG^{-1}H(t), \quad (\text{G.5})$$

we can recast the Hamiltonian system (G.4) in the following equivalent form:

$$\partial_t x(t) = A(t)x(t), \quad A^\dagger(t) = -A(t). \quad (\text{G.6})$$

It turns out that the matrizant $\Phi(t)$ of equation (G.6) with G -skew-Hermitian matrix $A(t)$ is a G -unitary matrix for each value of t . Indeed, using equation (G.6) together with equations (G.2) and (G.3), we obtain

$$\begin{aligned} \partial_t [\Phi^\dagger(t) \Phi(t)] &= \{\partial_t [\Phi(t)]\}^\dagger \Phi(t) + \Phi^\dagger(t) \partial_t [\Phi(t)] = \\ &= -\Phi^\dagger(t) A(t) \Phi(t) + \Phi^\dagger(t) A(t) \Phi(t) = 0, \end{aligned} \quad (\text{G.7})$$

implying that matrizant $\Phi(t)$ satisfies

$$\Phi^\dagger(t) \Phi(t) = \mathbb{I}, \text{ or equivalently } \Phi^*(t) G \Phi(t) = G, \quad (\text{G.8})$$

implying that $\Phi(t)$ is a G -unitary matrix for each value of t . Identity (G.8) implies in turn that for any two solutions $x(t)$ and $y(t)$ to the Hamiltonian system (G.4) we always have

$$\langle x(t), y(t) \rangle = x^*(t) G y(t) = x^*(0) \Phi^*(t) G \Phi(t) y(0) = \langle x(0), y(0) \rangle, \quad (\text{G.9})$$

that is $\langle x(t), y(t) \rangle$ does not depend on t .

G.1. Symmetry of the spectra. G -unitary, G -skew-Hermitian and G -Hermitian matrices have special properties described in Table 7. These properties can be viewed as symmetries, and not surprisingly, they imply consequent symmetries of the spectra of the matrices. Let $\sigma\{A\}$ denote the spectrum of matrix A . It is a straightforward exercise to verify based on matrix properties described in Table 7 that the following statements hold.

Theorem 26 (spectral symmetries). *Suppose that matrix A is either G -unitary or G -skew-Hermitian or G -Hermitian. Then the following statements hold:*

(i) *If A is G -unitary then $\sigma\{A\}$ is symmetric with respect to the unit circle, that is*

$$\zeta \in \sigma\{\Phi\} \Rightarrow \frac{1}{\bar{\zeta}} \in \sigma\{\Phi\}. \quad (\text{G.10})$$

(ii) *If A is G -skew-Hermitian then $\sigma\{A\}$ is symmetric with respect to the imaginary axis, that is*

$$\zeta \in \sigma\{\Phi\} \Rightarrow -\bar{\zeta} \in \sigma\{\Phi\}. \quad (\text{G.11})$$

(iii) *If A is G -Hermitian then $\sigma\{A\}$ is symmetric with respect to the real axis, that is*

$$\zeta \in \sigma\{\Phi\} \Rightarrow \bar{\zeta} \in \sigma\{\Phi\}. \quad (\text{G.12})$$

The following statement describes the G -orthogonality of invariant subspaces of G -unitary, G -skew-Hermitian and G -Hermitian matrices, [DalKre, 1.8].

Theorem 27 (eigenspaces). *Suppose that matrix A is either G -unitary or G -skew-Hermitian or G -Hermitian. Then the following statements hold. Let $\Lambda \subset \sigma\{A\}$ be a subset of the spectrum $\sigma\{A\}$ of the matrix A , and let $\tilde{\Lambda}$ be the relevant symmetric image of Λ defined by*

$$\tilde{\Lambda} = \begin{cases} \left\{ \frac{1}{\bar{\zeta}} : \zeta \in \Lambda \right\} & \text{if } A \text{ is } G\text{-unitary} \\ \left\{ -\bar{\zeta} : \zeta \in \Lambda \right\} & \text{if } A \text{ is } G\text{-skew-Hermitian} \\ \left\{ \bar{\zeta} : \zeta \in \Lambda \right\} & \text{if } A \text{ is } G\text{-Hermitian} \end{cases}.$$

Let $\Lambda_1, \Lambda_2 \subset \sigma\{A\}$ be two subsets of the spectrum $\sigma\{A\}$ so that $\tilde{\Lambda}_1$ and Λ_2 are separated from each other by non-intersecting contours $\tilde{\Gamma}_1$ and Γ_2 . Then the invariant subspaces E_1 and E_2 of the matrix A corresponding to Λ_1 and Λ_2 are G -orthogonal.

The statement below describes a special property of eigenvectors of a G -unitary matrix.

Lemma 28 (isotropic eigenvector). *Let A be a G -unitary matrix and ζ be its eigenvalue that does not lie on the unit circuit, that is, $|\zeta| \neq 1$. Then if x is the eigenvector corresponding to ζ it is isotropic, that is*

$$\langle x, x \rangle = x^* G x = 0, \quad Ax = \zeta x, \quad |\zeta| \neq 1. \quad (\text{G.13})$$

Proof. Since $Ax = \zeta x$ and A is a G -unitary, we have

$$\langle Ax, Ax \rangle = \langle \zeta x, \zeta x \rangle = |\zeta|^2 \langle x, x \rangle, \quad \langle Ax, Ax \rangle = \langle x, x \rangle.$$

Combining the two equation above with $|\zeta| \neq 1$ we conclude that $\langle x, x \rangle = 0$ which is the desired equation (G.10). \square

G.2. Special Hamiltonian systems. With equation (3.37) in mind we introduce the following system

$$\partial_t x(t) = A(t) x(t), \quad (\text{G.14})$$

where 4×4 matrix function $A(z)$ is of the following form special form

$$A(z) = \begin{bmatrix} 0 & 0 & 1 & 0 \\ 0 & 0 & 0 & 1 \\ a_1(z) & a(z) a_2 & i c_1 & 0 \\ a(z) a_3 & a_4(z) & 0 & i c_2 \end{bmatrix}, \quad a_1(z), a_2, a_3, a_4(z), c_1, c_2, a(z) \in \mathbb{R}. \quad (\text{G.15})$$

The system (G.14), (G.14) is Hamiltonian if we select Hermitian matrix G to be

$$G = \begin{bmatrix} c_1 & 0 & i & 0 \\ 0 & \frac{c_2 a_2}{a_3} & 0 & i \frac{a_2}{a_3} \\ -i & 0 & 0 & 0 \\ 0 & -i \frac{a_2}{a_3} & 0 & 0 \end{bmatrix}, \quad G^{-1} = \begin{bmatrix} 0 & 0 & i & 0 \\ 0 & 0 & 0 & i \frac{a_3}{a_2} \\ -i & 0 & -c_1 & 0 \\ 0 & -i \frac{a_3}{a_2} & 0 & -\frac{c_2 a_3}{a_2} \end{bmatrix}, \quad \det \{G\} = \frac{a_2^2}{a_3^2}. \quad (\text{G.16})$$

Indeed, it is an elementary exercise to verify that for each value of z matrix $A(z)$ is G -skew-Hermitian, that is

$$GA(z) + A^*(z)G = 0. \quad (\text{G.17})$$

APPENDIX H. FOLDED WAVEGUIDE TWT DISPERSION RELATIONS

Using a number of approximations the authors of [CanArm] arrive at the following expression of the dispersion relation similar to that of the Pierce theory

$$\delta k' (\Delta - \delta k')^2 \left(1 + \frac{\delta k'}{2} \right) - C^3 = 0, \quad k' = \frac{k}{k_c}, \quad (\text{H.1})$$

where (i) ω_c is the cut-off frequency of TE_{10} -mode; (ii) $k_c = \frac{\omega_c}{c}$, c is the velocity of light; (iii) C are respectively Δ are the coupling (Pierce) parameter and the detuning parameter represented by explicit formulas involving folded waveguide TWT parameters and frequency ω ; (iv) δk is defined by

$$k_m = k_m^0 + \delta k, \quad k_m^0 = \frac{2\pi m}{a} + \frac{a+h}{a} \sqrt{\frac{\omega^2 - \omega_c^2}{c^2}}, \quad (\text{H.2})$$

where k_m^0 is unperturbed propagation constant. In the case $C^3 \rightarrow 0$ there four solutions to equation (...): $\delta k = 0$ (unperturbed forward propagating wave), $2k_0^0$ (unperturbed contra propagating wave), and $k = k_c \Delta$ (degenerate e-beam mode). If the interaction with the contra propagating wave is neglected, $|\delta k| \ll 2|k_0^0|$, then we obtain from (H.1) the following third-order dispersion equation

$$\delta k'^3 - 2\Delta \delta k'^2 + \Delta^2 \delta k' - C^3 = 0. \quad (\text{H.3})$$

APPENDIX I. CAPACITANCE

According to [GreEM, I.1], [Zahn, 3.5.2] the following formulas hold for capacitance of capacitors of different geometries in Gaussian system of units.

Capacitance for the parallel-plate capacitor consisting of two parallel plates of area A that are separated by distance d is

$$C = \frac{A}{4\pi d}. \quad (\text{I.1})$$

Capacitance for the spherical capacitor consisting of two concentric spherical shells of radii $r_1 < r_2$ is

$$C = \frac{r_1 r_2}{r_2 - r_1}; \quad C \cong \frac{r_1^2}{2(r_2 - r_1)}, \text{ if } 0 < \frac{r_2 - r_1}{r_1} \ll 1. \quad (\text{I.2})$$

Capacitance of the cylindrical capacitor consisting of two coaxial cylinders of radii $r_1 < r_2$ and height h is

$$C = \frac{h}{2 \ln \left\{ \frac{r_2}{r_1} \right\}}; \quad C \cong \frac{h r_1}{2(r_2 - r_1)}, \text{ if } 0 < \frac{r_2 - r_1}{r_1} \ll 1. \quad (\text{I.3})$$

Capacitances for a number of different geometric shapes are available in [Landk, II.3] including capacitance of the disk of radius r :

$$C = \frac{2r}{\pi^2}. \quad (\text{I.4})$$

Since often the data is available in SI system of units rather than in Gaussian it is useful to know that the capacitances in these two systems are related as follows, [Jack, App. on units, 4]

$$C_{\text{SI}} = 4\pi\epsilon_0 C_{\text{Gaussian}}, \quad \epsilon_0 = 8.854187813 \cdot 10^{-12} \text{ F/m}. \quad (\text{I.5})$$

DATA AVAILABILITY: The data that supports the findings of this study are available within the article.

REFERENCES

- [ArnODE] Arnold V., *Ordinary Differential Equations*, 3rd ed., Springer, 1992. B
- [ArnMech] Arnold V., *Mathematical Methods of Classical Mechanics*, Springer, (1989). 11
- [ArfWeb] Arfken G. and Weber H., *Mathematical Methods for Physicists - A Comprehensive Guide*, 7th edn., Academic Press, 2013. A
- [Baum] Baumgartel H., *Analytic Perturbation Theory for Matrices and Operators*, Birkhauser, 1985. D, D
- [BenSweScha] Benford J., Swegle A. and Schamiloglu E., *High Power Microwaves*, 3rd ed., CRC Press, 2016. 8, 9
- [BernM] Bernstein D., *Matrix Mathematics: Theory, Facts, and Formulas*, 2 edn., Princeton University Press, 2009. B, C, C, C
- [BraMih] Branch G. and Mihran T., *Plasma-frequency Reduction Factors in Electron Beams*, IRE Trans.-Electron Devices, April, 3-11, 1955. 2
- [Caryo] Caryotakis G., *High Power Klystrons: Theory and Practice at the Stanford Linear Accelerator Center, Part I*, SLAC-PUB 10620, 2005. 10.1
- [CheN] Chen W. et. al., *Exceptional points enhance sensing in an optical microcavity*, Nature, **548**, 192-196, (2017). 6.2
- [ChoCra] Chodorow M. and Craig R., *Some new circuits for high power traveling wave tubes*, Proc. IRE., Aug., 1106-1118, (1957). 1
- [ChoWes] Chodorow M. and Wessel-Berg T., *A high-efficiency klystron with distributed interaction*, IRE Trans. on Electron Devices, **8**(1): 44-55, (1961). 1, 10.1
- [DalKre] Dalekii Ju. and Krein M., *Stability of solutions of differential equations in Banach space*, AMS 1974. F, G, G.1
- [FigKly] Figotin A., *Analytic theory of multicavity klystrons*, J. Math. Phys., **63**(6), (2022). 1, 8, 8.2, 8.2
- [FigTWTbk] Figotin A., *An Analytic Theory of Multi-stream Electron Beams in Traveling Wave Tubes*, World Scientific, 2020. 1, 2, 2, 2, 2, 2.1, 2.1, 2.2, 2.2, 2.2, 2.2, 2.2, 6.1, 6.2, 8

- [FigwtEPD] Figotin A., *Exceptional points of degeneracy in traveling wave tubes*, J. Math. Phys., **62**, 082701 (2021). 6.2
- [FigRey1] Figotin A. and Reyes G., *Multi-transmission-line-beam interactive system*, J. Math. Phys., **54**, 111901, (2013). 2
- [FigRey2] Figotin A. and Reyes G., *Lagrangian variational framework for boundary value-problems*, J. Math. Phys., **56**, 093506, (2015). 11, 11, 11
- [Foll] Folland G., *Fourier analysis and its applications*, Wadsworth & Brooks, 1992. A, A
- [CanArm] Ganguly A., Choi J. and Armstrong C., *Linear theory of slow wave cyclotron interaction in double-ridged folded rectangular waveguide*, IEEE Trans. on Electronic Devices, , **42**, 2, 348-355, (1995). H
- [GantM] Gantmacher F., *Lectures in Analytical Mechanics*, Mir, 1975. 11
- [GelFom] Gelfand I. and Fomin S., *Calculus of Variations*, Dover Publications (2000). 11, 11
- [GewWat] Gewartowski J. and Watson H., *Principles of Electron Tubes*, Van Nostrand, 1965.
- [Gilm1] Gilmour A., *Principles of Klystrons, Traveling Wave Tubes, Magnetrons, Cross-Field Amplifiers, and Gyrotrons*, Artech House, 2011. 1, 1, 2, 2, 2, 2, 2, 10.1
- [Gilm] Gilmour A., *Principles of Traveling Wave Tubes*, Artech House, 1994. 2
- [GoldM] Goldstein H. et. al. *Classical Mechanics*, 3rd edition, Addison Wesley, 2000. 11
- [GoLaRo] Gohberg I., Lancaster P. L. and Rodman L., *Matrix Polynomials*, SIAM, 2009. D, D, E
- [GoLaRo2] Gohberg I., Lancaster P. and Rodman L., *Invariant Subspaces of Matrices with Applications*, SIAM, 2006. E, E.1
- [Gran] Granger R., *Fluid Mechanics*, Dover, 1995. 10.1
- [GraParArm] Grandstein V. Parker R. Armstrong C., *Vacuum Electronics at the Dawn of the Twenty-First Century*, Proc. IEEE ., **87**, No.5, 702-716, (1999). 1
- [GreEM] Greiner W., *Classical Electrodynamics*, Springer, 1998. I
- [Grigo] Grigoriev A. et.al., *Microwave Electronics*, Springer, 2018. 8.2, 10.1
- [Jack] Jackson J., *Classical Electrodynamics*, Wiley, 3rd edition, 1999. I
- [Hale] Hale J., *Ordinary Differential Equations*, 2nd ed., Krieger Publishing Co., 1980. B, E, F
- [HorJohn] Horn R. and Johnson C., *Matrix Analysis*, 2nd ed., Cambridge University Press, 2013. B, B
- [Kato] Kato T., *Perturbation theory for linear operators*, Springer 1995. 6.2
- [KNAC] Kazemi H., Nada M., Mealy T., Abdelshafy A. and Capolino F., *Exceptional Points of Degeneracy Induced by Linear Time-Periodic Variation*, Phys. Rev. Applied, **11**, 014007 (2019). 6.2
- [Landk] Landkof N., *Foundations of Modern Potential Theory*, S, 1972. I
- [LanTsi] Lancaster P. and Tismenetsky M., *The Theory of Matrices*, 2nd ed., Academic Press, 1985. C, C, E.1
- [Lamb] Lamb H. *Hydrodynamics*, 6th ed., Cambridge University Press, 1975. 10.1
- [MAEAD] Minenna D., Andre F., Elskens Y., Auboin J-F., Doveil F., *The Traveling-Wave Tube in the History of Telecommunication*, Eur. Phys. J., **44**(1), 1-36, 2019. 1, 2
- [MeyCD] Meyer C., *Matrix analysis and applied linear algebra*, SIAM, 2010. B, C, E
- [OGC] Othman M., Galdi V. and Capolino F., *Exceptional points of degeneracy and PT symmetry in photonic coupled chains of scatterers*, Phys. Rev. B, **95**, 104305 (2017). 6.2
- [OTC] Othman M., Tamma V., and Capolino F., *Theory and new amplification regime in periodic multimodal slow wave structures with degeneracy interacting with an electron beam*, IEEE Trans. Plasma Sci., **44**, 594 (2016). 6.2
- [OVFC] Othman M., Veysi M., A. Figotin A. and Capolino F., *Low starting electron beam current in degenerate band edge oscillators*, IEEE Trans. Plasma Sci., **44**, 918 (2016). 6.2
- [OVFC1] Othman M., Veysi M., Figotin A. and Capolino F., *Giant amplification in degenerate band edge slow-wave structures interacting with an electron beam*, Phys. Plasmas, **23**, 033112 (2016). 6.2
- [Nusi] Barker R., Booske J., Luhmann N. and G. Nusinovich, *Modern Microwave and Millimeter-Wave Power Electronics*, Wiley, 2005. 2, 2, 2
- [PierTWT] Pierce J., *Traveling-Wave Tubes*, D. van Nostrand, 1950. 2
- [Pier51] Pierce J., *Waves in Electron Streams and Circuits*, Bell Sys. Tech. J., **30**, 626-651, 1951. 2
- [Redd] Reddy J., *An introduction to continuum mechanics*, Cambridge University Press, 2008. 10.1
- [SchaB] Schachter L., *Beam-Wave Interaction in Periodic and Quasi-Periodic Structures*, 2nd ed., Springer, 2011. 2, 2
- [Solnt] Solntsev V., *Beam-Wave Interaction in the Passbands and Stopbands of Periodic Slow-Wave Systems*, IEEE Trans. on Plasma Sc., **43**, No.7, 2114-2122, (2015). 6

- [Shev] Shevchik V., *Fundamentals of Microwave Electronics*, Pergamon Press, 1963. 1, 1, 1, 10.1, 10.1, 10.3
- [Stap] Staprans E. et.al., *High-power linear-beam tubes*, Proc. IEEE, **61**, No.3, 299-330, (1973).
- [Tsim] Tsimring S., *Electron Beams and Microwave Vacuum Electronics*, Wiley, 2007. 1, 1, 1, 2, 2, 3, 8, 8.2, 10.1
- [ValMid] Valkenburg M. Middleton W., eds., *Reference Data for Engineers - Radio, Electronics, Computer, and Communications*, 9th ed., Newnes, 2002. 8.2
- [VOFC] Veysi M., Othman M., Figotin A. and Capolino F., *Degenerate band edge laser*, Phys. Rev. B, **97**, 195107 (2018). 6.2
- [Werne] Warnecke R. et.al., *Velocity Modulated Tubes*, a chapter in Morton L. et. al. eds. "Advances in Electronics", v. III, Academic Press, 1951. 1, 8
- [Wie] Wiersig J., *Enhancing the Sensitivity of Frequency and Energy Splitting Detection by Using Exceptional Points - Application to Microcavity Sensors for Single-Particle Detection*, Phys. Rev. Lett., **112**, 203901 (2014). 6.2
- [Wiel] Wiersig J., *Sensors operating at exceptional points: General theory*, Phys. Rev. A, **93**, 033809 (2016). 6.2
- [YagCG] Yaglom I., *Complex Numbers in Geometry*, Academic Press, 1968. 12
- [YakStar] Yakubovich V. and Starzhinskij V., *Linear Differential Equation with Periodic Coefficients*, Vol. 1, Wiley & Sons, 1975. F, G
- [Zahn] Zahn M., *Electromagnetic Field theory - A Problem-Solving Approach*, 2nd ed., Wiley, 1979.

I

UNIVERSITY OF CALIFORNIA AT IRVINE, CA 92967